Electronic Supplementary Material (ESI) for Chemical Communications

Hybrid Charged Heterometallic Pt Ir Complexes: Tailoring Excited States by Taking the Best of Both Worlds

Ahmed M. Soliman, Daniel Fortin, Pierre D. Harvey and Eli Zysman-Colman*.*

Département de chimie, Université de Sherbrooke,
2500 Boul. Université, Sherbrooke, QC, J1K 2R1

Pierre.Harvey@usherbrooke.ca; *Eli.Zysman-Colman@usherbrooke.ca*

SUPPORTING INFORMATION

Table of Contents: **Pages**

Experimental section

Synthesis:

General Procedures:

Commercial chemicals were used as supplied. All experiments were carried out with freshly distilled anhydrous solvents obtained from a Pure Solv™ solvent purification system from Innovative Technologies except where specifically mentioned. *N*,*N*,*N*-Triethylamine (Et_3N), *N*,*N*-di*iso*propylamine (*i*-Pr_2NH) were distilled over CaH_2 under a nitrogen atmosphere. $PtCl_2(PBu_3)_2$ was obtained following standard literature protocol[1] and heated to 165 °C to obtain the *trans* form. CuI,[2] $[(ppy)_2Ir\text{-}\mu\text{-}Cl]_2$[3] dimer and 1-ethynyl-4-methylbenzene[4] were purified or prepared following literature procedures. All reagents wherein the synthesis is not explicitly described in the SI were purchased and used without further purification. Flash column chromatography was performed using silica gel (Silia-P from Silicycle, 60 Å, 40-63 μm). Analytical thin layer chromatography (TLC) was performed with silica plates with aluminum backings (250 μm with indicator F-254). Compounds were visualized under UV light. ^1H and ^{13}C NMR spectra were recorded on a Brucker Avance spectrometer at 400 MHz and 100 MHz, respectively or a Brucker Avance spectrometer at 300 MHz and 75MHz, respectively. ^{31}P NMR spectra was recorded on a Brucker Avance spectrometer at 121 MHz. The following abbreviations have been used for multiplicity assignments: "s" for singlet, "d" for doublet, "t" for triplet and "m" for multiplet. Deuterated cholorform ($CDCl_3$) was used as the solvent of record. Melting points (Mp's) were recorded using open end capillaries on a Meltemp melting point apparatus and are uncorrected. GC-MS samples were separated on a Shimadzu QP 2010 Plus equipped with a HP5-MS 30 m x 0.25 mm ID x 0.25 μm film thickness column. High resolution mass spectra were recorded on either a VG Micromass ZAB-2F or a Waters Synapt MS G1 (ES-Q-TOF) at the Université de Sherbrooke.

5-Bromo-2-iodopyridine (6):[5]

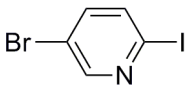

To a mixture of 2,5-dibromopyridine (4.00 g, 16.88 mmol, 1.00 equiv.) and KI (8.41 g, 50.63 mmol, 3.00 equiv.) was added HI (48 % wt., 20 mL). The reaction mixture was heated to reflux for 72 h. The reaction was followed by GC-MS and upon consumption of the starting material, was then cooled to 0 ^{o}C. An aqueous solution of KOH (40 %, 30 mL) followed by Et_2O (30 mL) was then added to the reaction mixture. The layers were separated and the aqueous phase was washed with Et_2O (2 x 30 mL). The combined organic phases were dried over $MgSO_4$, filtered and concentrated. The residue was purified by flash chromatography (10% EtOAc/Hexanes on silica gel) to yield 4.25 g of white solid (Yield: 90 %). **R*f*:** 0.28 (10% EtOAc/Hexanes). **Mp:** 112.8-113.6°C. (**Litt.:** 112.5-113.5^{o}C).[5] **^{1}H NMR (400 MHz, $CDCl_3$)** δ **(ppm):** 8.43 (d, *J* = 2.5 Hz, 1H), 7.58 (dd, *J* = 8.3 Hz, 1H), 7.42 (dd, *J* = 8.4, 2.7 Hz, 1H). **^{13}C NMR (100 MHz, $CDCl_3$)** δ **(ppm):** 152.1, 140.5, 136.3, 121.4, 115.4. **LR-MS (EI, 70eV) (*m/z*):** 283 (M^+), 75. **HR-MS (EI, 70eV): Calculated** (C_5H_3BrIN)**:** 282.8494; **Found**: 282.8493. The ^{1}H and ^{13}C NMR spectrum each correspond to that found in the literature.[6]

5-bromo-2,2'-bipyridine (7):

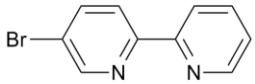

To a solution of 2-bromopyridine (4.80 mL, 50.4 mmol, 1.05 equiv.) in THF (65 mL) at -78 ^{o}C was added *n*-BuLi 2.2 M in hexanes (24.0 mL, 52.8 mmol, 1.10 equiv.) over 40 min. The mixture was stirred for 30 min at -78 ^{o}C, then a solution of $ZnCl_2$ (7.19 g, 52.8 mmol, 1.10 equiv.) in THF (60 mL) was canulated in over 40 min. The mixture was stirred at room temperature for 2 h. The zincate solution was canulated into a mixture of 5-bromo-2-iodopyridine **(6)** (13.6 g, 48.0 mmol, 1.00 equiv.) and $Pd(PPh_3)_4$ (2.91 g, 2.52 mmol, 5 mol %) in THF (60 mL). The reaction mixture was heated to reflux for 16 h. The reaction was followed by GC-MS. Upon cooling to room temperature, a gray solid precipitate was observed. The reaction mixture was concentrated under reduced pressure, but not dried. The suspension was cooled to -20 ^{o}C. The gray solid was filtered and washed with cold THF (2 x 20 mL). It was added to an aqueous solution of EDTA:$NaHCO_{3\ (sat.)}$ (1:1,15 mL) then stirred for 2 h at room temperature. To the mixture was added DCM and then the phases were separated. The organic phase was further washed with an aqueous solution of EDTA:$NaHCO_{3\ (sat.)}$ (1:1, 2 x 15 mL). The organic phase was dried over $MgSO_4$ and concentrated under reduced pressure.

The residue was purified by flash chromatography (15% EtOAc/Hexanes on silica gel) to yield 7.00 g of white solid (Yield: 60%). **R*f*:** 0.45 (10% EtOAc/Hexanes). **Mp:** 72-73.8°C. (**Litt.:** 74-75°C).[7] **^{1}H NMR (300 MHz, $CDCl_3$)** δ **(ppm):** 8.72 (d, *J* = 2.2 Hz, 1H), 8.68 (d, *J* = 4.7 Hz, 1H), 8.38 (d, *J* = 8.0 Hz, 1H), 8.32 (d, *J* = 8.5 Hz, 1H), 7.96 (dd, *J* = 8.5, 2.4 Hz, 1H), 7.82 (td, *J* = 7.8, 1.8 Hz, 1 H), 7.33 (ddd, *J* = 7.3, 4.7, 1.1 Hz, 1H). **^{13}C NMR (75 MHz, $CDCl_3$)** δ **(ppm):** 155.1, 154.6, 150.1, 149.2, 139.4, 137.0, 123.9, 122.3, 121.1, 120.9. **LR-MS (EI, 70eV) (*m/z*):** 234 (M^+), 155, 128. **HR-MS (EI, 70eV): Calculated** ($C_{10}H_7BrN_2$): 233.9793; **Found**: 233.9797. The ^{1}H and ^{13}C NMR spectra each correspond to that found in the literature.[7]

5-trimethylsilylethynyl-2,2'-bipyridine (8):

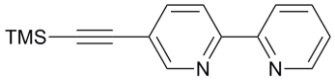

To a solution of 5-bromo-2,2'-bipyridine **(7)** (2.00 g, 8.55 mmol, 1.00 equiv.) in THF (90 mL) and *i*-Pr_2NH (30 mL) was added TMSA (2.90 mL, 20.5 mmol, 2.40 equiv.), $Pd(PPh_3)_4$ (0.59 g, 0.51 mmol, 6 mol %) and CuI (0.25 mg, 1.37 mmol, 0.16 equiv.). The solution was degassed and stirred for 48 h at room temperature. The reaction was followed by GC-MS. The solvent was evaporated under reduced pressure. The residue was purified by flash chromatography (10% EtOAc/Hexanes on silica gel) to yield 2.03 g of gray solid (Yield: 94%). **R*f*:** 0.38 (10% EtOAc/Hexanes). **Mp:** 53.2-54.7 °C. (**Litt.:** 55-56 °C).[8] **^{1}H NMR (300 MHz, $CDCl_3$)** δ **(ppm):** 8.73 (d, *J* = 1.8 Hz, 1H), 8.68 (d, *J* = 4.3 Hz, 1H), 8.38 (dd, *J* = 11.7, 8.1 Hz, 2H), 7.87 (dd, *J* = 8.3, 2.2 Hz, 1H), 7.85 – 7.77 (m, 1H), 7.32 (ddd, *J* = 7.3, 4.7, 0.9 Hz, 1H), 0.28 (s, 9H). **^{13}C NMR (75 MHz, $CDCl_3$)** δ **(ppm):** 155.4, 154.9, 152.0, 149.1, 139.8, 136.9, 123.9, 121.4, 120.0, 101.7, 99.1, -0.3. **LR-MS (EI, 70eV) (*m/z*):** 252 (M^+), 237, 221. **HR-MS (EI, 70eV): Calculated** ($C_{15}H_{16}N_2Si$): 252.1083; **Found:** 252.1088. The ^{1}H NMR spectrum corresponds to that found in the literature, but the ^{13}C NMR spectrum was found to be different.[9]

5-Ethynyl-2,2'-bipyridine (5) :

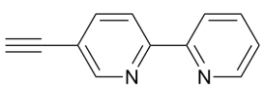

To a solution of the protected 5-trimethylsilylethynyl-2,2'-bipyridine **(8)** (0.10 g, 0.40 mmol, 1.00 equiv.) in MeOH (5 mL) was added K_2CO_3 (0.13 g, 0.91 mmol, 2.30 equiv.). The reaction was stirred for 2 h at room temperature and followed by GC-MS. The reaction was poured into a solution of H_2O/Et_2O (1:1), the layers were separated and the organic phase was washed with H_2O (twice). The combined aqueous fractions were extracted with Et_2O (three times). The organic phase were combined and dried over $MgSO_4$, the organic phase was filtered and then concentrated under reduced pressure to yield 0.07 g of light brown solid (Yield: 99 %). **Mp:** 87.6-88.5 °C. (**Litt.:** 87-89°C).[9] **R*f*:** 0.30 (10% EtOAc/Hexanes). **^{1}H NMR (300 MHz, $CDCl_3$)** δ **(ppm):** 8.78 (d, *J* = 1.4 Hz, 1H), 8.69 (d, *J* = 4.4 Hz, 1H), 8.40 (dd, *J* = 8.1, 4.3 Hz, 2H), 7.91 (dd, *J* = 8.2, 2.1 Hz, 1H), 7.83 (td, *J* = 7.9, 1.6 Hz, 1H), 7.33 (ddd, *J* = 7.4, 4.9, 0.5 Hz, 1H), 3.29 (s, 1H). **^{13}C NMR (75 MHz, $CDCl_3$)** δ **(ppm):** δ 155.4, 155.3, 152.2, 149.2, 140.0, 137.0, 124.0, 121.4, 120.2, 119.1, 81.32, 80.7. **LR-MS (EI, 70eV) (*m/z*):** 180 (M^+). **HR-MS (EI, 70eV): Calculated** ($C_{12}H_8N_2$)**:** 180.0687; **Found**: 180.0682.

Synthesis of 5' and 2':

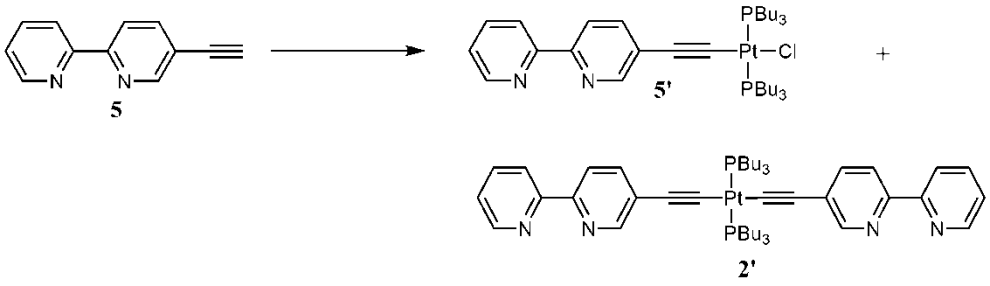

A) Procedure leading to (5') as the major product:

***trans*-(5-ethynyl-2,2'-bipyridine)-chloro-bis(tri-*n*-butylphosphine)platinum (5'):**

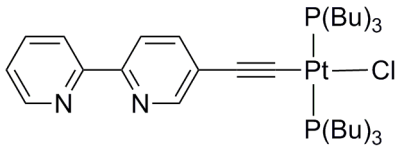

In A dry flask charged with excess *trans*-$PtCl_2(PBu_3)_2$ (0.99 g, 1.48 mmol, 8.90 equiv.), CuI (9.5 mg, 0.05 mmol, 0.30 equiv.) was added followed by DCM (50 mL) and *i*-Pr_2NH (50 mL). The

reaction mixture was purged with N_2 for 30 min, then 5-Ethynyl-2,2'-bipyridine **(5)** (30 mg, 0.17 mmol, 1.00 equiv.), dissolved in DCM (15 mL) and *i*-Pr_2NH (15 mL), was added dropwise over 2 h. The mixture was stirred at room temperature for 16 h. The solvent was removed under reduced pressure and the residue was redissolved in DCM (50 mL). The organic phase was washed with H_2O twice then dried over $MgSO_4$ and concentrated under reduced pressure. The residue was purified by flash chromatography (50% DCM/Hexanes on silica gel) to recuperate the excess *trans*-$PtCl_2(PBu_3)_2$, then (30% EtOAc/Hexanes) to yield 100 mg (Yield: 73%) of light yellow solid of **5'** and finally flushed with (20% MeOH/DCM) to yield 42 mg (Yield: 13%) of **2'**. **R*f***: 0.75 (30% EtOAc/Hexanes). **Mp** = 67.3-69.7 °C; **^{1}H NMR (400 MHz, $CDCl_3$)** δ **(ppm):** 8.65 (d, *J* = 4.7 Hz, 1H), 8.55 (d, *J* = 2.0 Hz, 1H), 8.34 (d, *J* = 8.0 Hz, 1H), 8.24 (d, *J* = 8.2 Hz, 1H), 7.79 (td, *J* = 7.7, 1.4 Hz, 1H), 7.61 (dd, *J* = 8.2, 1.9 Hz, 1H), 7.31 – 7.23 (m, 1H), 2.15 – 1.80 (m, 12H), 1.68 – 1.33 (m, 24H), 0.93 (dd, *J* = 13.1, 6.8 Hz, 18H). **^{13}C NMR (75 MHz, $CDCl_3$)** δ **(ppm):** 156.2, 151.8, 151.1, 149.2, 138.1, 136.8, 125.7, 123.2, 120.8, 120.2, 98.2, 90.5, 26.4, 24.2, 22.2, 13.8. **^{31}P NMR (162 MHz, $CDCl_3$)** δ **(ppm):** 8.45 (d, *J* = 2353.5 Hz). **LR-MS (EI, 70eV) (*m/z*):** 814 (M^+), 381, 202, 173. **HR-MS (EI, 70eV): Calculated** ($C_{36}H_{61}Cl_1N_2P_2Pt$): 812.3625; **Found**: 812.3600.

B) Procedure leading to (2') as the major product:

***trans*-bis(tri-*n*-butylphosphine)-bis(5-ethynyl-2,2'-bipyridine)platinum (2'):**

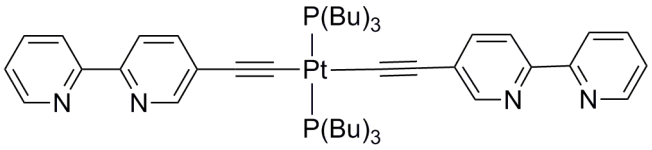

In A dry flask charged with excess *trans*-$PtCl_2(PBu_3)_2$ (0.40 g, 0.60 mmol, 4.00 equiv.), CuI (8.6 mg, 0.04 mmol, 0.3 equiv.) was added followed by DCM (30 mL) and *i*-Pr_2NH (30 mL). The reaction mixture was purged with N_2 for 30 min, then 5-Ethynyl-2,2'-bipyridine **(5)** (27 mg, 0.15 mmol, 1.00 equiv.), dissolved in DCM (10 mL) and *i*-Pr_2NH (10 mL), and added dropwise over 2 h. The mixture was stirred at room temperature for 16 h. The reaction was followed the same way as **5'**. The residue was purified by flash chromatography (50% DCM/Hexanes on silica gel) to recuperate the excess *trans*-$PtCl_2(PBu_3)_2$, then (30% EtOAc/Hexanes) to yield 8 mg (Yield: 7%) of light yellow

solid of **5'** and finally flushed with (20% MeOH/DCM) to yield 80 mg (Yield: 28%) of **2'**. **R*f*:** 0.18 (20% MeOH/DCM). **Mp:** 138.7-140.8°C. **^{1}H NMR (400 MHz, $CDCl_3$)** δ **(ppm):** 8.58 (d, *J* = 4.1 Hz, 2H), 8.51 (s, 2H), 8.27 (d, *J* = 8.0 Hz, 2H), 8.18 (d, *J* = 8.2 Hz, 2H), 7.71 (td, *J* = 7.8, 0.9 Hz, 2H), 7.57 (dd, *J* = 8.2, 2.1 Hz, 2H), 7.22 – 7.17 (m, 2H), 2.15 – 1.97 (m, 12H), 1.63 – 1.48 (m, 12H), 1.46 – 1.31 (m, 12H), 0.86 (t, *J* = 7.3 Hz, 18H). **^{13}C NMR (101 MHz, $CDCl_3$)** δ **(ppm):** 156.5, 151.9, 151.4, 149.4, 138.4, 137.0, 126.0, 123.4, 121.0, 120.4, 114.9, 106.5, 26.4, 24.7, 24.0, 13.8. **^{31}P NMR (162 MHz, $CDCl_3$)** δ **(ppm):** 4.31 (d, *J* = 2328.0 Hz). **LR-MS (EI, 70eV) (*m/z*):** 957 (M^+), 381, 173. **HR-MS (EI, 70eV): Calculated** ($C_{48}H_{68}N_4P_2Pt$): 956.4546; **Found**: 956.4539

***trans*-(5-ethynyl-2,2'-bipyridine)-4-tolylethynyl-bis(tri-*n*-butylphosphine)platinum (2):**

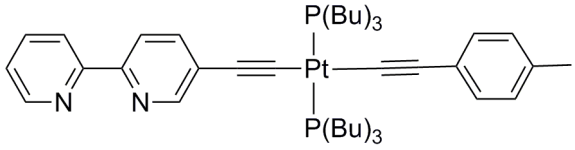

A dry flask charged with **5'** (76 mg, 0.09, 1.00 equiv.), CuI (5.3 mg, 0.03 mmol, 0.30 equiv.), DCM (40 mL) and *i*-Pr_2NH (6 mL) was purged with N_2 for 30 min. Excess 1-ethynyl-4-methylbenzene (50 mg, 0.43 mmol, 4.60 equiv.), dissolved in DCM (10 mL), was then added. The mixture was stirred at room temperature for 16 h. The solvent was removed under reduced pressure and the residue was redissolved in DCM (20 ml). The organic phase was washed with H_2O twice then dried over $MgSO_4$ and concentrated under reduced pressure. The residue was purified by flash chromatography (50% DCM/Hexane on silica gel) to yield 64 mg of yellow liquid (Yield: 78%). **R*f***: 0.84 (50% DCM/Hexanes). **^{1}H NMR (400 MHz, $CDCl_3$)** δ **(ppm):** 8.65 (d, *J* = 3.4 Hz, 1H), 8.57 (s, 1H), 8.36 – 8.31 (m, 1H), 8.23 (d, *J* = 8.4 Hz, 1H), 7.83 – 7.74 (m, 1H), 7.64 (td, *J* = 8.3, 1.8 Hz, 1H), 7.30 – 7.22 (m, 1H), 7.16 (d, *J* = 7.9 Hz, 2H), 7.01 (d, *J* = 7.9 Hz, 2H), 2.29 (s, 3H), 2.26 – 2.06 (m, 12H), 1.68 – 1.36 (m, 24H), 0.92 (t, *J* = 7.3 Hz, 18H). **^{13}C NMR (101 MHz, $CDCl_3$)** δ **(ppm):** 156.5, 151.7, 151.4, 149.4, 138.4, 137.0, 134.8, 130.8, 128.8, 126.2, 126.1, 123.3, 121.0, 120.4, 109.3, 106.1, 106.0, 105.9, 26.6, 24.7, 24.1, 21.5, 14.1. **^{31}P NMR (162 MHz, $CDCl_3$)** δ **(ppm):** 4.17 (d, *J* = 2349.4 Hz). **LR-MS (EI, 70eV) (*m/z*):** 893 (M^+); 381, 317. **HR-MS (EI, 70eV): Calculated** ($C_{45}H_{68}N_2P_2Pt$): 892.4484. **Found**: 892.4470.

[Ir(ppy)$_2$(5-ethynyl-2,2'-bipyridine)] Hexafluorophosphate (1):[10]

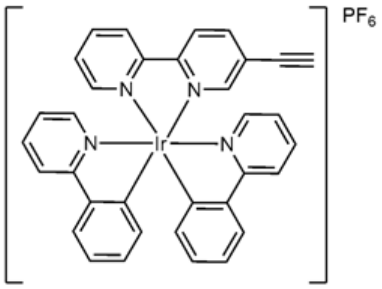

The dimeric complex $[(ppy)_2Ir\text{-}\mu\text{-}Cl]_2$ (86 mg, 0.08 mmol, 0.45 equiv.) was dissolved in DCM (6 mL) and methanol (6 mL) and 5-ethynyl-2,2'-bipyridine **(5)** (32 mg, 0.18 mmol, 1.00 equiv.) was added. The mixture was heated to 60 °C over 18 h. The color of the solution turned from orange to red. The solution was cooled to RT and extracted with water (3 x 50 mL), then washed with ether (3 x 50 mL) to remove unreacted bipyridine (**5**). To the aqueous solution was slowly added a solution of NH_4PF_6 (10 mL, 10 % w/w in H_2O) under gentle stirring. The first drop caused the precipitation of an orange solid. The suspension was conserved for 2 h at 0 °C, filtered and the resulting solid was washed with cold water. The residue was purified by flash chromatography (10% MeOH/DCM on silica gel) to yield 110 mg of a red solid (Yield: 76%). **R*f*:** 0.53 (10% MeOH/DCM). **Mp:** >350 ^{o}C. **^{1}H NMR (300 MHz, $CDCl_3$)** δ **(ppm):** 8.68 (d, *J* = 6.5 Hz, 2H), 8.17 (dd, *J* = 13.1, 4.8 Hz, 2H), 7.98 – 7.86 (m, 4H), 7.78 (t, *J* = 7.6 Hz, 2H), 7.69 (dd, *J* = 7.7, 4.0 Hz, 2H), 7.50 (t, *J* = 6.9 Hz, 2H), 7.42 (t, *J* = 6.9, 1H), 7.05 (t, *J* = 6.9 Hz, 4H), 6.98 – 6.86 (m, 2H), 6.27 (t, *J* = 6.6 Hz, 2H), 3.35 (s, 1H). **^{13}C NMR (75 MHz, $CDCl_3$):** δ **(ppm):** 168.0, 167.8, 155.4, 155.2, 152.8, 150.5, 149.8, 149.7, 148.9, 143.6, 143.5, 140.2, 138.5, 138.4, 131.9, 131.8, 131.2, 131.1, 128.5, 126.3, 125.2, 125.1, 125.0, 123.9, 123.7, 123.7, 123.1, 123.0, 120.0, 119.9, 85.6, 78.3. **LR-MS (EI, 70eV) (*m/z*):** 681 (M^+); 381, 317, 75.**HR-MS (EI, 70eV): Calculated** ($C_{34}H_{24}IrN_4$)**:** 681.1630. **Found:** 681.1649. The ^{1}H and ^{13}C NMR spectra each correspond to that found in the literature.[10] The structure was resolved by single crystal X-ray diffractometry and has been deposited into the CCDB.

***trans*-[Ir(ppy)$_2$(5-Ethynyl-2,2'-bipyridine)]-4-tolylethynyl-bis(tri-*n*-butylphosphine)platinum Hexafluorophosphate (3):**

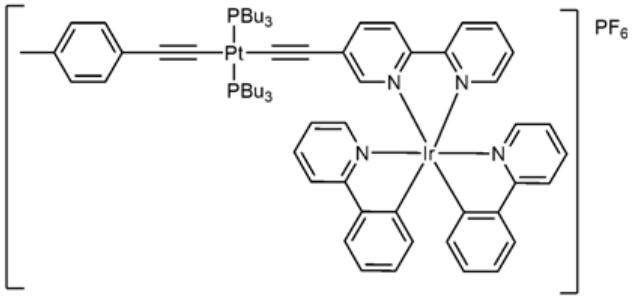

The dimeric complex $[(ppy)_2Ir\text{-}\mu\text{-}Cl]_2$ (15.20 mg, 0.01 mmol, 0.45 equiv.) was dissolved in DCM (5 mL) and methanol (5 mL), and **2** (28 mg, 0.03 mmol, 1.00 equiv.) was added and the mixture was heated to 60 °C over 18 h. The color of the solution turned from orange to red. The solution was cooled to RT and washed with water (3 x 50 mL) then extracted with ether (3x)**.** The organic solution was evaporated to obtain the chloride complex as a red solid. This complex was dissolved in a minimum amount of methanol and a solution of NH_4PF_6 (3 mL, 10% w/w in H_2O) was slowly added under stirring. The resulting suspension was re-cooled to 0 °C for 2 h, filtered, washed with cold water and the solid was dried under vacuum. The residue was purified by flash chromatography (10% MeOH/DCM on silica gel) to yield 40 mg of red solid (Yield: 87%). **R*f***: 0.47 (10% MeOH/DCM). **Mp:** >350 °C. **^{1}H NMR (300 MHz, $CDCl_3$)** δ **(ppm)**: 8.61 (d, *J* = 8.1 Hz, 1H), 8.45 (d, *J* = 8.5 Hz, 1H), 8.13 (t, *J* = 7.8 Hz, 1H), 7.99 – 7.82 (m, 3H), 7.77 (t, *J* = 8.1 Hz, 4H), 7.65 (dd, *J* = 16.7, 7.7 Hz, 3H), 7.52 (t, *J* = 4.8 Hz, 2H), 7.32 (dd, *J* = 12.5, 6.3 Hz, 2H), 7.14 (d, *J* = 7.8 Hz, 2H), 7.10 – 6.96 (m, 4H), 6.95 – 6.83 (m, 2H), 6.27 (d, *J* = 7.4 Hz, 2H), 2.29 (s, 3H), 2.11 – 1.81 (m, 12H), 1.72 – 1.26 (m, 24H), 0.87 (t, *J* = 7.0 Hz, 18H). **^{13}C NMR (101 MHz, $CDCl_3$)** δ **(ppm):** 169.0, 168.8, 153.2, 153.1, 151.9, 151.7, 151.6, 151.0, 149.9, 149.5, 144.6, 144.5, 141.3, 141.0, 140.5, 140.3, 139.1, 139.0, 136.1, 132.8, 132.8, 132.0, 131.7, 131.4, 131.2, 129.8, 128.2, 127.5, 127.3, 126.0, 125.9, 125.7, 124.5, 124.2, 123.7, 123.4, 120.7, 120.5, 27.4, 25.4, 25.0, 22.4, 14.8. **^{31}P NMR (162 MHz, $CDCl_3$)** δ **(ppm):** 5.28 (d, *J* = 2318.2 Hz). **LR-MS (EI, 70eV) (*m/z*):** 1394 (M^+); **Calculated** ($C_{67}H_{84}IrN_4P_2Pt$): 1394.5458. **Found:** 1394.5421.

***trans*-bis[Ir(ppy)$_2$(5-Ethynyl-2,2'-bipyridine)]-bis(tri-*n*-butylphosphine)platinum Hexafluorophosphate (4):**

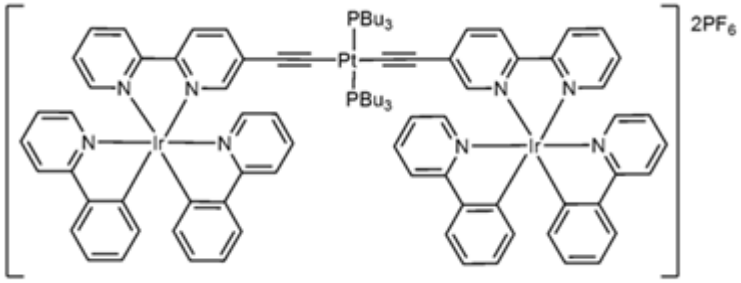

The dimeric complex $[(ppy)_2Ir\text{-}\mu\text{-}Cl]_2$ (0.06 g, 0.05 mmol, 1.50 equiv.) was dissolved in DCM (6 mL) and methanol (6 mL) and Pt complex **2'** (35 mg, 0.04 mmol, 1 equiv.) was added as a solid. The mixture was heated to 60 °C over 18 h. The reaction was followed the same way as described for **1** to yield 33 mg of a red solid (Yield: 40%). **R*f***: 0.52 (10% MeOH/DCM). **Mp**: >350 °C. **^{1}H NMR (300 MHz, $CDCl_3$)** δ **(ppm)**: 8.46 (t, *J* = 9.1 Hz, 4H), 8.00 (t, *J* = 8.1 Hz, 4H), 7.95 – 7.88 (m, 4H), 7.87 – 7.71 (m, 8H), 7.64 (d, *J* = 7.5 Hz, 4H), 7.60 – 7.52 (m, 2H), 7.46 (dd, *J* = 9.8, 5.6 Hz, 4H), 7.29 (d, *J* = 6.4 Hz, 4H), 6.99 (dt, *J* = 14.5, 6.8 Hz, 2H), 6.91 – 6.80 (m, 4H), 6.77 (d, *J* = 7.6 Hz, 2H), 6.23 (dd, *J* = 11.6, 7.6 Hz, 4H), 1.91 – 1.66 (m, 12), 1.48 – 1.22 (m, 24), 0.86 (t, *J* = 6.7 Hz, 18H). **^{13}C NMR (75 MHz, $CDCl_3$)** δ **(ppm):** 167.9, 167.7, 155.8, 151.9, 151.0, 150.6, 150.3, 150.0, 148.7, 148.3, 143.5, 143.4, 140.3, 139.7, 138.1, 138.0, 131.6, 130.8, 130.6, 130.1, 130.0, 127.3, 126.3, 126.2, 124.8, 124.6, 123.4, 123.1, 122.6, 122.4, 119.7, 119.5, 110.1, 105.2, 26.2, 24.3, 23.8, 13.8. **^{31}P NMR (162 MHz, $CDCl_3$)** δ **(ppm):** 4.38 (d, *J* = 2326.3 Hz). **LR-MS (EI, 70eV) (*m/z*):** 979 (M^{2+}); 501, 360, 249. **HR-MS (EI, 70eV): Calculated** ($C_{92}H_{100}Ir_2N_8P_2Pt$)**:** 979.3216 ($M^{2+}$); Found: 979.3270 ($M^{2+}$).

Photophysical characterization: All samples were prepared in 2-methyltetrahydrofuran (2-MeTHF), which was distilled over CaH_2 under nitrogen or HPLC grade acetonitrile (ACN) for the external reference. Absorption spectra were recorded at room temperature and at 77 K in a 1.0 cm capped quartz cuvette and an NMR tube inserted into a liquid nitrogen filled quartz dewar, respectively, using a Shimadzu UV-1800 double beam spectrophotometer. Molar absorptivity determination was verified by linear least squares fit of values obtained from at least three independent solutions at varying concentrations with absorbances ranging from 0.01-2.6. Steady-state emission spectra were obtained by exciting at the lowest energy absorption maxima using a Horiba Jobin Yvon Fluorolog-3 spectrofluorometer equipped with double monochromators and a photomultiplier tube detector (Hamamatsu model R955). Emission quantum yields were determined

using the optically dilute method.[11 12] A stock solution with absorbance of ca. 0.5 was prepared and then four dilutions were prepared with dilution factors of 40, 20, 13.3 and 10 to obtain solutions with absorbances of ca. 0.013, 0.025, 0.038 and 0.05, respectively. The Beer-Lambert law was found to be linear at the concentrations of the solutions. The emission spectra were then measured after the solutions were rigorously degassed with solvent-saturated nitrogen gas (N_2) for 20 minutes prior to spectrum acquisition using septa-sealed quartz cells from Starna. For each sample, linearity between absorption and emission intensity was verified through linear regression analysis and additional measurements were acquired until the Pearson regression factor (R^2) for the linear fit of the data set surpassed 0.9. Individual relative quantum yield values were calculated for each solution and the values reported represent the slope value. The equation $\Phi_s = \Phi_r(A_r/A_s)(I_s/I_r)(n_s/n_r)^2$ was used to calculate the relative quantum yield of each of the sample, where Φ_r is the absolute quantum yield of the reference, n is the refractive index of the solvent, A is the absorbance at the excitation wavelength, and I is the integrated area under the corrected emission curve. The subscripts s and r refer to the sample and reference, respectively. A solution of $[Ru(bpy)_3](PF_6)_2$ in ACN (Φ_r = 0.095 %) was used as the external reference.[13] The experimental uncertainty in the emission quantum yields is conservatively estimated to be 10%, though we have found that statistically we can reproduce PLQYs to 3% relative error. The emission lifetimes were measured on a TimeMaster model TM-3/2003 apparatus from PTI. The source was a nitrogen laser with high-resolution dye laser (fwhm ~1400 ps), and the excited state lifetimes were obtained from deconvolution or distribution lifetimes analysis.

Computational Methodology. Calculations were performed with Gaussian 09[14] at the Université de Sherbrooke with Mammouth super computer supported by Calcul Québec. The DFT[15] and TDDFT[16] were calculated with the B3LYP[17] method. The 3-21G*[18] basis set was used for C, H and N, and VDZ (valence double ζ) with SBKJC effective core potentials[18a, 19] for iridium and platinum. The predicted phosphorescence wavelengths were obtained by energy differences between the Triplet and Singlet optimized states.[20] The calculated absorption spectra and related MO contributions were obtained from the TD-DFT/Singlets output file and gausssum 2.1.[21] A THF quantum mechanical continuum solvation model was employed.[22]

Figure S1: Absorptivities of **1** (blue), **2** (red), **3** (mauve), **4** (green)**:**

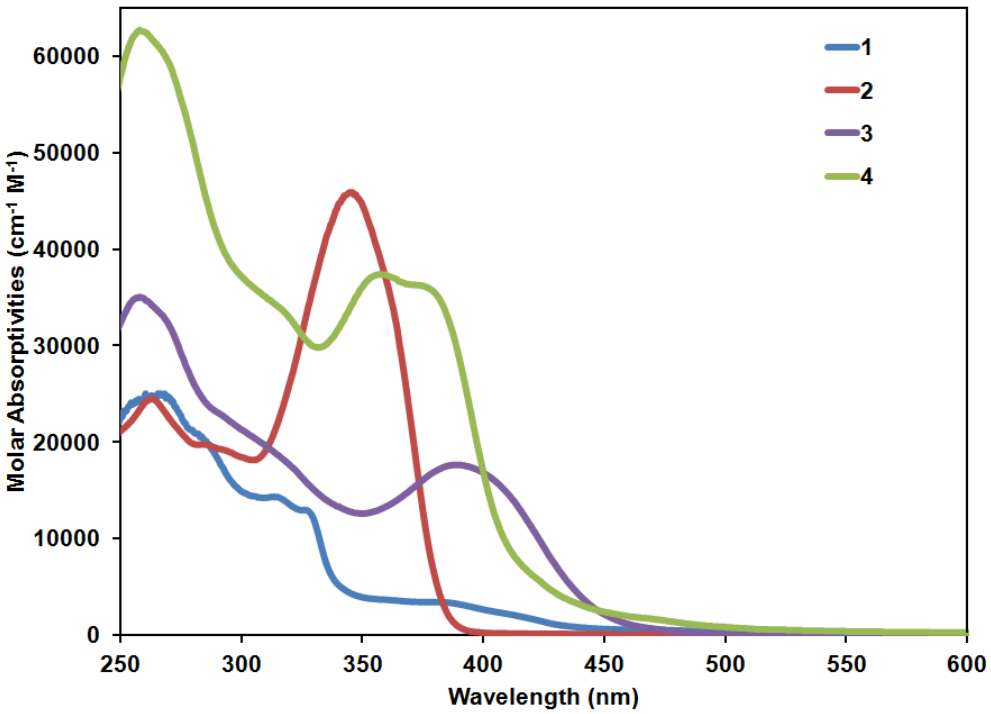

Figure S2: Absorption (green) and emission spectra at 298 K (red) and 77 K (blue) for **1**:

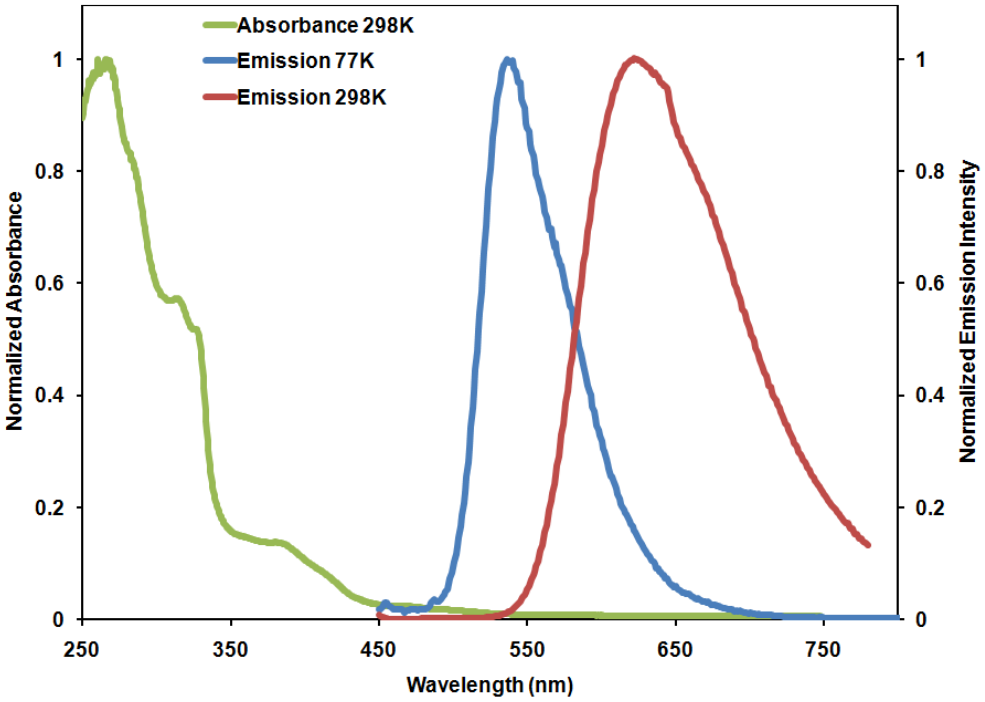

Figure S3: Absorption (green) and emission spectra at 298 K (red) and 77 K (blue) for **2**:

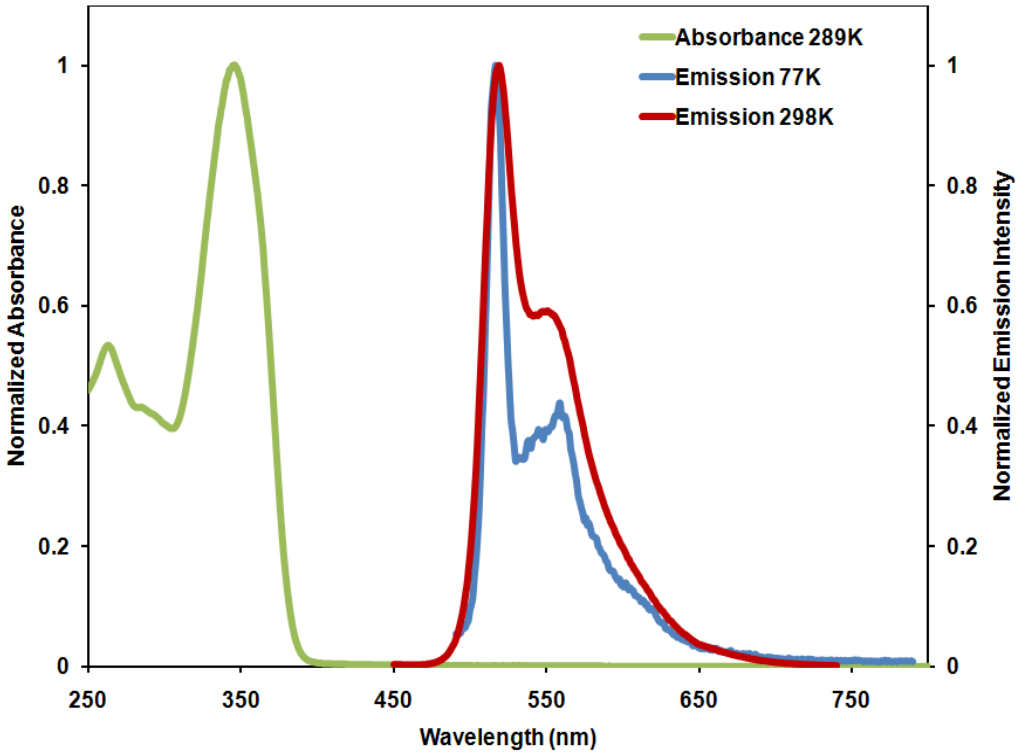

Figure S4: Absorption (green) and emission spectra at 298 K (red) and 77 K (blue) for **3**:

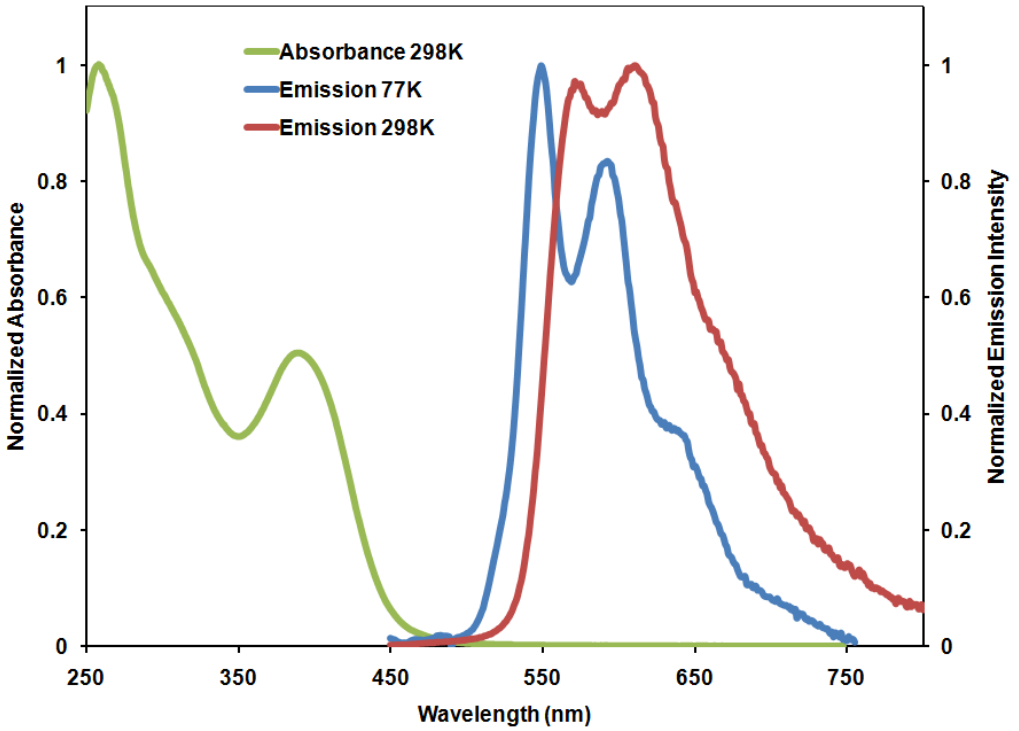

Figure S5: Absorption (green) and emission spectra at 298 K (red) and 77 K (blue) for **4**:

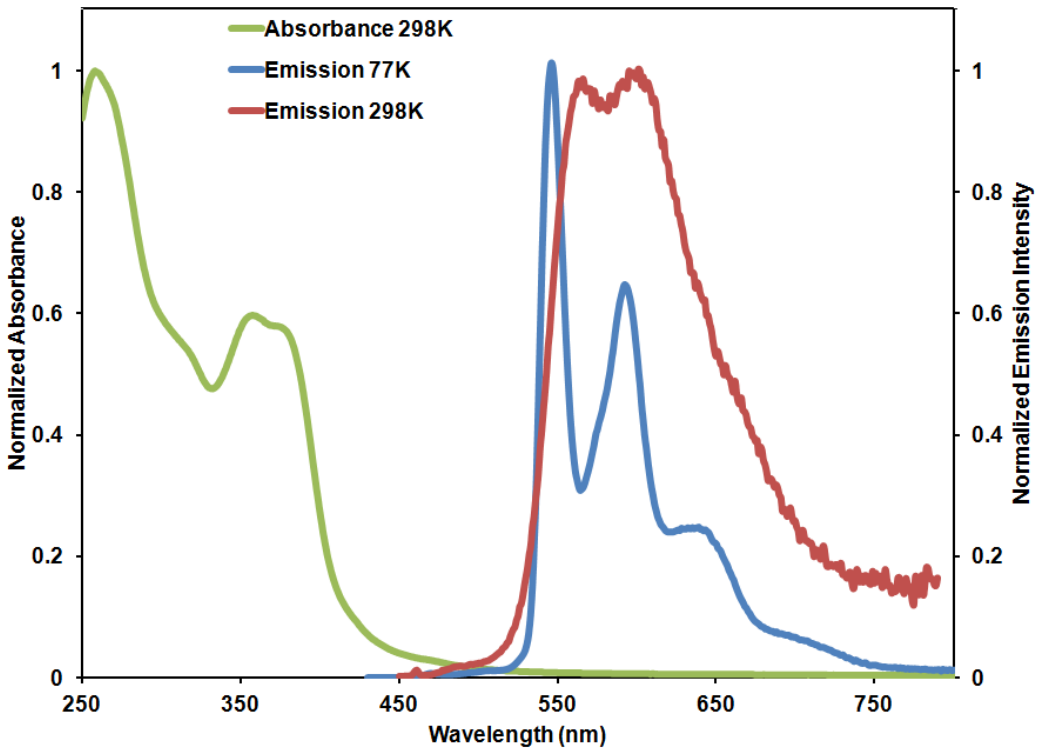

Figure S6: Calculated and experimental absorption spectra for **1**:

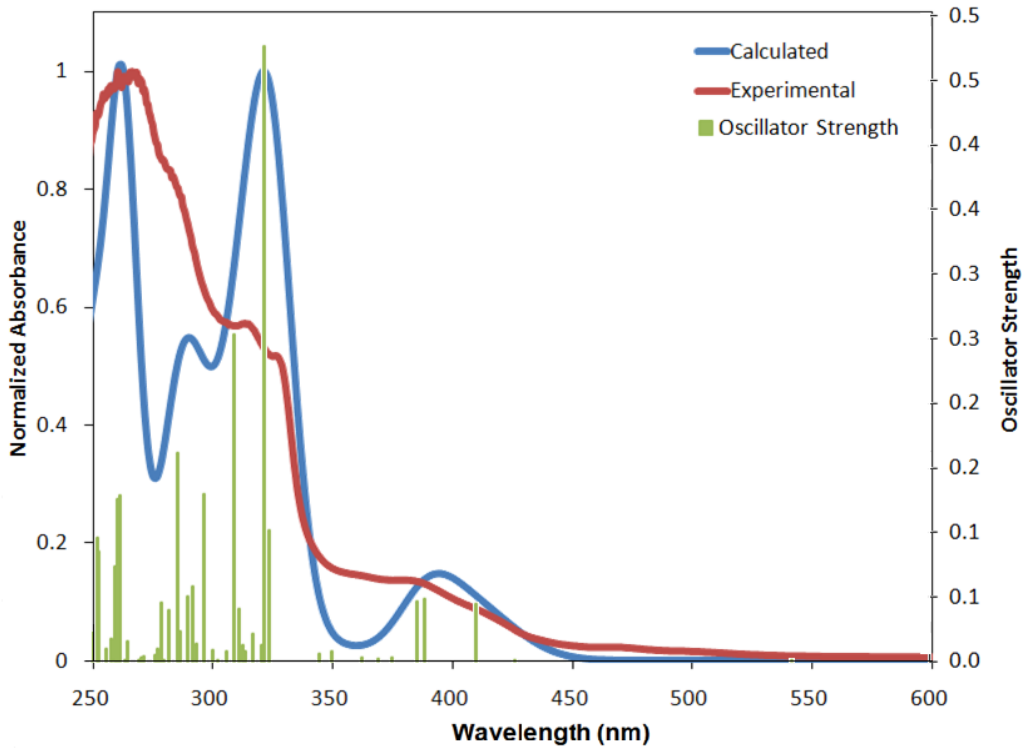

Figure S7: Calculated and experimental absorption spectra for **2**:

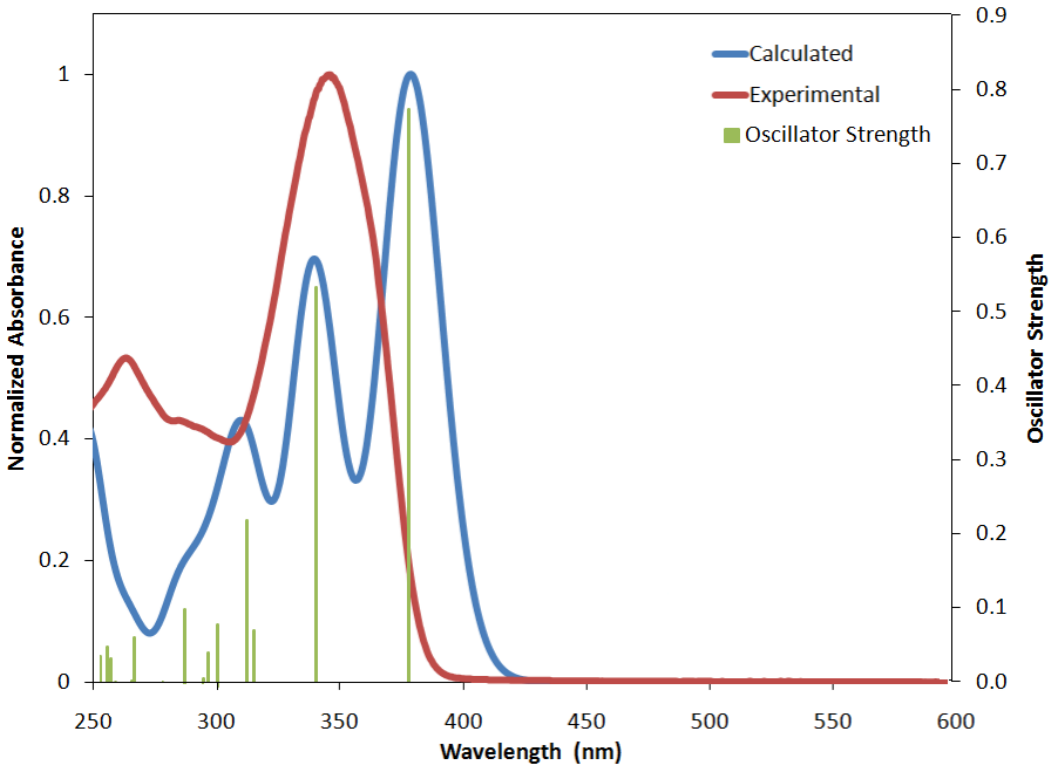

Figure S8: Calculated and experimental absorption spectra for **3**:

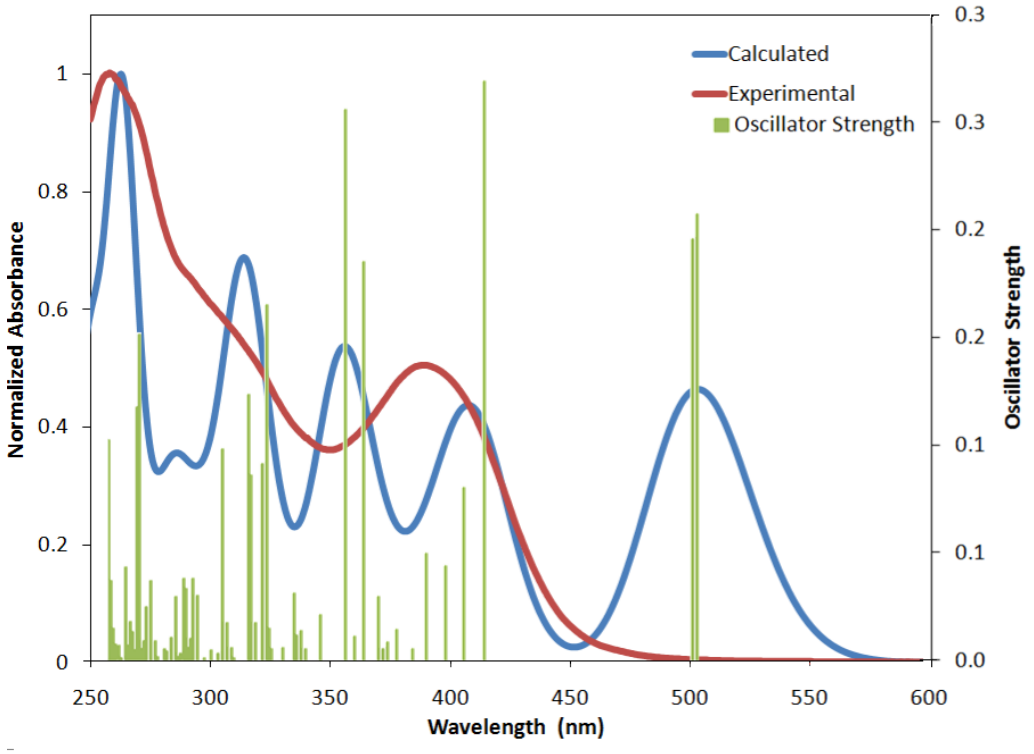

Figure S9: Calculated and experimental absorption spectra for **4**:

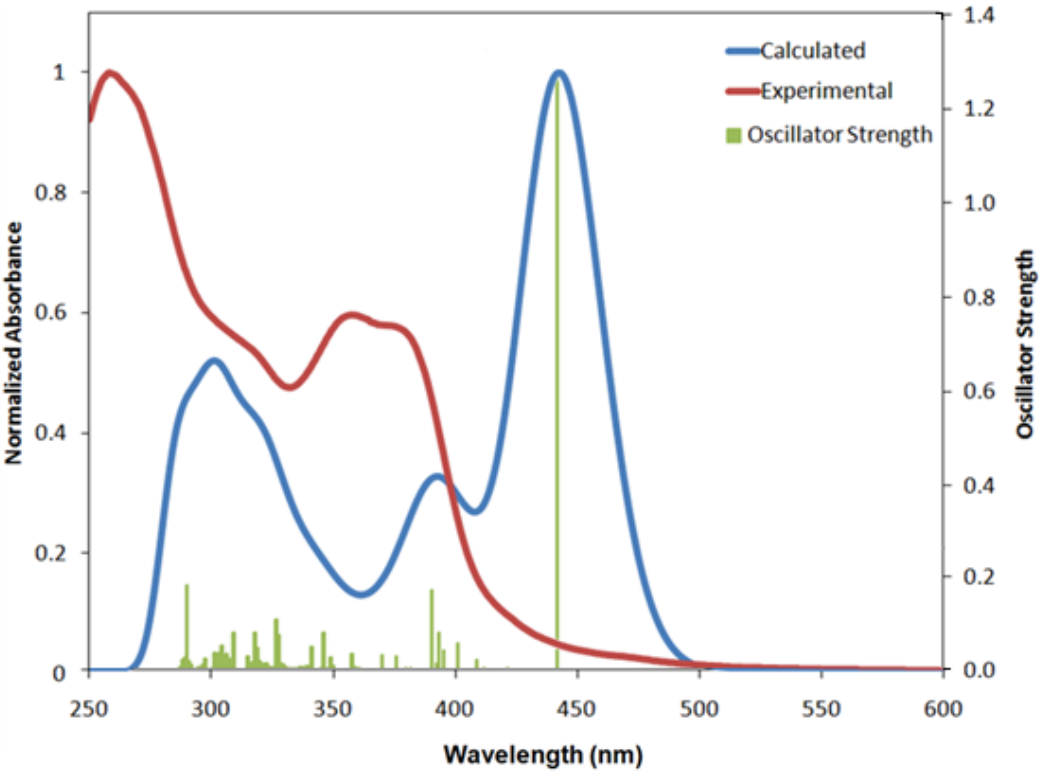

Table S1: Visualization of MOs of **1:**

Orbital Energy (eV)	Image	Orbital Energy (eV)	Image	Orbital Energy (eV)	Image
HOMO -5.97	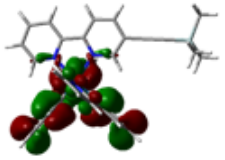	LUMO -3.04	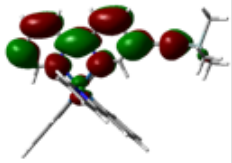	HSOMO -3.90	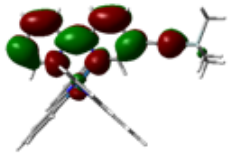
HOMO -1 -6.59	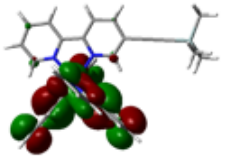	LUMO+1 -2.05	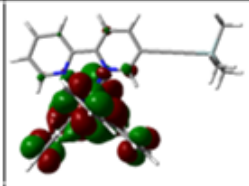		
HOMO -2 -6.67	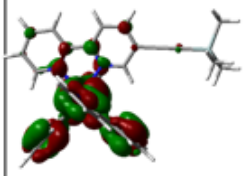				

Table S2: Visualization of MOs of **2:**

Orbital Energy (eV)	Image	Orbital Energy (eV)	Image	Orbital Energy (eV)	Image
HOMO -5.27	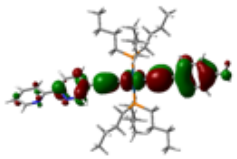	LUMO -1.56	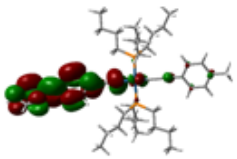	HSOMO -3.18	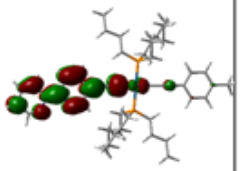
HOMO -1 -5.79	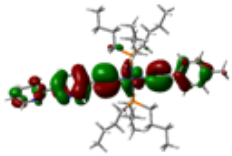	LUMO+1 -0.77	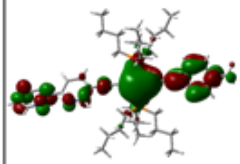		
HOMO -2 -6.20	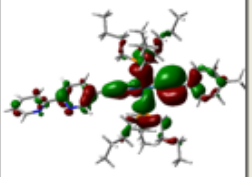				

Table S3: Visualization of MOs of **3:**

Orbital Energy (eV)	Image	Orbital Energy (eV)	Image	Orbital Energy (eV)	Image
HOMO -5.58	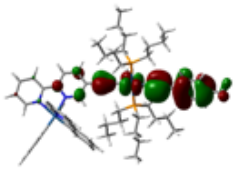	LUMO -2.78	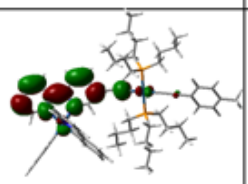	HSOMO -3.87	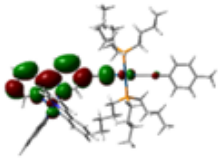
HOMO -1 -5.93	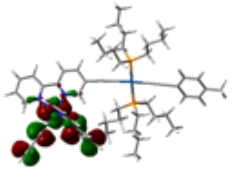	LUMO+1 -2.02	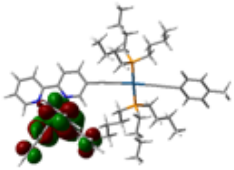		
HOMO -2 -6.25	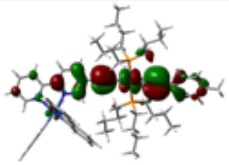				

Table S4: Visualization of MOs of **4:**

Orbital Energy (eV)	Image	Orbital Energy (eV)	Image	Orbital Energy (eV)	Image
HOMO -8.60	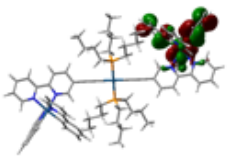	LUMO -5.81	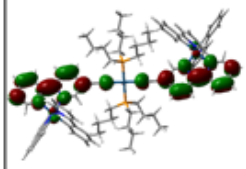	HSOMO -6.82	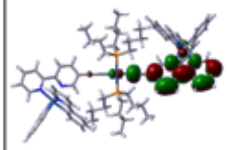
HOMO -1 -8.61	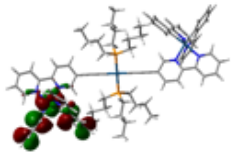	LUMO+1 -5.66	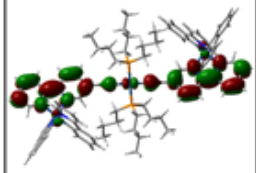		
HOMO -2 -8.96	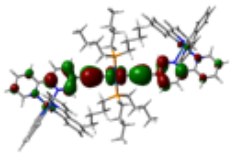				

Table S5: Energy and composition of TD-DFT calculated transitions of **1:**

No.	Energy (cm^{-1})	Wavelength (nm)	Oscillator Strength	Symmetry	Major contributions
1	18155.6656	550.7922552	0.0002	Singlet-A	HOMO->LUMO (98%)
2	23140.2064	432.1482629	0.0012	Singlet-A	H-2->LUMO (94%)
3	24080.65536	415.27109	0.0451	Singlet-A	H-1->LUMO (92%)
4	25446.968	392.9741256	0.0489	Singlet-A	HOMO->L+1 (96%)
5	25633.28336	390.1177957	0.0468	Singlet-A	H-3->LUMO (87%)
6	26384.99728	379.0032606	0.0033	Singlet-A	HOMO->L+2 (-12%), HOMO->L+3 (83%)
7	26810.0544	372.9943942	0.002	Singlet-A	HOMO->L+2 (82%), HOMO->L+3 (12%)
8	27318.1872	366.0565003	0.0028	Singlet-A	H-4->LUMO (91%)
9	28289.28544	353.4907243	0.0085	Singlet-A	H-5->LUMO (96%)
10	28725.6344	348.1211193	0.0064	Singlet-A	HOMO->L+4 (98%)
11	30646.86032	326.2976989	0.1022	Singlet-A	H-2->L+1 (73%)
12	30847.69376	324.1733427	0.4761	Singlet-A	H-6->LUMO (77%), H-2->L+2 (13%)
13	30988.0352	322.7051969	0.013	Singlet-A	H-3->L+1 (16%), H-2->L+3 (14%), H-1->L+1 (61%)
14	31387.2824	318.6003768	0.0214	Singlet-A	HOMO->L+5 (93%)
15	31646.99472	315.9857702	0.0083	Singlet-A	H-2->L+3 (-23%), HOMO->L+6 (59%)
16	31741.36224	315.04634	0.0131	Singlet-A	H-2->L+1 (-13%), H-2->L+2 (-11%), H-1->L+3 (47%)
17	31969.61872	312.7969741	0.0405	Singlet-A	H-2->L+3 (32%), H-1->L+1 (-18%), HOMO->L+6 (22%)
18	32133.3504	311.2031542	0.2533	Singlet-A	H-2->L+2 (61%), H-1->L+3 (16%)
19	32482.59088	307.8572161	0.008	Singlet-A	H-1->L+2 (68%)
20	32914.90704	303.8137093	0.0012	Singlet-A	H-7->LUMO (94%)
21	33127.83888	301.8609224	0.0092	Singlet-A	H-3->L+1 (58%), H-2->L+3 (-10%)
22	33502.08272	298.4889054	0.1298	Singlet-A	H-3->L+3 (68%), H-1->L+3 (-14%)
23	33936.81856	294.6652168	0.0134	Singlet-A	H-3->L+2 (31%), H-2->L+4 (49%)
24	34156.20288	292.7725905	0.0587	Singlet-A	H-3->L+4 (13%), H-1->L+4 (71%)
25	34328.00016	291.3073862	0.0501	Singlet-A	H-3->L+2 (40%), H-2->L+4 (-30%)
26	34745.79824	287.8045838	0.0239	Singlet-A	H-8->LUMO (83%)
27	34883.72	286.6666743	0.1616	Singlet-A	H-4->L+1 (67%)
28	35287.80656	283.3840064	0.0396	Singlet-A	H-5->L+1 (36%), H-4->L+3 (-25%), H-1->L+5 (14%)
29	35527.35488	281.4732488	0.0008	Singlet-A	H-5->L+1 (43%), H-4->L+3 (40%)
30	35705.60464	280.0680762	0.0458	Singlet-A	H-4->L+2 (48%), H-3->L+4 (-16%)
31	35815.2968	279.2103066	0.004	Singlet-A	H-4->L+2 (14%), HOMO->L+7 (64%)
32	35893.53312	278.6017182	0.0123	Singlet-A	H-3->L+4 (49%), H-1->L+4 (-14%), HOMO->L+7 (-21%)
33	35941.92672	278.2265981	0.0099	Singlet-A	H-5->L+3 (50%), H-2->L+5 (-12%)
34	36066.13696	277.2683975	0.0056	Singlet-A	H-9->LUMO (91%)
35	36697.67344	272.4968387	0.0045	Singlet-A	H-5->L+2 (73%)
36	36784.78192	271.8515505	0.0064	Singlet-A	H-2->L+5 (57%), H-1->L+6 (23%)

37	36891.24784	271.0670033	0.0035	Singlet-A	H-2->L+6 (57%), H-1->L+5 (28%)
38	37096.92064	269.5641532	0.0001	Singlet-A	H-10->LUMO (92%)
39	37766.36544	264.7858719	0.0154	Singlet-A	H-11->LUMO (-16%), H-6->L+2 (48%), H-4->L+4 (12%)
40	37867.18544	264.0808891	0.0014	Singlet-A	H-4->L+4 (74%)
41	37931.71024	263.6316669	0.3458	Singlet-A	H-6->L+1 (19%), H-5->L+3 (-11%), H-1->L+6 (32%)
42	38111.57312	262.3874897	0.1284	Singlet-A	H-4->L+3 (10%), H-2->L+6 (-18%), H-1->L+5 (39%)
43	38322.08528	260.946134	0.126	Singlet-A	H-6->L+1 (64%)
44	38519.69248	259.6074723	0.0734	Singlet-A	H-3->L+5 (65%)
45	38725.36528	258.2286811	0.0181	Singlet-A	H-5->L+4 (80%)
46	38822.95904	257.5795418	0.0073	Singlet-A	H-3->L+6 (76%), H-1->L+6 (-13%)
47	39102.0288	255.7412059	0.0102	Singlet-A	H-6->L+3 (86%)
48	39573.05984	252.6971642	0.0855	Singlet-A	H-11->LUMO (-23%), HOMO->L+11 (32%)
49	39616.61408	25242%	0.0955	Singlet-A	H-11->LUMO (38%), H-6->L+2 (10%), HOMO->L+11 (20%)
50	39998.11696	250.0117696	0.0221	Singlet-A	H-6->L+4 (67%)
51	40122.3272	249.237786	0.0664	Singlet-A	H-4->L+5 (19%), HOMO->L+8 (50%), HOMO->L+14 (12%)
52	40438.49872	24729%	0.0079	Singlet-A	H-12->LUMO (95%)
53	40561.9024	246.5367601	0.1197	Singlet-A	H-4->L+5 (72%), HOMO->L+8 (-10%)
54	40803.06384	245.0796352	0.0035	Singlet-A	H-4->L+6 (91%)
55	40965.98896	244.1049332	0.0015	Singlet-A	H-13->LUMO (88%)
56	41116.81568	243.2094955	0.0103	Singlet-A	H-5->L+5 (-18%), H-1->L+7 (58%)
57	41149.07808	243.0188103	0.011	Singlet-A	H-5->L+5 (65%), H-1->L+7 (12%)
58	41193.43888	242.7571058	0.0156	Singlet-A	H-8->L+1 (-10%), H-7->L+1 (-12%), H-2->L+7 (38%)
59	41269.25552	242.3111315	0.0023	Singlet-A	H-8->L+1 (21%), H-7->L+1 (32%), H-2->L+7 (15%)
60	41427.34128	241.3864779	0.0015	Singlet-A	H-7->L+2 (67%)
61	41467.66928	241.1517255	0.0312	Singlet-A	H-5->L+6 (79%)
62	41659.63056	240.0405348	0.0004	Singlet-A	H-9->L+1 (-19%), H-8->L+3 (17%), H-7->L+3 (23%)
63	41798.35888	239.2438428	0.0329	Singlet-A	H-2->L+11 (38%)
64	41846.75248	238.9671697	0.0124	Singlet-A	H-3->L+11 (21%), H-1->L+11 (12%)
65	42712.99792	234.1207709	0.0014	Singlet-A	H-15->LUMO (-34%), H-3->L+7 (39%)
66	42771.8768	233.7984851	0.0016	Singlet-A	H-15->LUMO (56%), H-3->L+7 (21%)
67	42773.48992	233.7896678	0.0206	Singlet-A	H-14->LUMO (52%), H-3->L+7 (20%)
68	43027.55632	232.4092013	0.0093	Singlet-A	H-9->L+1 (24%), H-8->L+1 (-15%), H-7->L+3 (25%)
69	43307.43264	23091%	0.0037	Singlet-A	H-8->L+2 (67%), H-7->L+4 (-12%)
70	43380.02304	230.520855	0.0935	Singlet-A	H-9->L+3 (-19%), H-8->L+3 (18%), HOMO->L+9 (20%)
71	43495.36112	229.9095752	0.0107	Singlet-A	H-6->L+5 (82%)
72	43600.21392	229.3566728	0.0329	Singlet-A	H-9->L+3 (22%), H-8->L+3 (-15%), HOMO->L+9 (18%), HOMO->L+11 (10%)
73	43916.38544	227.705443	0.0179	Singlet-A	H-16->LUMO (55%)
74	43995.42832	227.2963438	0.0051	Singlet-A	H-6->L+6 (84%)
75	44185.77648	226.3171726	0.0166	Singlet-A	H-17->LUMO (76%)
76	44212.39296	226.1809264	0.0227	Singlet-A	H-10->L+1 (60%)

77	44369.67216	225.3791726	0.0047	Singlet-A	H-8->L+2 (10%), H-8->L+4 (28%), H-7->L+4 (38%)
78	44432.58384	225.0600603	0.0613	Singlet-A	H-10->L+1 (-10%), HOMO->L+8 (10%), HOMO->L+10 (23%), HOMO->L+13 (17%), HOMO->L+14 (-19%)
79	44576.15152	224.335203	0.0073	Singlet-A	H-4->L+7 (88%)
80	44673.74528	223.8451228	0.0045	Singlet-A	H-9->L+2 (79%)
81	44918.13296	22263%	0.0008	Singlet-A	H-10->L+3 (61%)
82	45135.0976	221.5570705	0.0096	Singlet-A	H-2->L+8 (52%)
83	45211.7208	221.1815835	0.001	Singlet-A	H-10->L+1 (11%), H-9->L+1 (28%), H-8->L+1 (20%), H-7->L+1 (-24%)
84	45377.0656	220.3756428	0.0024	Singlet-A	H-5->L+7 (12%), HOMO->L+10 (40%), HOMO->L+13 (-13%)
85	45405.2952	22024%	0.0044	Singlet-A	H-5->L+7 (71%)
86	45707.7552	218.781254	0.0043	Singlet-A	H-10->L+2 (47%)
87	45773.89312	21847%	0.0026	Singlet-A	H-10->L+2 (-11%), H-1->L+8 (33%), HOMO->L+12 (-12%)
88	45981.17904	217.4802867	0.001	Singlet-A	H-10->L+2 (-11%), H-9->L+4 (-28%), H-8->L+4 (30%)
89	46031.99232	217.240217	0.0012	Singlet-A	H-10->L+3 (-14%), H-9->L+3 (-24%), H-8->L+3 (-18%), H-7->L+3 (24%)
90	46315.90144	21591%	0.0007	Singlet-A	H-18->LUMO (36%), H-11->L+2 (33%), H-6->L+7 (-19%)
91	46496.57088	215.0696236	0.0014	Singlet-A	H-19->LUMO (-25%), H-3->L+8 (19%), HOMO->L+12 (32%)
92	46583.67936	214.6674573	0.0016	Singlet-A	H-19->LUMO (58%), H-6->L+7 (13%)
93	46689.33872	214.1816585	0.0017	Singlet-A	H-20->LUMO (-22%), H-19->LUMO (-12%), H-6->L+7 (30%)
94	47035.35296	21261%	0.0028	Singlet-A	H-1->L+9 (-19%), HOMO->L+13 (17%), HOMO->L+14 (26%)
95	47045.83824	212.5586529	0.0095	Singlet-A	H-11->L+1 (61%)
96	47131.3336	212.1730755	0.0016	Singlet-A	H-2->L+9 (46%), H-2->L+10 (-11%)
97	47166.01568	212.0170605	0.0333	Singlet-A	H-20->LUMO (24%), H-11->L+1 (-18%), H-11->L+2 (18%), H-11->L+4 (13%)
98	47195.8584	211.8829986	0.0006	Singlet-A	H-10->L+4 (-22%), H-9->L+4 (25%), H-7->L+5 (-16%)
99	47260.3832	21159%	0.0018	Singlet-A	H-9->L+4 (11%), H-8->L+5 (19%), H-7->L+5 (38%)
100	47489.44624	210.5731019	0.0085	Singlet-A	H-12->L+1 (30%), H-8->L+6 (16%), H-7->L+6 (26%)

Table S6: Energy and composition of TD-DFT calculated transitions of **2:**

No.	Energy (cm^{-1})	Wavelength (nm)	Oscillator Strength	Symmetry	Major contributions
1	28194.11136	354.6839931	1.4361	Singlet-A	HOMO->LUMO (85%)
2	28408.65632	352.0053848	0.0759	Singlet-A	HOMO->L+1 (84%)
3	28867.58896	346.4092555	0.2333	Singlet-A	H-2->LUMO (23%), H-1->LUMO (62%)
4	30937.22192	323.2352286	0.6913	Singlet-A	H-1->L+1 (92%)
5	31097.72736	321.5669069	0.0002	Singlet-A	H-2->LUMO (49%), H-1->LUMO (-27%)
6	32207.55392	310.4861681	0.0009	Singlet-A	H-6->L+1 (11%), H-5->L+1 (16%), H-4->L+1 (55%)
7	33058.47472	302.4942949	0.0073	Singlet-A	H-6->LUMO (-16%), H-5->LUMO (55%), H-2->LUMO (-12%)
8	34275.57376	291.7529571	0.012	Singlet-A	H-3->LUMO (95%)
9	34350.58384	291.1158671	0.0069	Singlet-A	H-8->L+1 (20%), H-6->L+1 (-27%), H-5->L+1 (-10%), H-2->L+1 (34%)
10	35020.8352	285.5443036	0.004	Singlet-A	H-9->LUMO (-10%), H-7->LUMO (35%), HOMO->L+2 (-19%)
11	35136.17328	284.6069753	0.0555	Singlet-A	H-8->L+1 (-11%), H-7->LUMO (-12%), H-2->L+1 (23%), HOMO->L+2 (-18%)
12	35361.20352	282.7958046	0.0031	Singlet-A	H-2->L+1 (24%), HOMO->L+2 (42%)
13	35470.08912	281.9276818	0.0007	Singlet-A	H-3->L+1 (92%)
14	36012.09744	277.6844647	0.0034	Singlet-A	HOMO->L+3 (55%), HOMO->L+6 (15%)
15	36150.82576	276.6188542	0.0318	Singlet-A	HOMO->L+4 (56%)
16	36273.42288	275.6839362	0.0346	Singlet-A	H-1->L+2 (-28%), H-1->L+3 (-13%), H-1->L+4 (32%)
17	36455.70544	274.3054861	0.015	Singlet-A	H-1->L+3 (60%)
18	36915.44464	270.8893282	0.0284	Singlet-A	H-4->LUMO (51%), HOMO->L+4 (-11%)
19	37228.38992	268.6122076	0.004	Singlet-A	H-2->L+2 (24%), H-2->L+5 (12%), H-1->L+4 (25%)
20	37504.23344	266.6365656	0.0085	Singlet-A	HOMO->L+2 (-11%), HOMO->L+5 (75%)
21	37579.24352	266.1043455	0.0005	Singlet-A	HOMO->L+7 (91%)
22	37987.36288	263.2454385	0.0004	Singlet-A	H-8->L+1 (31%), H-6->L+1 (10%), H-5->L+1 (14%), H-4->L+1 (-20%)
23	38318.85904	260.9681042	0.0139	Singlet-A	H-1->L+3 (-12%), H-1->L+6 (69%)
24	38435.81024	260.1740392	0.0024	Singlet-A	H-4->L+6 (10%), HOMO->L+3 (-12%), HOMO->L+6 (38%)
25	38679.39136	258.535609	0.0002	Singlet-A	H-6->L+3 (15%), H-5->L+3 (13%), H-4->L+3 (29%), HOMO->L+3 (-22%)
26	38758.43424	258.0083586	0.003	Singlet-A	H-6->L+2 (-11%), H-5->L+2 (30%), H-5->L+5 (-12%)
27	39033.4712	256.1903846	0.0705	Singlet-A	H-6->LUMO (59%), H-5->LUMO (21%)
28	39289.15072	254.5231907	0.0047	Singlet-A	H-1->L+2 (53%), H-1->L+4 (16%)
29	39544.02368	252.8827132	0.0051	Singlet-A	H-1->L+7 (85%)
30	39794.86384	251.28871	0.0168	Singlet-A	H-6->L+1 (-29%), H-5->L+1 (50%)
31	39966.66112	250.2085418	0.0045	Singlet-A	H-8->L+3 (-16%), H-4->L+6 (-22%), HOMO->L+6 (25%)
32	40058.60896	249.6342299	0.0025	Singlet-A	H-9->LUMO (32%), H-8->LUMO (-20%), H-7->LUMO (22%)
33	40230.40624	248.5682083	0.0468	Singlet-A	H-2->L+2 (-17%), H-2->L+4 (44%), H-1->L+5 (15%)
34	40578.84016	246.4338547	0.0164	Singlet-A	H-10->LUMO (90%)
35	40621.58784	246.1745228	0.0234	Singlet-A	H-2->L+4 (-17%), H-1->L+5 (60%)
36	40857.90992	244.7506497	0.1069	Singlet-A	H-9->L+1 (23%), H-7->L+1 (38%), H-3->L+7 (14%)

37	40972.44144	244.0664908	0.0486	Singlet-A	H-9->LUMO (20%), H-8->LUMO (53%)
38	41123.26816	243.1713346	0.0406	Singlet-A	H-3->L+7 (76%)
39	41881.43456	238.7692806	0.026	Singlet-A	H-3->L+2 (-17%), H-3->L+4 (22%), H-2->L+2 (-14%)
40	41902.40512	238.6497856	0.0289	Singlet-A	H-3->L+2 (-19%), H-3->L+4 (32%), H-2->L+2 (10%)
41	42060.49088	237.7528125	0.0357	Singlet-A	H-9->L+1 (-37%), H-7->L+1 (37%)
42	42284.71456	236.4920777	0.0013	Singlet-A	H-10->L+1 (94%)
43	42458.93152	235.5217063	0.0265	Singlet-A	H-9->L+1 (10%), H-2->L+3 (71%)
44	42557.33184	234.9771371	0.0338	Singlet-A	H-11->LUMO (27%), H-2->L+5 (-26%)
45	42742.03408	233.9617245	0.0136	Singlet-A	H-11->LUMO (22%), H-2->L+5 (26%)
46	43157.41248	231.7099063	0.0029	Singlet-A	HOMO->L+8 (68%)
47	43496.16768	229.905312	0.01	Singlet-A	H-3->L+3 (22%), HOMO->L+8 (11%)
48	43524.39728	229.7561971	0.0015	Singlet-A	H-3->L+3 (30%), H-1->L+8 (-11%)
49	43542.1416	22966%	0.0012	Singlet-A	H-4->L+3 (-11%), H-3->L+3 (32%), H-2->L+6 (18%)
50	43674.41744	228.9669923	0.0055	Singlet-A	H-3->L+2 (45%), H-3->L+4 (34%), H-3->L+5 (12%)
51	43761.52592	228.5112274	0.0101	Singlet-A	H-12->L+1 (11%), H-11->L+1 (28%), H-4->L+2 (11%)
52	43877.67056	22791%	0.0002	Singlet-A	H-12->LUMO (43%), H-11->LUMO (11%), H-9->LUMO (-12%)
53	44227.7176	226.1025561	0.0042	Singlet-A	H-14->LUMO (17%), H-7->L+2 (11%), H-4->L+5 (16%)
54	44259.98	225.9377433	0.0004	Singlet-A	H-4->L+6 (-10%), H-2->L+6 (35%)
55	44369.67216	225.3791726	0.0032	Singlet-A	H-11->L+1 (-10%), H-4->L+4 (15%), H-1->L+8 (-13%)
56	44651.1616	223.9583393	0.0788	Singlet-A	H-4->L+4 (22%), H-1->L+8 (10%), HOMO->L+9 (13%)
57	44713.26672	223.6472692	0.0042	Singlet-A	H-7->L+5 (16%), H-6->L+5 (17%), H-5->L+5 (-14%)
58	44850.38192	222.9635417	0.0018	Singlet-A	H-5->L+4 (14%), HOMO->L+9 (35%)
59	44918.93952	222.6232433	0.0102	Singlet-A	H-8->L+6 (30%), H-6->L+6 (-29%)
60	44951.20192	222.463462	0.0129	Singlet-A	H-12->L+1 (33%), H-11->L+1 (-10%)
61	45077.02528	221.8425004	0.2722	Singlet-A	H-2->L+7 (77%)
62	45281.08496	220.8427649	0.071	Singlet-A	H-6->L+4 (-10%), H-5->L+4 (13%), H-4->L+4 (15%)
63	45503.69552	219.7623706	0.0018	Singlet-A	H-3->L+2 (-13%), H-3->L+5 (82%)
64	45605.32208	219.2726538	0.0001	Singlet-A	H-3->L+3 (-14%), H-3->L+6 (83%)
65	45781.95872	218.4266528	0.0124	Singlet-A	H-13->L+1 (19%), H-8->L+3 (-13%), H-5->L+3 (-11%), H-4->L+3 (10%)
66	45936.81824	217.6903056	0.0099	Singlet-A	H-16->LUMO (15%), H-6->L+2 (10%), H-4->L+2 (15%)
67	46004.56928	217.3697125	0.0171	Singlet-A	H-13->L+1 (13%), H-12->L+1 (-10%)
68	46245.73072	216.2361767	0.0095	Singlet-A	H-5->L+2 (16%), H-4->L+2 (10%), H-1->L+9 (17%)
69	46332.03264	21583%	0.0068	Singlet-A	H-1->L+9 (42%)
70	46575.61376	214.7046317	0.0066	Singlet-A	H-13->L+1 (13%), H-12->L+1 (11%), H-9->L+3 (-11%), H-7->L+3 (-10%)
71	46960.34288	212.9456343	0.0053	Singlet-A	H-7->L+4 (57%)
72	47161.98288	212.03519	0.0147	Singlet-A	H-6->L+4 (19%), H-5->L+4 (12%)
73	47214.40928	211.7997483	0.0032	Singlet-A	H-6->L+3 (-22%), H-5->L+3 (42%)
74	47378.14096	211.0678004	0.0029	Singlet-A	H-5->L+8 (10%), H-4->L+8 (38%)
75	47481.38064	210.6088716	0.0859	Singlet-A	H-10->L+2 (-16%), H-10->L+4 (42%)
76	47515.25616	210.4587202	0.0084	Singlet-A	H-14->LUMO (-12%), H-5->L+5 (12%), H-4->L+5 (42%)

77	47739.47984	209.4702337	0.0059	Singlet-A	H-10->L+7 (25%), H-9->L+4 (-13%)
78	47929.02144	208.6418562	0.0322	Singlet-A	H-10->L+7 (11%), H-6->L+2 (-14%), H-4->L+7 (20%)
79	47990.32	208.3753557	0.0423	Singlet-A	H-10->L+7 (-12%), H-4->L+7 (40%)
80	48136.30736	207.7433968	0.0021	Singlet-A	H-8->L+6 (16%), H-5->L+6 (27%), H-4->L+6 (-13%)
81	48144.37296	20771%	0.0094	Singlet-A	H-10->L+7 (19%), H-9->L+4 (10%)
82	48447.63952	206.408405	0.0003	Singlet-A	H-13->LUMO (91%)
83	48700.89936	205.335017	0.0097	Singlet-A	H-9->L+2 (-14%), H-2->L+9 (27%)
84	48754.13232	205.1108188	0.0136	Singlet-A	H-16->LUMO (-14%), H-8->L+2 (27%)
85	48863.82448	20465%	0.0141	Singlet-A	H-7->L+3 (30%), H-2->L+8 (11%)
86	48954.96576	204.2693697	0.0026	Singlet-A	H-17->LUMO (15%), H-15->LUMO (16%), H-2->L+8 (12%)
87	49078.36944	20376%	0.0054	Singlet-A	H-17->LUMO (11%), H-15->LUMO (21%), H-2->L+9 (-15%)
88	49096.11376	203.6821091	0.0178	Singlet-A	H-6->L+5 (21%), H-2->L+8 (-12%)
89	49158.21888	203.4247828	0.0185	Singlet-A	H-6->L+6 (24%), H-5->L+6 (-20%)
90	49214.67808	20319%	0.0001	Singlet-A	H-9->L+2 (-10%), H-9->L+4 (-13%), H-8->L+4 (13%), H-7->L+3 (14%)
91	49425.9968	202.3226773	0.0237	Singlet-A	H-9->L+3 (29%), H-9->L+6 (14%), H-7->L+3 (-21%)
92	49546.9808	201.828645	0.0001	Singlet-A	H-14->L+1 (96%)
93	49647.8008	201.4187907	0.0117	Singlet-A	H-17->LUMO (-13%), H-8->L+4 (20%)
94	49787.33568	20085%	0.0034	Singlet-A	H-19->L+1 (-13%), H-16->L+1 (31%), H-2->L+8 (16%)
95	49825.244	200.7014757	0.0016	Singlet-A	H-17->LUMO (34%), H-15->LUMO (-33%)
96	49934.93616	200.2605945	0.0011	Singlet-A	H-3->L+8 (78%)
97	49996.23472	200.0150623	0.0052	Singlet-A	H-19->LUMO (-11%), H-18->LUMO (52%)
98	50025.27088	199.8989675	0.0029	Singlet-A	H-8->L+8 (16%), H-6->L+8 (-10%), H-4->L+8 (11%), H-3->L+8 (-14%), H-2->L+8 (-13%)
99	50138.99584	19945%	0.0016	Singlet-A	H-19->LUMO (43%), H-18->LUMO (28%)
100	50277.72416	198.8952397	0.0074	Singlet-A	H-10->L+3 (65%), H-10->L+6 (10%)

Table S7: Energy and composition of TD-DFT calculated transitions of **3:**

No.	Energy (cm^{-1})	Wavelength (nm)	Oscillator Strength	Symmetry	Major contributions
1	19829.2776	504.3048063	0.2067	Singlet-A	H-1->LUMO (-45%), HOMO->LUMO (53%)
2	19920.41888	501.9974761	0.195	Singlet-A	H-1->LUMO (53%), HOMO->LUMO (44%)
3	24293.5872	411.6312637	0.2684	Singlet-A	H-4->LUMO (-10%), H-2->LUMO (74%)
4	24823.49712	402.8441259	0.0797	Singlet-A	H-6->LUMO (36%), H-5->LUMO (-27%), H-4->LUMO (-12%)
5	25314.69216	395.0275175	0.0431	Singlet-A	H-1->L+1 (97%)
6	25860.73328	386.6866377	0.0488	Singlet-A	H-4->LUMO (13%), H-3->LUMO (64%)
7	26235.78368	381.1588067	0.0049	Singlet-A	H-1->L+2 (89%)
8	26274.49856	380.5971778	0.0034	Singlet-A	HOMO->L+1 (92%)
9	26725.3656	374.1763593	0.0134	Singlet-A	H-5->LUMO (57%), H-4->LUMO (-15%), H-2->LUMO (-10%)
10	27011.6944	370.2100228	0.0079	Singlet-A	H-6->LUMO (51%), H-4->LUMO (23%)
11	27160.10144	368.1871374	0.0046	Singlet-A	HOMO->L+2 (89%)
12	27319.80032	366.0348862	0.0291	Singlet-A	H-8->LUMO (74%)
13	27799.70352	359.7160665	0.1843	Singlet-A	HOMO->L+3 (85%)
14	28096.5176	355.9159944	0.0107	Singlet-A	H-1->L+3 (86%)
15	28408.65632	352.0053848	0.2549	Singlet-A	H-7->LUMO (54%), H-4->LUMO (-16%), H-1->L+3 (-11%)
16	29320.87568	341.053934	0.0204	Singlet-A	H-9->LUMO (94%)
17	29830.6216	335.2260015	0.0047	Singlet-A	HOMO->L+4 (80%)
18	30009.67792	333.2258356	0.0131	Singlet-A	H-1->L+4 (90%)
19	30249.22624	330.5869684	0.0111	Singlet-A	H-10->LUMO (91%)
20	30313.75104	329.8832925	0.0307	Singlet-A	H-6->L+1 (27%), H-5->L+1 (-11%), H-4->L+1 (-21%), H-2->L+1 (16%)
21	30778.3296	324.903922	0.0052	Singlet-A	H-8->L+1 (15%), H-6->L+2 (-10%), H-3->L+1 (41%)
22	31276.78368	319.72597	0.0045	Singlet-A	H-2->L+1 (63%)
23	31368.73152	318.7887911	0.0142	Singlet-A	H-1->L+5 (84%)
24	31418.73824	318.2814002	0.1645	Singlet-A	HOMO->L+5 (68%), HOMO->L+7 (-15%)
25	31454.22688	317.9222951	0.0037	Singlet-A	H-1->L+6 (60%)
26	31674.41776	315.7121964	0.0908	Singlet-A	H-3->L+2 (51%)
27	31901.86768	313.4612713	0.0167	Singlet-A	H-3->L+1 (-22%), H-2->L+2 (-22%), H-1->L+6 (27%)
28	31968.0056	312.812758	0.0926	Singlet-A	HOMO->L+6 (75%), HOMO->L+7 (-19%)
29	32106.73392	311.4611416	0.0851	Singlet-A	H-2->L+2 (-13%), H-2->L+3 (38%)
30	32257.56064	310.0048423	0.1228	Singlet-A	H-2->L+2 (10%), HOMO->L+5 (20%), HOMO->L+6 (11%), HOMO->L+7 (45%)
31	32273.69184	309.8498941	0.0029	Singlet-A	H-2->L+2 (28%), H-2->L+3 (28%)
32	32893.93648	304.0073968	0.0002	Singlet-A	H-11->LUMO (99%)
33	33012.5008	302.9155549	0.0054	Singlet-A	H-8->L+1 (38%), H-7->L+1 (12%)
34	33187.52432	301.3180466	0.0167	Singlet-A	H-8->L+2 (-10%), H-6->L+3 (21%), H-5->L+3 (-14%)
35	33438.36448	299.0576888	0.0973	Singlet-A	H-8->L+2 (41%), H-7->L+2 (12%), H-3->L+2 (-15%)
36	33614.19456	297.4933694	0.0028	Singlet-A	H-12->LUMO (47%), H-3->L+3 (32%)

37	33648.07008	297.1938651	0.0228	Singlet-A	H-12->LUMO (38%), H-3->L+3 (-29%)
38	34062.64192	293.5767585	0.004	Singlet-A	H-5->L+1 (-30%), H-4->L+1 (49%)
39	34311.0624	291.451191	0.0003	Singlet-A	H-6->L+1 (37%), H-5->L+1 (33%)
40	34322.35424	291.3553054	0.0182	Singlet-A	H-13->LUMO (15%), H-2->L+4 (33%), H-2->L+7 (11%)
41	34373.97408	290.9177733	0.0225	Singlet-A	H-13->LUMO (49%), H-2->L+4 (-17%)
42	34672.40128	288.4138286	0.0294	Singlet-A	H-2->L+4 (-11%), H-2->L+7 (38%)
43	34920.82176	286.3621042	0.0374	Singlet-A	H-9->L+1 (40%)
44	34974.86128	285.9196473	0.0073	Singlet-A	H-5->L+2 (-25%), H-4->L+2 (37%)
45	35020.8352	285.5443036	0.0472	Singlet-A	H-7->L+1 (17%), H-6->L+4 (-14%), H-5->L+4 (14%)
46	35117.6224	284.7573189	0.0092	Singlet-A	H-7->L+1 (34%)
47	35161.9832	284.3980655	0.0052	Singlet-A	H-8->L+3 (25%), H-7->L+3 (16%)
48	35264.41632	283.5719698	0.0023	Singlet-A	H-6->L+2 (31%), H-5->L+2 (34%)
49	35371.6888	28271%	0.0324	Singlet-A	H-10->L+1 (10%), H-3->L+4 (19%)
50	35464.4432	281.9725646	0.0375	Singlet-A	H-14->LUMO (11%), H-3->L+4 (13%)
51	35590.26656	280.9756983	0.0023	Singlet-A	H-10->L+1 (15%), H-5->L+3 (16%)
52	35684.63408	28023%	0.0007	Singlet-A	H-10->L+1 (30%), H-9->L+2 (41%)
53	35703.18496	280.087057	0.0046	Singlet-A	H-6->L+3 (33%), H-5->L+3 (15%), H-4->L+3 (12%)
54	35814.49024	279.2165945	0.0291	Singlet-A	H-15->LUMO (39%), H-14->LUMO (-11%), H-3->L+4 (12%)
55	35870.14288	278.7833891	0.0005	Singlet-A	H-1->L+7 (76%)
56	35895.9528	278.5829382	0.0224	Singlet-A	H-10->L+2 (31%), H-7->L+2 (-20%)
57	36111.30432	276.9215953	0.0099	Singlet-A	H-10->L+2 (19%), H-8->L+2 (-17%), H-7->L+2 (35%)
58	36333.91488	275.2249526	0.0036	Singlet-A	H-10->L+2 (13%), H-2->L+5 (32%), H-2->L+6 (-14%)
59	36442.80048	274.4026219	0.0044	Singlet-A	H-8->L+3 (-11%), H-7->L+3 (28%)
60	36527.48928	273.7664208	0.011	Singlet-A	HOMO->L+9 (76%)
61	36554.91232	273.5610446	0.0025	Singlet-A	H-7->L+3 (10%), H-3->L+5 (16%), H-2->L+6 (20%)
62	36901.73312	270.9899822	0.0012	Singlet-A	H-6->L+5 (-13%), H-2->L+5 (20%)
63	37025.94336	270.0808971	0.0084	Singlet-A	H-8->L+4 (20%), H-3->L+4 (-10%), H-2->L+6 (10%)
64	37091.27472	269.6051855	0.0075	Singlet-A	H-2->L+5 (14%), H-2->L+6 (41%)
65	37309.04592	268.0315123	0.0364	Singlet-A	H-16->LUMO (31%), H-14->LUMO (-10%), H-8->L+4 (16%)
66	37375.18384	267.5572124	0.0026	Singlet-A	H-16->LUMO (19%), H-9->L+3 (70%)
67	37583.27632	266.0757917	0.0243	Singlet-A	H-16->LUMO (-11%), H-14->LUMO (-13%), H-5->L+4 (17%), H-4->L+4 (-10%), HOMO->L+8 (-14%)
68	37665.54544	265.4946287	0.0083	Singlet-A	H-16->LUMO (-12%), H-5->L+4 (-18%), H-4->L+4 (27%), HOMO->L+8 (-10%)
69	37846.21488	26423%	0.0045	Singlet-A	H-10->L+3 (11%), H-6->L+4 (31%), H-5->L+4 (19%), H-4->L+4 (12%)
70	37913.15936	263.7606617	0.2923	Singlet-A	H-10->L+3 (-10%), H-3->L+6 (22%)
71	37968.812	263.3740555	0.1508	Singlet-A	H-10->L+3 (27%)
72	38163.99952	262.0270445	0.1167	Singlet-A	H-14->LUMO (-11%), HOMO->L+8 (46%)
73	38317.24592	260.9790907	0.0042	Singlet-A	H-4->L+7 (35%), HOMO->L+8 (15%)
74	38364.83296	260.655377	0.1129	Singlet-A	H-10->L+3 (25%), H-3->L+5 (-17%)
75	38460.8136	260.0049002	0.0126	Singlet-A	H-8->L+5 (46%), H-7->L+5 (19%)
76	38591.47632	259.1245776	0.0173	Singlet-A	H-10->L+3 (11%), H-8->L+4 (-12%), H-8->L+5 (-11%), H-7->L+4 (37%)

77	38663.26016	258.643476	0.0428	Singlet-A	H-8->L+6 (53%), H-7->L+6 (16%), H-3->L+6 (-20%)
78	38734.23744	258.1695332	0.0062	Singlet-A	H-11->L+7 (12%), HOMO->L+11 (68%)
79	38868.93296	257.2748784	0.0428	Singlet-A	H-6->L+5 (-10%), H-6->L+7 (26%), H-5->L+5 (-13%), H-5->L+7 (35%)
80	38910.87408	256.9975678	0.0043	Singlet-A	H-18->LUMO (88%)
81	39252.04896	25476%	0.0001	Singlet-A	H-11->L+1 (96%)
82	39408.5216	253.752224	0.006	Singlet-A	H-9->L+4 (86%)
83	39485.1448	253.2598032	0.0066	Singlet-A	H-5->L+5 (-13%), H-4->L+5 (30%), H-4->L+6 (-12%)
84	39666.6208	252.1011318	0.0142	Singlet-A	H-1->L+8 (-14%), H-1->L+14 (34%)
85	39755.3424	25154%	0.0416	Singlet-A	H-17->LUMO (17%), H-6->L+5 (-10%), H-5->L+5 (-14%), H-5->L+6 (13%), H-5->L+7 (-11%)
86	39795.6704	251.283617	0.0364	Singlet-A	H-17->LUMO (21%)
87	39886.81168	25071%	0.0022	Singlet-A	H-5->L+6 (-17%), H-4->L+5 (11%), H-4->L+6 (39%)
88	39990.05136	250.0621945	0.1015	Singlet-A	H-1->L+8 (-24%), H-1->L+10 (24%)
89	40072.32048	249.5488128	0	Singlet-A	H-11->L+2 (97%)
90	40135.23216	24916%	0.0007	Singlet-A	H-7->L+5 (14%), H-6->L+6 (-10%), H-5->L+6 (-11%), H-1->L+8 (23%)
91	40199.75696	248.7577228	0.0005	Singlet-A	H-6->L+5 (11%), H-6->L+6 (18%), H-5->L+6 (20%), H-1->L+8 (10%)
92	40269.92768	248.3242602	0.1275	Singlet-A	H-10->L+4 (39%), H-1->L+10 (-20%)
93	40344.93776	247.862571	0.0172	Singlet-A	H-10->L+4 (-26%), H-8->L+5 (-10%), H-7->L+5 (30%)
94	40729.66688	24552%	0.015	Singlet-A	H-7->L+6 (-18%), H-2->L+9 (22%)
95	40758.70304	245.346374	0.0066	Singlet-A	H-12->L+1 (-14%), H-2->L+9 (29%)
96	40793.38512	245.1377833	0.0077	Singlet-A	H-12->L+1 (-12%), H-9->L+5 (19%), H-7->L+6 (-18%)
97	40805.48352	245.0651025	0.0808	Singlet-A	H-9->L+5 (47%)
98	40942.59872	244.2443888	0.0033	Singlet-A	H-9->L+6 (23%)
99	40964.37584	24411%	0.0196	Singlet-A	H-6->L+9 (14%), H-5->L+9 (16%), H-2->L+9 (10%), HOMO->L+13 (-13%)
100	41013.576	243.8217043	0.0065	Singlet-A	H-9->L+6 (39%), H-7->L+6 (17%), H-3->L+7 (10%)

Table S8: Energy and composition of TD-DFT calculated transitions of **4:**

No.	Energy (cm^{-1})	Wavelength (nm)	Oscillator Strength	Symmetry	Major contributions
1	17574.9424	568.9919075	0.0002	Singlet-A	HOMO->LUMO (62%), HOMO->L+1 (-36%)
2	17612.04416	567.7932618	0.0001	Singlet-A	H-1->LUMO (64%), H-1->L+1 (34%)
3	21617.42112	462.5898688	0.0175	Singlet-A	HOMO->LUMO (37%), HOMO->L+1 (61%)
4	21713.40176	460.5450639	0.001	Singlet-A	H-1->LUMO (-35%), H-1->L+1 (63%)
5	22036.83232	453.7857281	0.9277	Singlet-A	H-2->LUMO (87%)
6	22926.468	436.1770858	0.0053	Singlet-A	H-5->LUMO (48%), H-5->L+1 (-18%)
7	23167.62944	431.6367381	0.0748	Singlet-A	H-6->LUMO (45%), H-6->L+1 (15%), H-5->L+1 (-12%)
8	23549.93888	424.6295522	0.0112	Singlet-A	H-3->LUMO (61%), H-3->L+1 (-27%)
9	23674.95568	422.3872743	0.0163	Singlet-A	H-4->LUMO (63%), H-4->L+1 (26%)
10	24168.5704	413.7605094	0.0596	Singlet-A	H-2->L+1 (68%)
11	24692.8344	404.9757852	0.1381	Singlet-A	H-9->LUMO (-10%), H-8->LUMO (-12%), H-7->LUMO (44%)
12	24745.2608	404.1177857	0.0352	Singlet-A	HOMO->L+2 (49%), HOMO->L+3 (22%), HOMO->L+4 (15%)
13	24806.55936	403.1191853	0.0343	Singlet-A	H-1->L+2 (-14%), H-1->L+3 (66%), H-1->L+4 (-14%)
14	25323.56432	394.8891188	0.021	Singlet-A	H-9->LUMO (52%), H-8->L+1 (-24%)
15	25392.12192	393.8229358	0.0862	Singlet-A	H-9->L+1 (-13%), H-8->LUMO (41%), H-7->LUMO (13%), H-7->L+1 (-11%)
16	25813.9528	387.3873977	0.0066	Singlet-A	HOMO->L+2 (-15%), HOMO->L+4 (16%), HOMO->L+5 (37%)
17	25843.79552	386.9400682	0.0044	Singlet-A	H-1->L+6 (72%)
18	25878.4776	386.4214949	0.0085	Singlet-A	H-1->L+4 (33%), H-1->L+5 (-19%), H-1->L+6 (-23%)
19	25990.58944	384.7546445	0.0026	Singlet-A	HOMO->L+7 (77%)
20	26066.40608	383.6355487	0.0114	Singlet-A	H-10->LUMO (18%), H-9->L+1 (-12%), H-7->L+1 (20%), HOMO->L+7 (11%)
21	26457.58768	377.9634077	0.0219	Singlet-A	H-12->L+1 (-11%), H-11->LUMO (50%), H-10->L+1 (-14%), H-6->LUMO (-10%)
22	26506.78784	377.2618569	0.0047	Singlet-A	H-12->LUMO (17%), H-11->L+1 (-13%), H-10->LUMO (13%), H-3->LUMO (11%), H-3->L+1 (29%)
23	26570.50608	376.3571522	0.0005	Singlet-A	H-12->LUMO (-15%), H-3->LUMO (18%), H-3->L+1 (38%)
24	26736.65744	374.0183313	0.0005	Singlet-A	H-4->LUMO (-29%), H-4->L+1 (69%)
25	27203.65568	367.5976537	0.002	Singlet-A	H-13->LUMO (98%)
26	27280.27888	366.5651676	0.0229	Singlet-A	H-12->LUMO (-18%), H-10->LUMO (15%), H-5->LUMO (19%), H-5->L+1 (29%)
27	27468.20736	364.0572488	0.0025	Singlet-A	HOMO->L+8 (56%), HOMO->L+9 (-39%)
28	27544.83056	363.0445277	0.0033	Singlet-A	H-1->L+8 (35%), H-1->L+9 (50%)
29	27630.32592	361.9211742	0.0095	Singlet-A	H-14->LUMO (18%), H-6->LUMO (15%), H-6->L+1 (-12%), H-5->L+1 (11%)
30	27656.13584	361.5834135	0.003	Singlet-A	H-15->LUMO (-15%), H-14->LUMO (23%), H-14->L+1 (-11%), H-6->L+1 (17%)
31	27743.24432	360.4481107	0.0149	Singlet-A	H-15->LUMO (20%), H-15->L+1 (10%), H-14->LUMO (17%), H-5->L+1 (-14%)
32	27804.54288	359.6534582	0.002	Singlet-A	H-15->LUMO (19%), H-6->L+1 (32%)
33	28353.81024	352.686285	0.0122	Singlet-A	H-13->L+1 (89%)
34	28389.29888	352.2454021	0.101	Singlet-A	H-12->L+1 (-15%), H-10->L+1 (49%)
35	28732.08688	348.0429403	0.0065	Singlet-A	H-9->LUMO (11%), H-9->L+1 (36%), H-8->LUMO (14%), H-8->L+1 (14%), H-7->L+1 (13%)
36	28769.18864	347.5940919	0.0057	Singlet-A	H-9->LUMO (11%), H-9->L+1 (-15%), H-8->LUMO (-14%), H-8->L+1 (43%)

37	29404.75792	340.0810177	0.0007	Singlet-A	HOMO->L+2 (-23%), HOMO->L+3 (72%)
38	29433.79408	339.745531	0.0001	Singlet-A	H-1->L+2 (71%), H-1->L+3 (22%)
39	29631.40128	337.479821	0.0033	Singlet-A	HOMO->L+4 (56%), HOMO->L+5 (-34%)
40	29693.5064	336.7739689	0.0006	Singlet-A	H-12->L+1 (13%), H-11->LUMO (24%), H-11->L+1 (44%)
41	29797.55264	335.5980312	0.0002	Singlet-A	H-1->L+4 (31%), H-1->L+5 (59%)
42	29809.65104	335.461827	0.0006	Singlet-A	H-12->LUMO (-17%), H-12->L+1 (40%), H-11->L+1 (-17%)
43	29988.70736	333.4588544	0.0472	Singlet-A	H-5->L+2 (-10%), H-2->L+2 (44%)
44	30062.10432	332.6447109	0.0288	Singlet-A	H-6->L+3 (-13%), H-2->L+3 (33%)
45	30149.2128	331.6836186	0.0881	Singlet-A	H-2->L+4 (42%)
46	30234.70816	330.7457094	0.0142	Singlet-A	HOMO->L+10 (73%)
47	30325.04288	329.760457	0.0065	Singlet-A	H-16->LUMO (-22%), H-2->L+5 (31%), H-1->L+11 (-10%)
48	30354.8856	329.4362605	0.0097	Singlet-A	H-1->L+11 (72%)
49	30525.87632	327.590923	0.0001	Singlet-A	HOMO->L+6 (98%)
50	30542.81408	32741%	0.0068	Singlet-A	H-14->LUMO (27%), H-14->L+1 (59%)
51	30608.952	326.7018093	0.0167	Singlet-A	H-3->L+2 (27%), H-3->L+3 (10%)
52	30640.40784	326.366413	0.0096	Singlet-A	H-15->LUMO (-25%), H-15->L+1 (59%)
53	30712.19168	32560%	0.0171	Singlet-A	H-4->L+2 (-11%), H-4->L+3 (47%)
54	30751.71312	325.1851356	0	Singlet-A	H-1->L+7 (99%)
55	30939.6416	323.2099495	0.0015	Singlet-A	H-1->L+12 (70%)
56	30972.71056	322.8648646	0.0087	Singlet-A	H-5->L+2 (15%), H-2->L+2 (24%), H-2->L+3 (11%), H-2->L+4 (15%)
57	30988.0352	322.7051969	0.0183	Singlet-A	H-6->L+3 (23%), H-2->L+3 (25%), H-1->L+12 (-17%)
58	30999.32704	322.587648	0.0083	Singlet-A	HOMO->L+13 (86%)
59	31175.96368	320.7599323	0.0017	Singlet-A	H-16->LUMO (37%), H-2->L+5 (29%), H-2->L+9 (10%)
60	31334.04944	319.1416424	0.0224	Singlet-A	H-3->L+7 (15%), HOMO->L+8 (15%), HOMO->L+9 (23%)
61	31349.37408	318.9856351	0.0086	Singlet-A	H-3->L+7 (-12%), HOMO->L+8 (24%), HOMO->L+9 (33%)
62	31388.89552	318.5840035	0.0002	Singlet-A	H-1->L+8 (58%), H-1->L+9 (-41%)
63	31421.15792	318.25689	0.012	Singlet-A	H-6->L+6 (-19%), H-4->L+6 (20%)
64	31449.38752	317.9712162	0.0081	Singlet-A	H-5->L+7 (24%), H-3->L+2 (-10%), H-3->L+5 (17%)
65	31508.2664	317.3770297	0.0264	Singlet-A	H-4->L+4 (22%), H-4->L+5 (-15%), H-4->L+6 (-14%)
66	31638.12256	316.0743809	0.0022	Singlet-A	H-5->L+5 (19%)
67	31709.09984	315.3668837	0.0083	Singlet-A	H-3->L+5 (-10%), H-3->L+7 (15%), H-2->L+7 (-10%)
68	31733.29664	315.1264148	0.0181	Singlet-A	H-4->L+4 (22%), H-4->L+5 (-11%), H-4->L+6 (11%), H-2->L+6 (-14%)
69	31806.6936	314.3992307	0.0057	Singlet-A	H-4->L+6 (11%), H-3->L+7 (15%), H-2->L+6 (-14%)
70	32112.37984	31141%	0.1433	Singlet-A	H-16->L+1 (53%), H-2->L+6 (-14%)
71	32187.38992	310.6806742	0.0601	Singlet-A	H-4->L+6 (14%), H-2->L+6 (23%)
72	32222.072	310.3462744	0.031	Singlet-A	H-2->L+7 (52%)
73	32271.27216	309.8731265	0.0704	Singlet-A	H-2->L+7 (-11%), H-2->L+8 (50%)
74	32277.72464	309.8111813	0.01	Singlet-A	H-2->L+5 (-13%), H-2->L+9 (49%)
75	32604.38144	306.7072448	0.0214	Singlet-A	H-7->L+2 (13%), H-2->L+8 (-10%)
76	32710.84736	305.7089867	0.0298	Singlet-A	H-8->L+3 (19%), H-8->L+6 (10%)

77	33002.01552	303.0117962	0.0324	Singlet-A	H-3->L+8 (36%), H-3->L+9 (-25%)
78	33025.40576	302.7971881	0.0397	Singlet-A	H-8->L+6 (23%)
79	33092.35024	302.1846417	0.0747	Singlet-A	H-5->L+8 (21%), H-5->L+9 (-17%)
80	33131.06512	301.8315277	0.0481	Singlet-A	
81	33184.29808	301.3473413	0.0105	Singlet-A	H-4->L+8 (20%), H-4->L+9 (28%)
82	33237.53104	30086%	0.0122	Singlet-A	H-6->L+9 (16%), H-4->L+9 (12%)
83	33354.48224	299.8097805	0.0075	Singlet-A	H-7->L+4 (12%)
84	33526.27952	298.2734781	0.0103	Singlet-A	H-7->L+5 (19%)
85	33589.99776	297.7076709	0.0034	Singlet-A	H-17->LUMO (95%)
86	33631.93888	29734%	0.0283	Singlet-A	H-11->L+2 (11%)
87	33675.49312	296.9518505	0.009	Singlet-A	
88	33802.12304	29584%	0.0255	Singlet-A	H-12->L+3 (20%), H-11->L+3 (-11%), H-10->L+3 (13%)
89	33829.54608	295.5995914	0.0064	Singlet-A	H-19->L+1 (18%), H-18->LUMO (42%)
90	33872.29376	295.2265374	0.0168	Singlet-A	H-18->LUMO (-10%), H-9->L+5 (13%)
91	33983.59904	29426%	0.0038	Singlet-A	H-19->LUMO (51%), H-18->L+1 (26%)
92	34208.62928	292.3239022	0.0007	Singlet-A	H-1->L+10 (62%), H-1->L+14 (-26%)
93	34233.63264	292.1103964	0.0004	Singlet-A	HOMO->L+11 (74%), HOMO->L+14 (13%)
94	34271.54096	291.7872882	0.0001	Singlet-A	H-3->L+2 (-22%), H-3->L+3 (72%)
95	34398.97744	29071%	0.0025	Singlet-A	H-4->L+2 (56%), H-4->L+3 (18%)
96	34414.30208	290.5768647	0.0166	Singlet-A	H-11->L+5 (14%), H-4->L+2 (12%)
97	34478.02032	290.0398546	0.0154	Singlet-A	H-3->L+4 (13%)
98	34498.18432	289.8703279	0.0094	Singlet-A	H-3->L+4 (29%), H-3->L+5 (-16%)
99	34553.83696	289.4034608	0.0077	Singlet-A	H-11->L+7 (10%)
100	34558.67632	28936%	0.0215	Singlet-A	H-15->L+3 (15%)

Figure S9: ^{1}H NMR data for **5-Bromo-2-iodopyridine (6):**

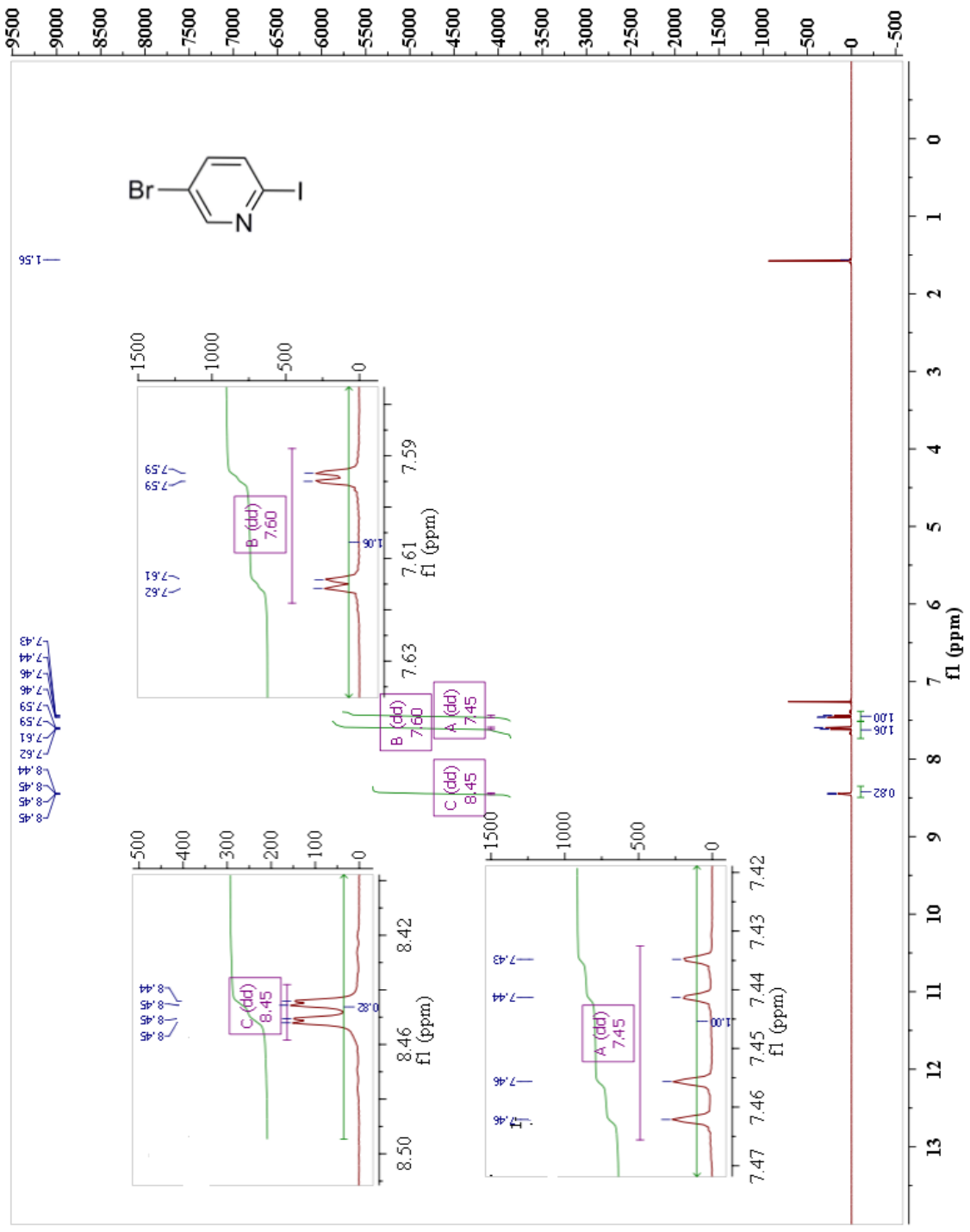

Figure S10: ^{13}C NMR data for **5-Bromo-2-iodopyridine (6):**

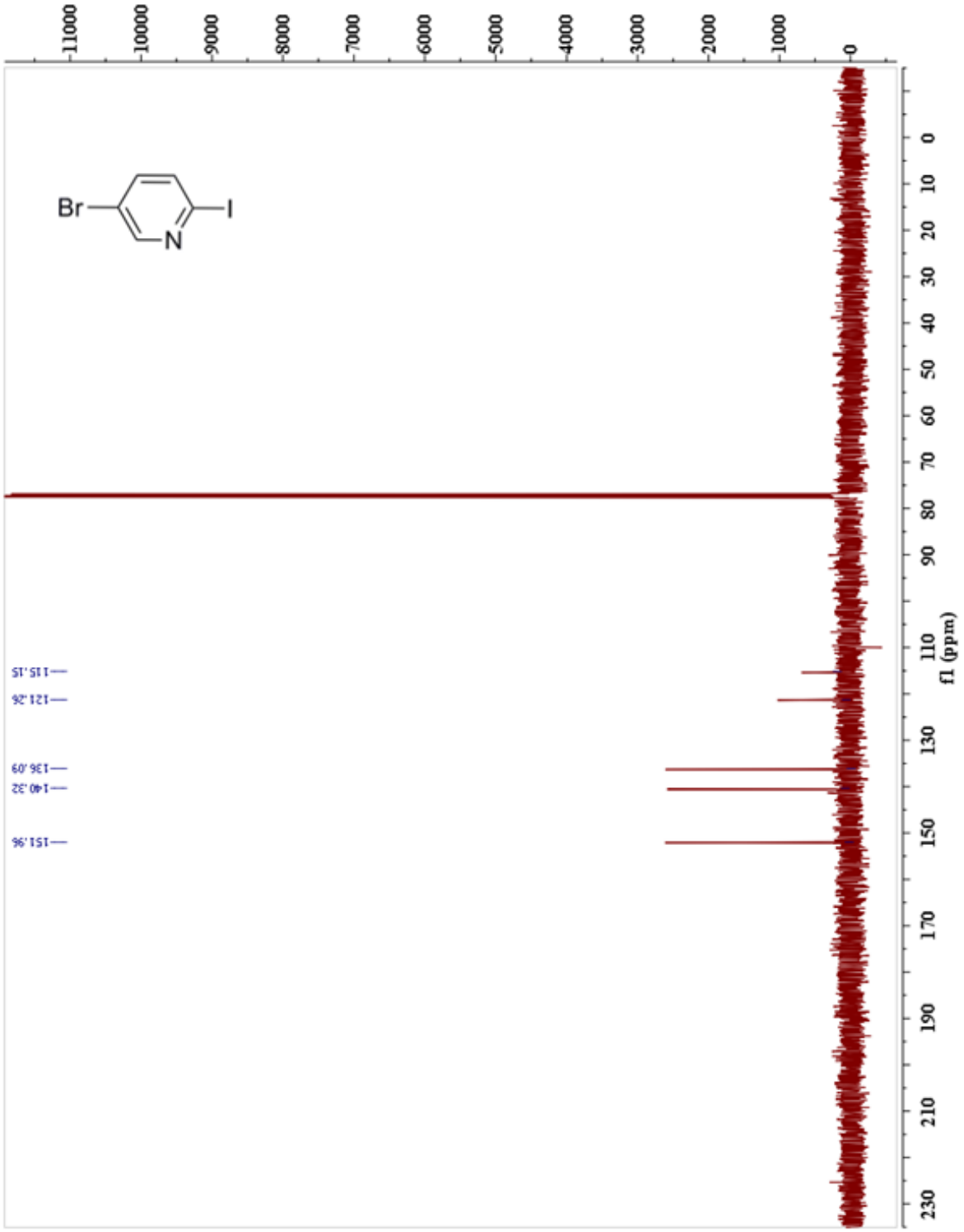

Figure S11: ^{1}H NMR data for **5-bromo-2,2'-bipyridine (7):**

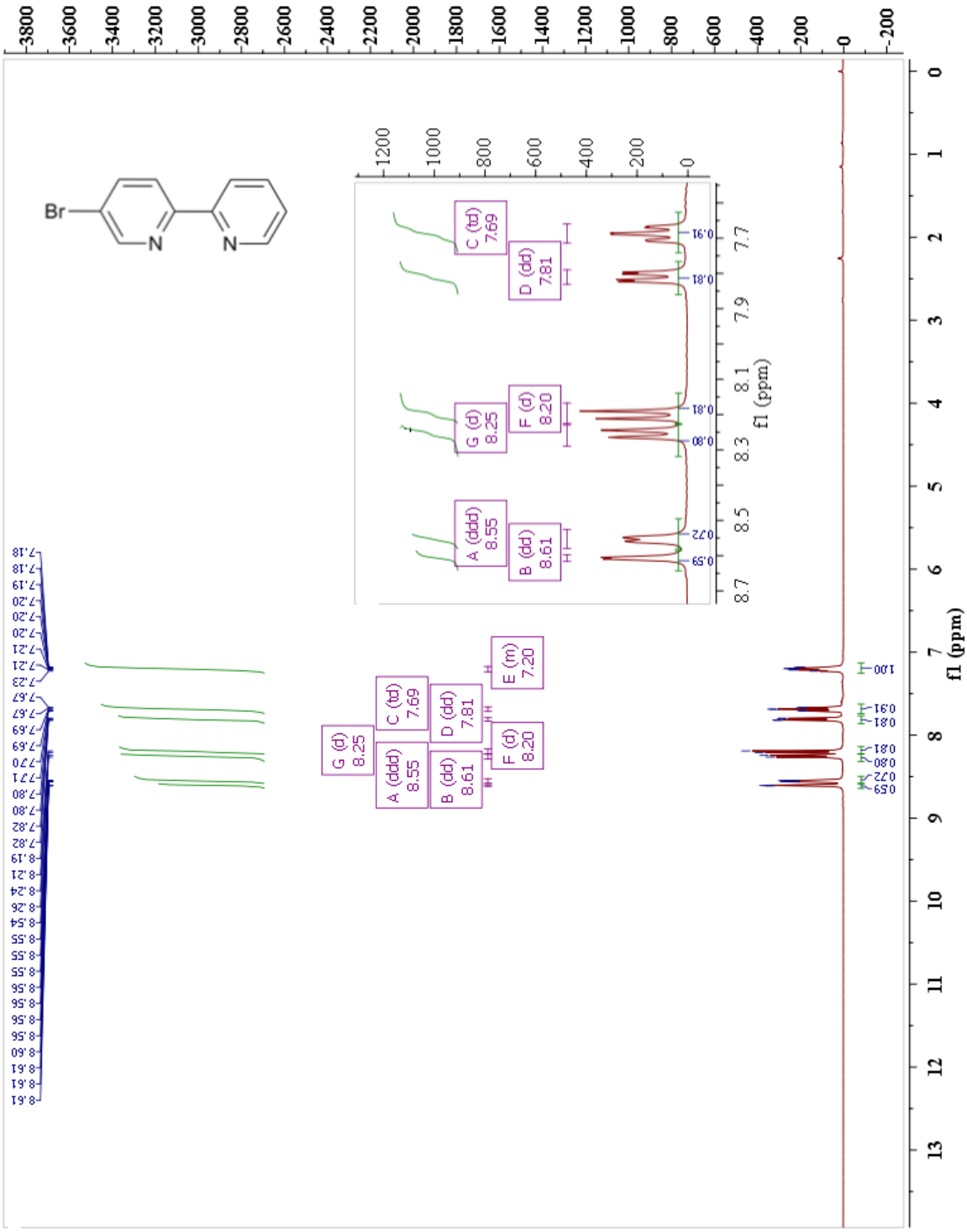

Figure S12: ^{13}C NMR data for **5-bromo-2,2'-bipyridine (7):**

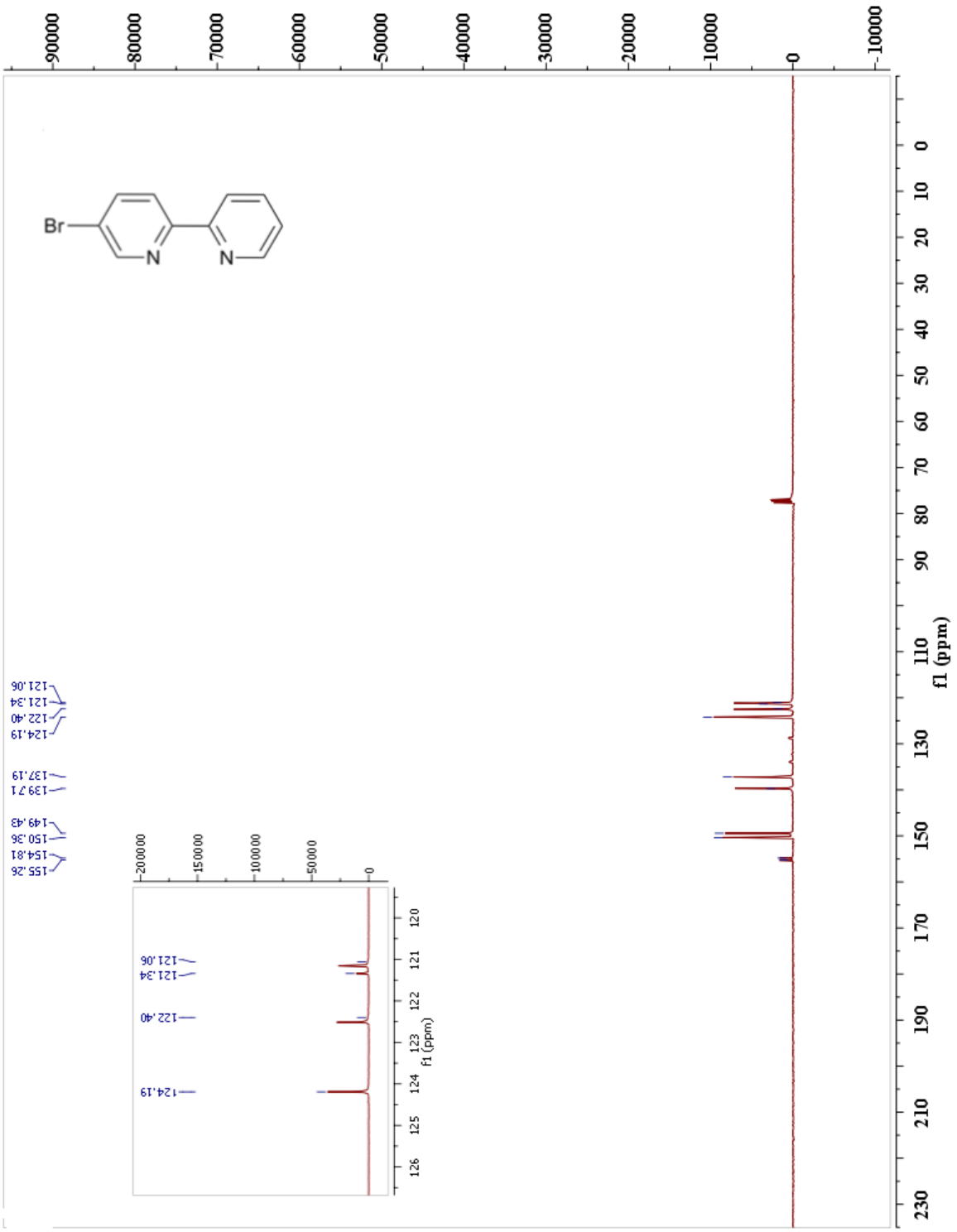

Figure S13: ^{1}H NMR data for **5-trimethylsilylethynyl-2,2'-bipyridine (8):**

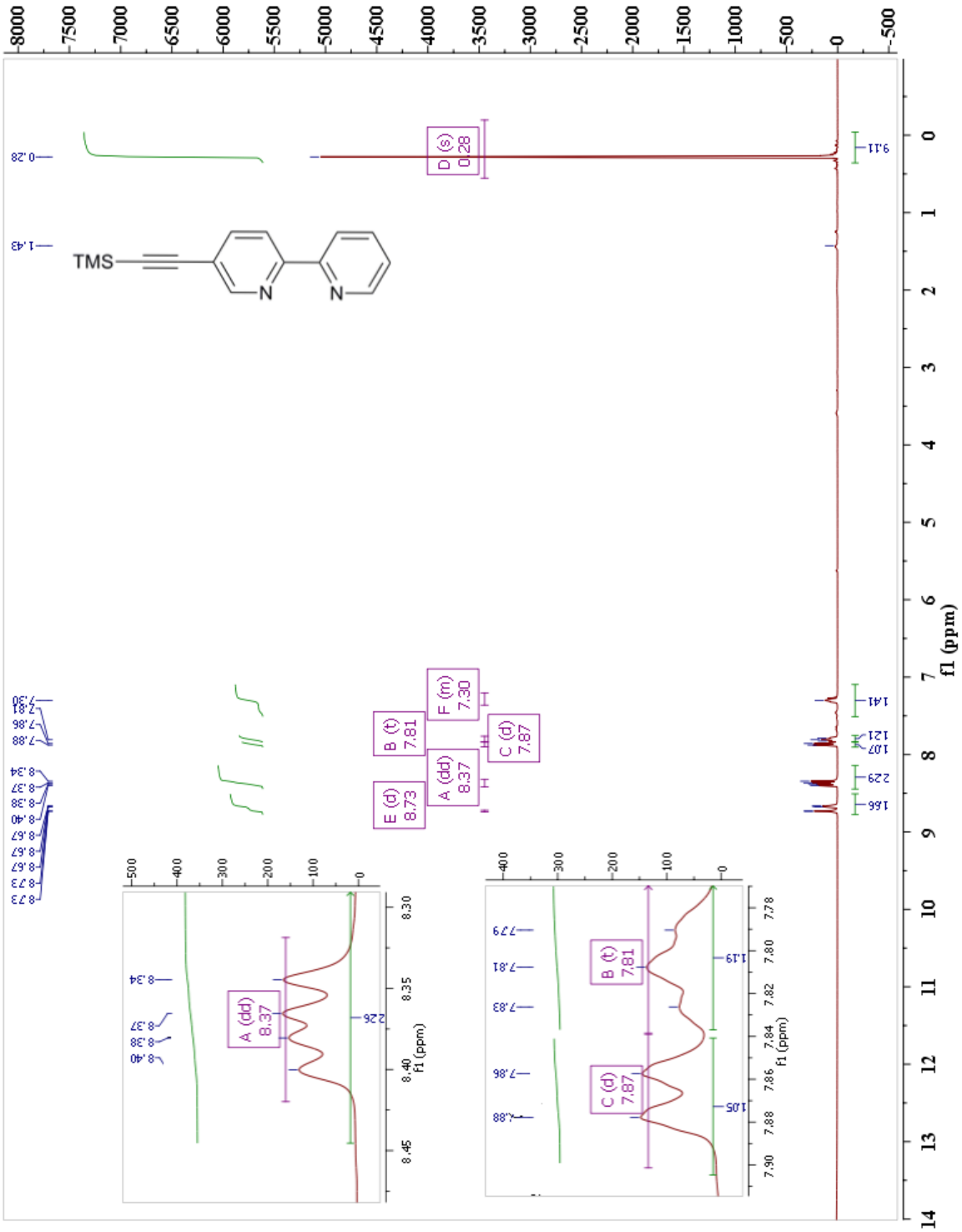

Figure S14: ^{13}C NMR data for **5-trimethylsilylethynyl-2,2'-bipyridine (8):**

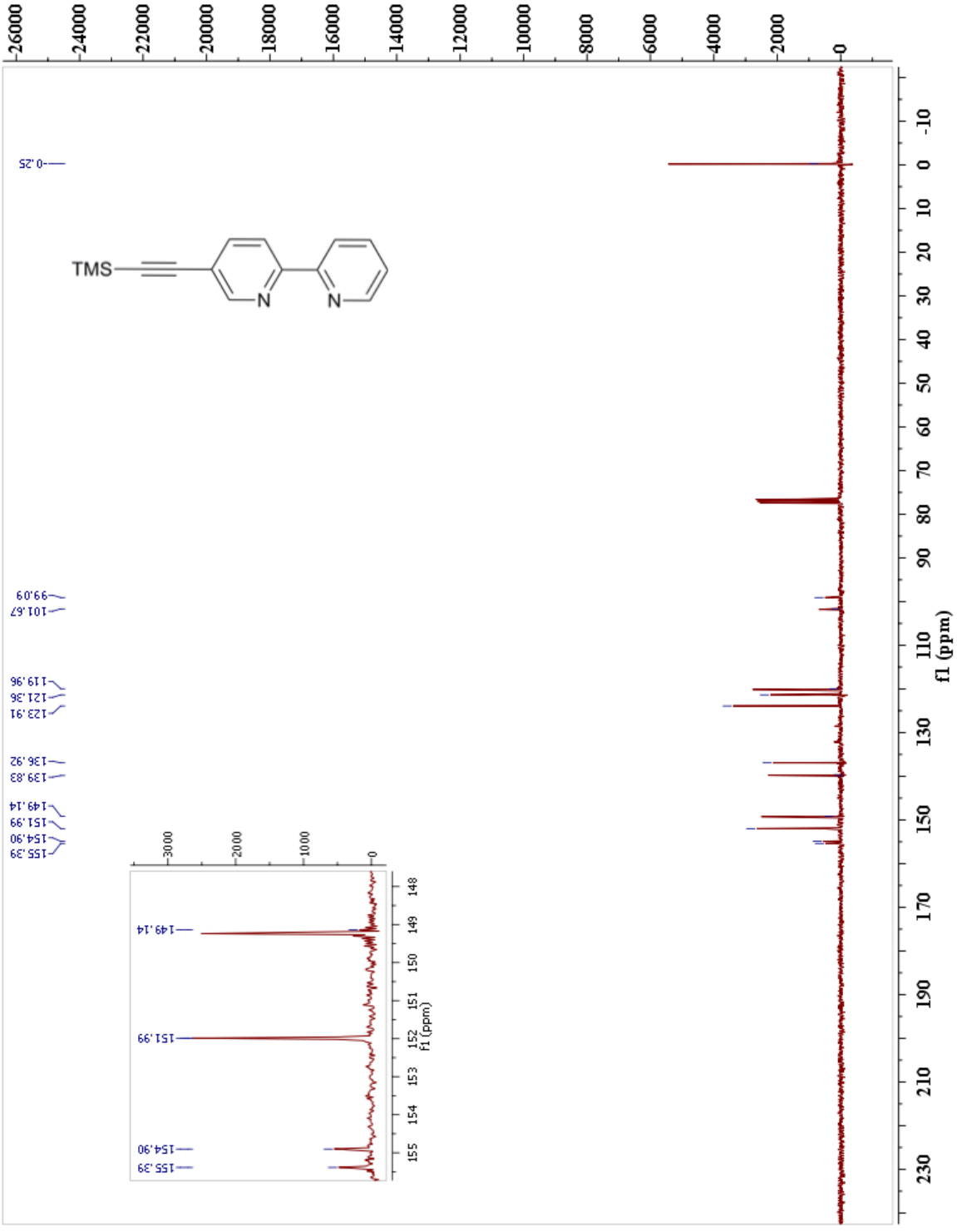

Figure S15: ^{1}H NMR data for **5-Ethynyl-2,2'-bipyridine (5) :**

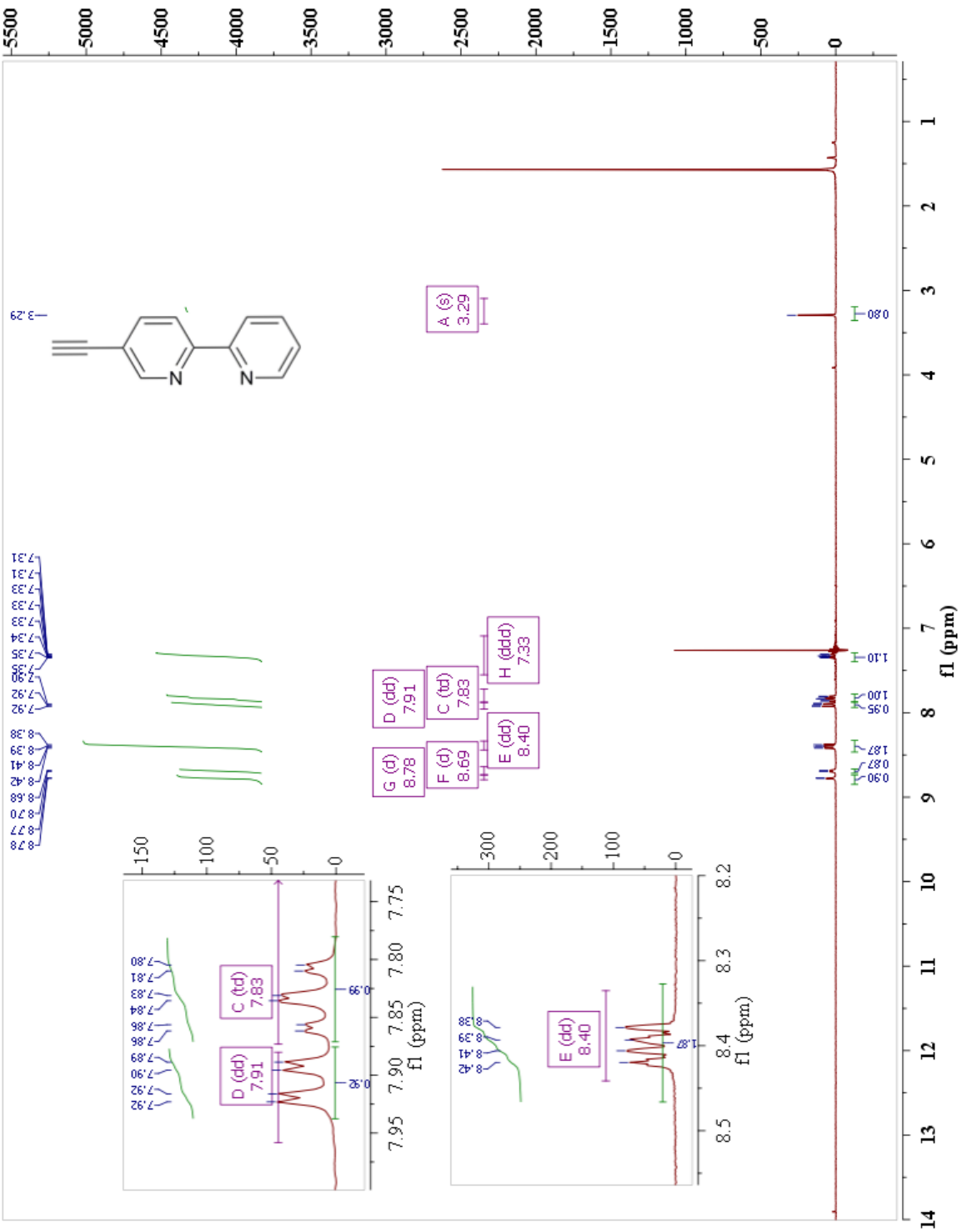

Figure S16: ^{13}C NMR data for **5-Ethynyl-2,2'-bipyridine (5) :**

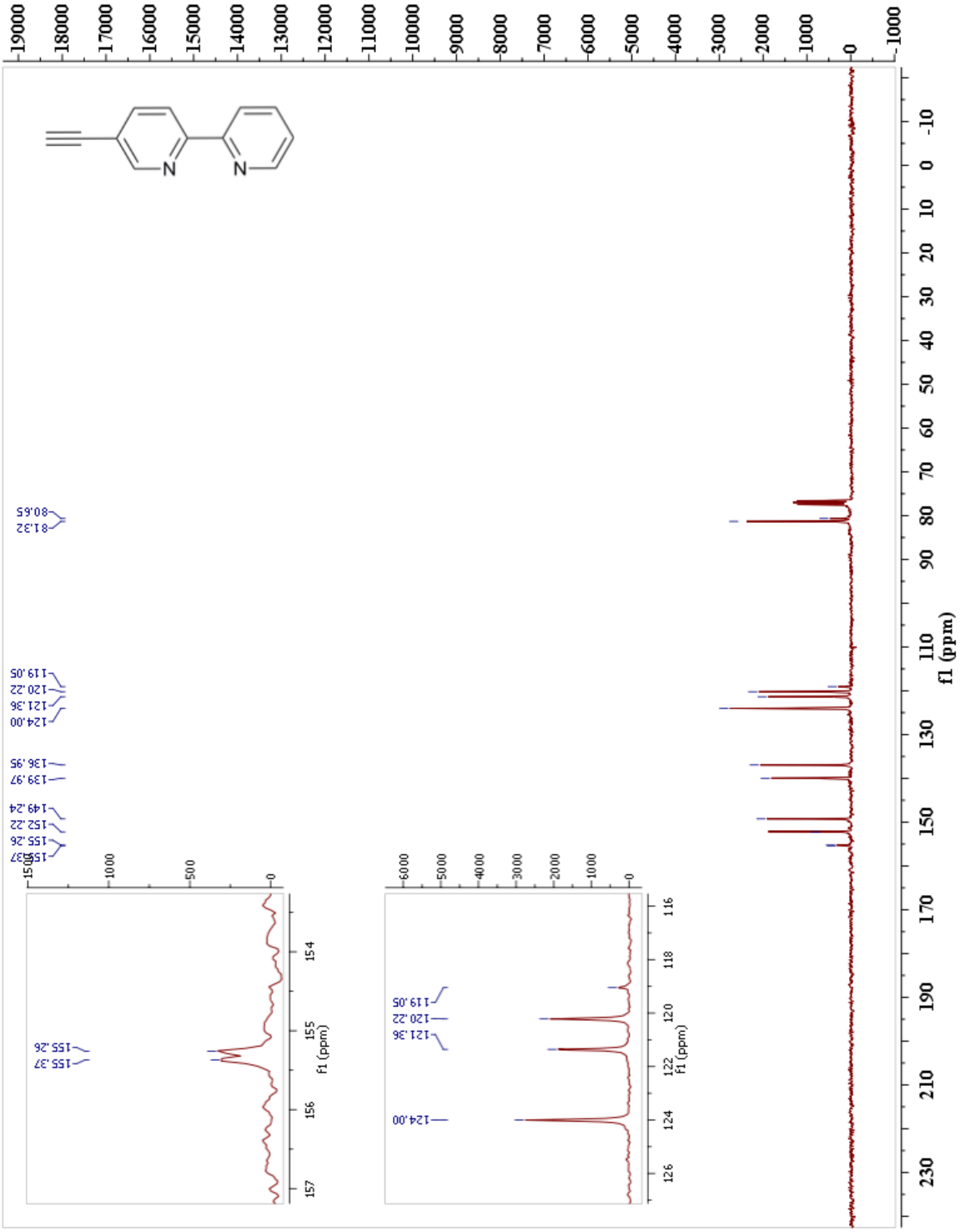

Figure S17: ^{1}H NMR data for ***trans*-(5-ethynyl-2,2'-bipyridine)-chloro-bis(tri-*n*-butylphosphine)platinum (5'):**

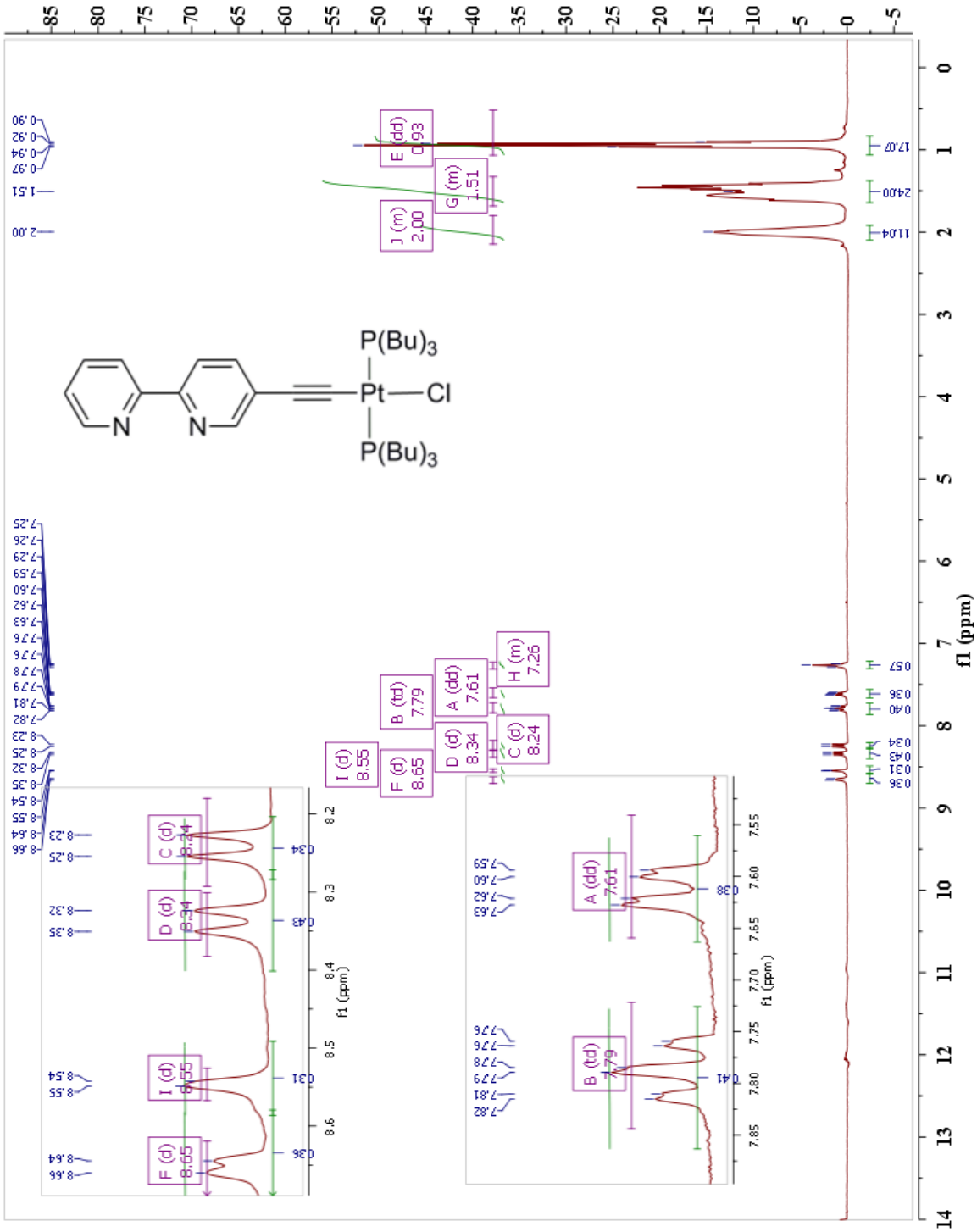

Figure S18: ^{13}C NMR data for ***trans*-(5-ethynyl-2,2'-bipyridine)-chloro-bis(tri-*n*-butylphosphine)platinum (5'):**

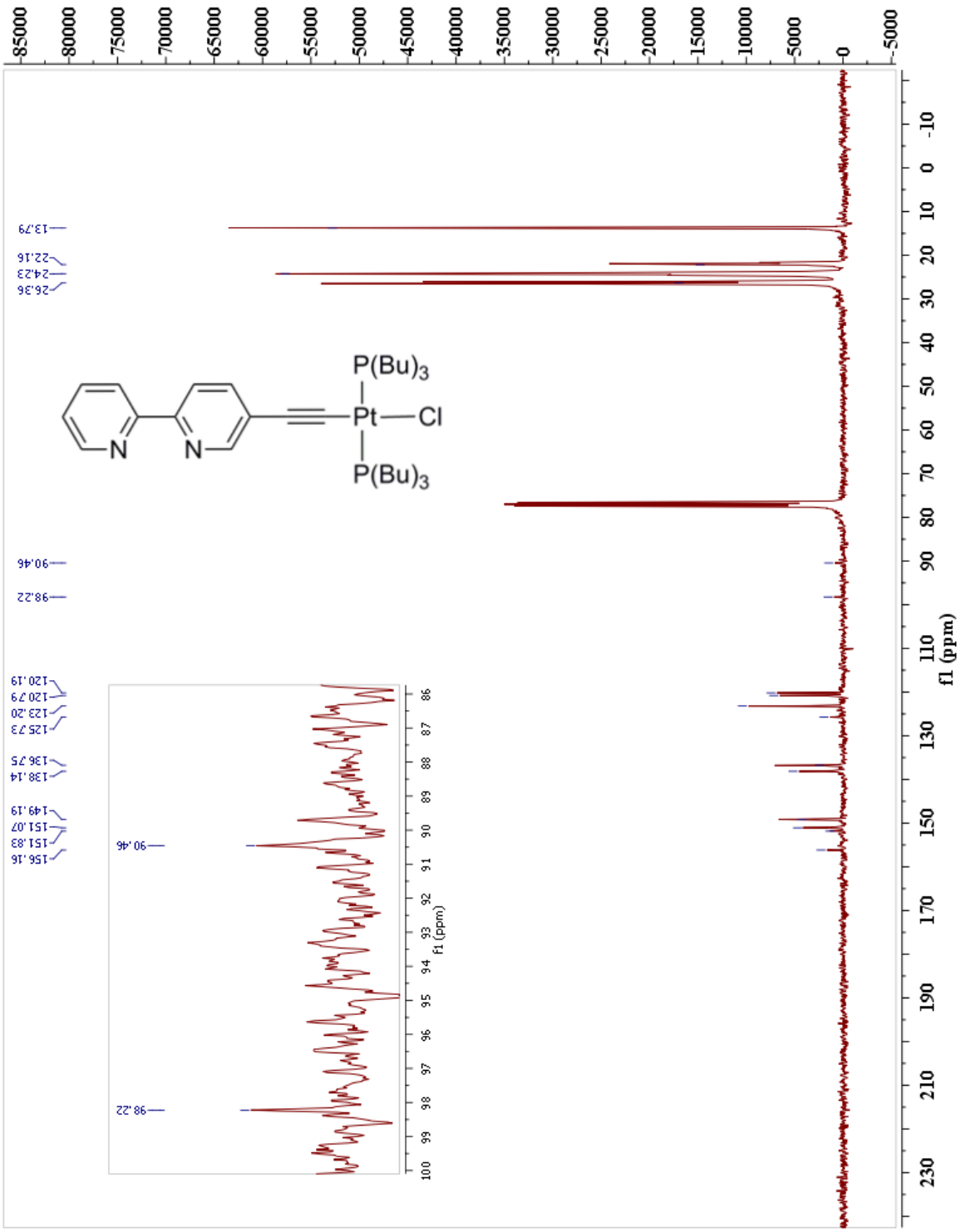

Figure S19: ^{31}P NMR data for ***trans*-(5-ethynyl-2,2'-bipyridine)-chloro-bis(tri-*n* butylphosphine)platinum (5'):**

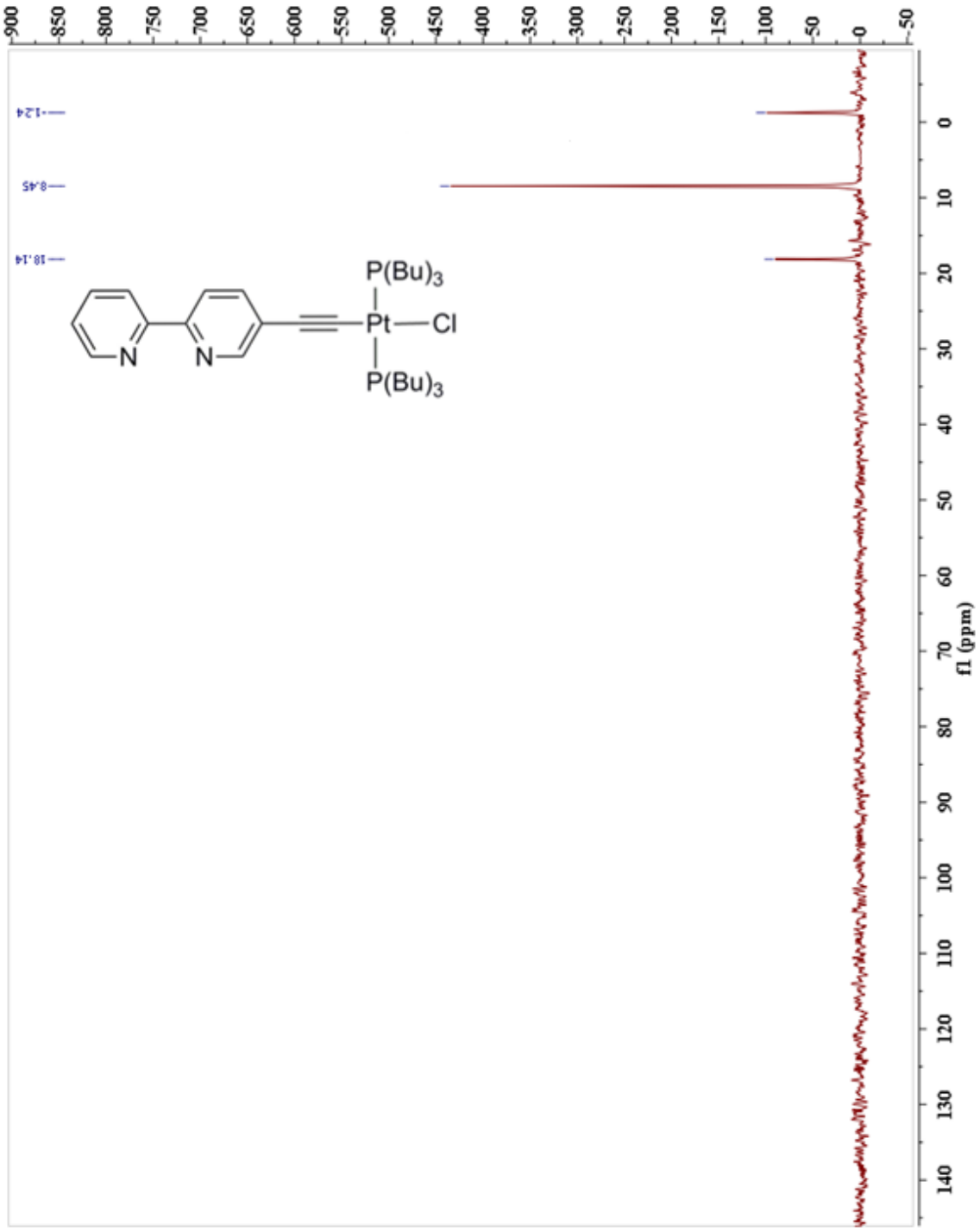

Figure S20: ^{1}H NMR data for ***trans*-(5-ethynyl-2,2'-bipyridine)-4-tolylethynyl-bis(tri-*n*-butylphosphine)platinum (2):**

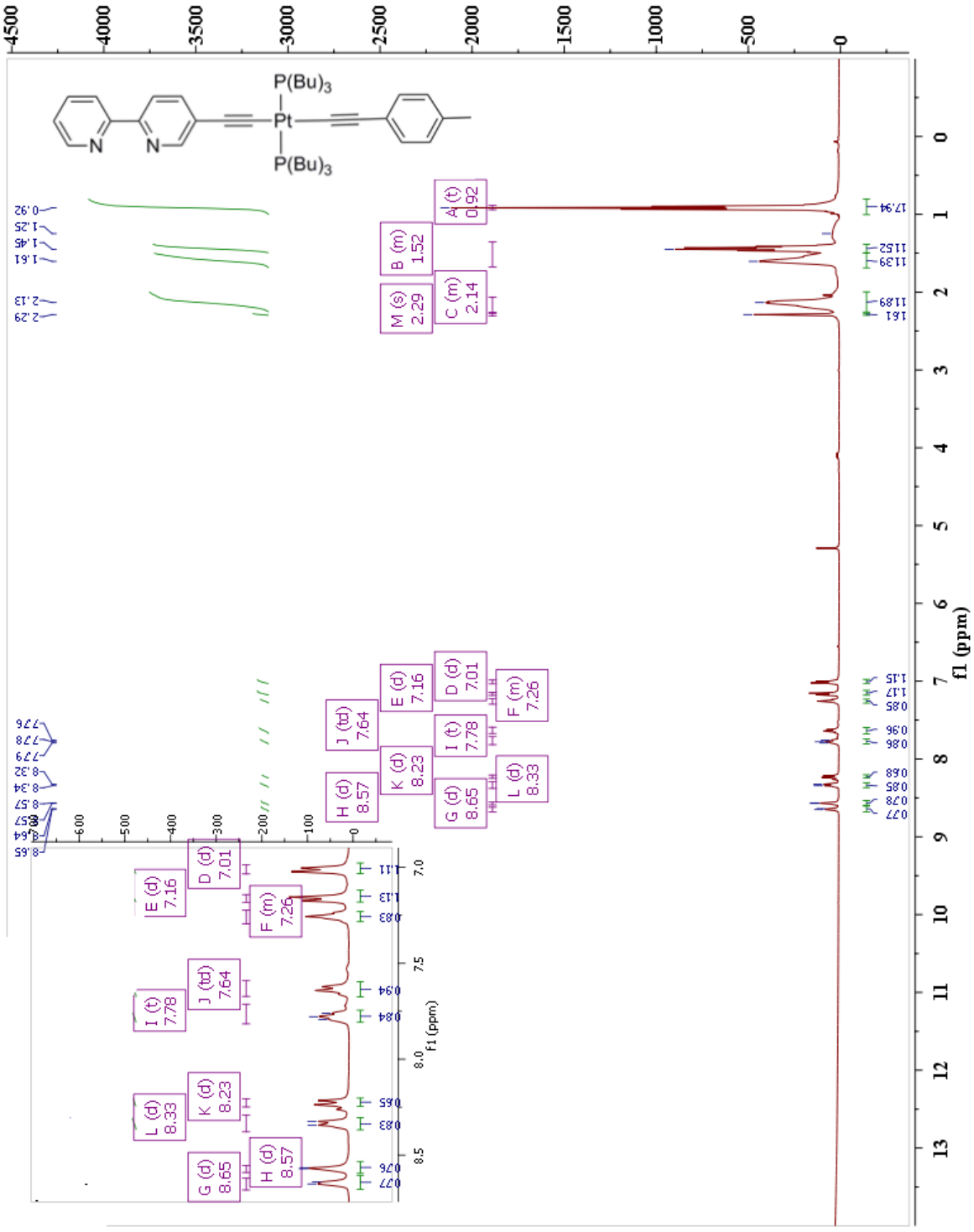

Figure S21: ^{13}C NMR data for ***trans*-(5-ethynyl-2,2'-bipyridine)-4-tolylethynyl-bis(tri-*n*-butylphosphine)platinum (2):**

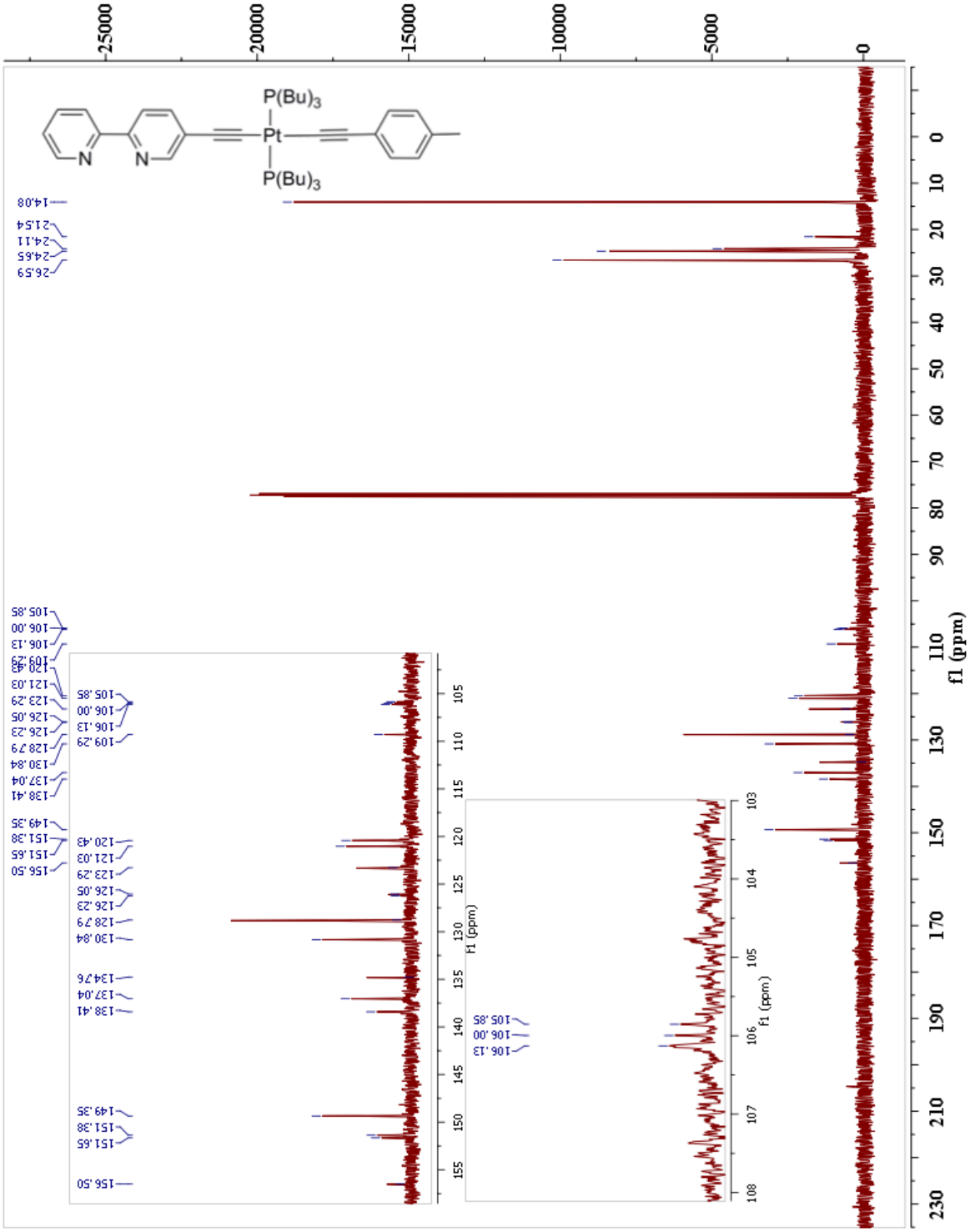

Figure S22: ^{31}P NMR data for ***trans*-(5-ethynyl-2,2'-bipyridine)-4-tolylethynyl-bis(tri-*n*-butylphosphine)platinum (2):**

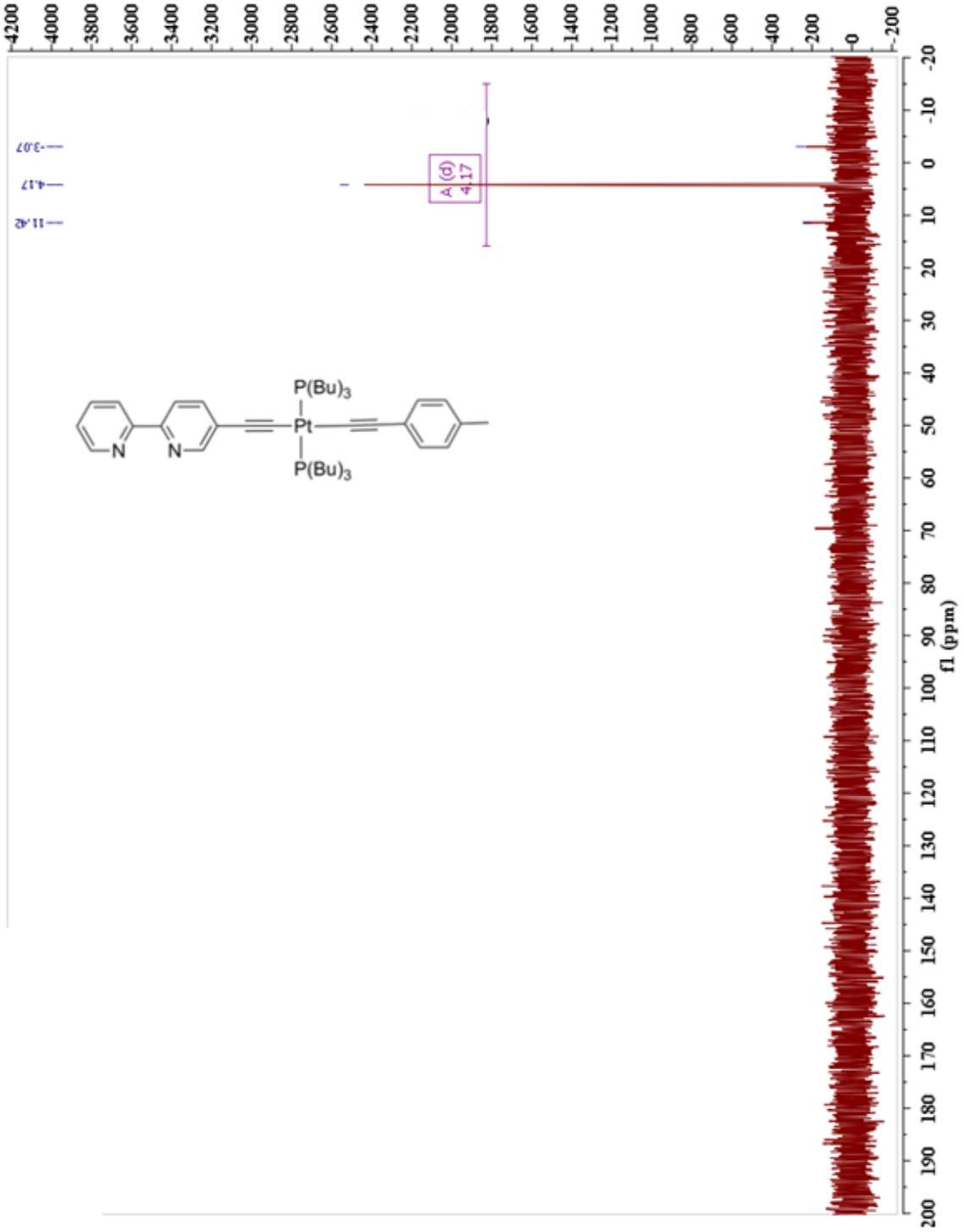

Figure S23: ^{1}H NMR data for ***trans*-bis(tri-*n*-butylphosphine)-bis(5-ethynyl-2,2'-bipyridine)platinum (2'):**

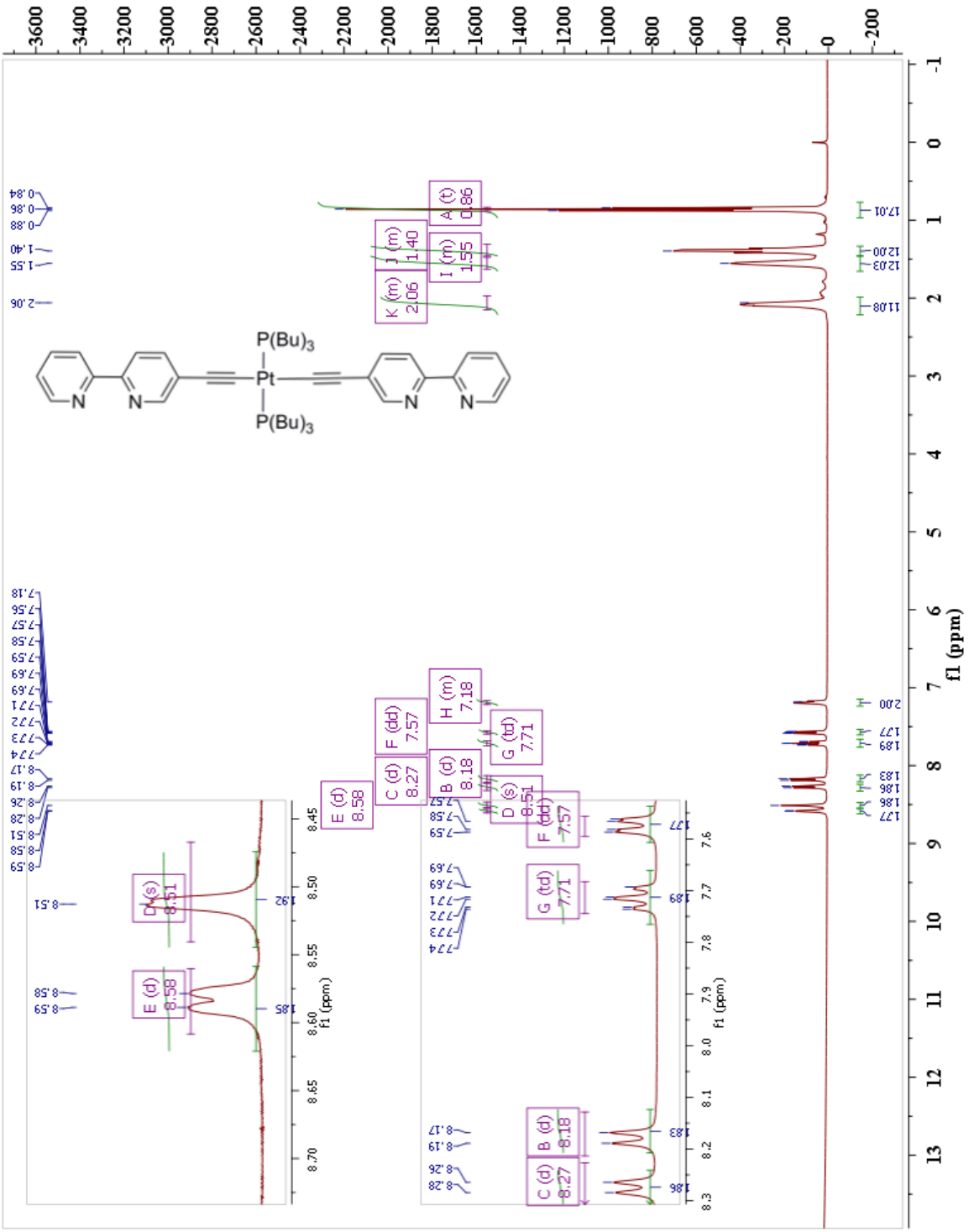

Figure S24: ^{13}C NMR data for ***trans*-bis(tri-*n*-butylphosphine)-bis(5-ethynyl-2,2'-bipyridine)platinum (2'):**

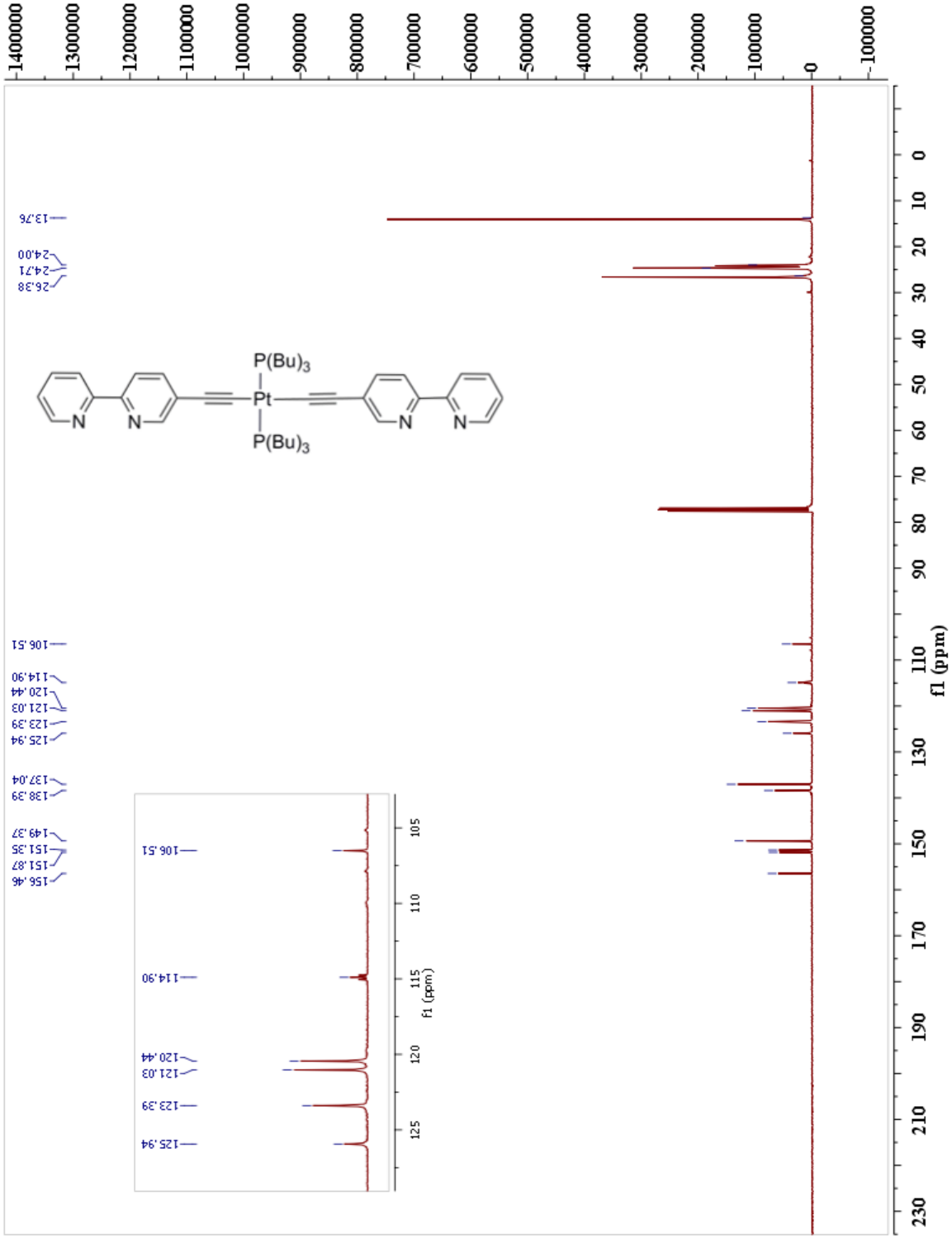

Figure S25: ^{31}P NMR data for ***trans*-bis(tri-*n*-butylphosphine)-bis(5-ethynyl-2,2'-bipyridine)platinum (2'):**

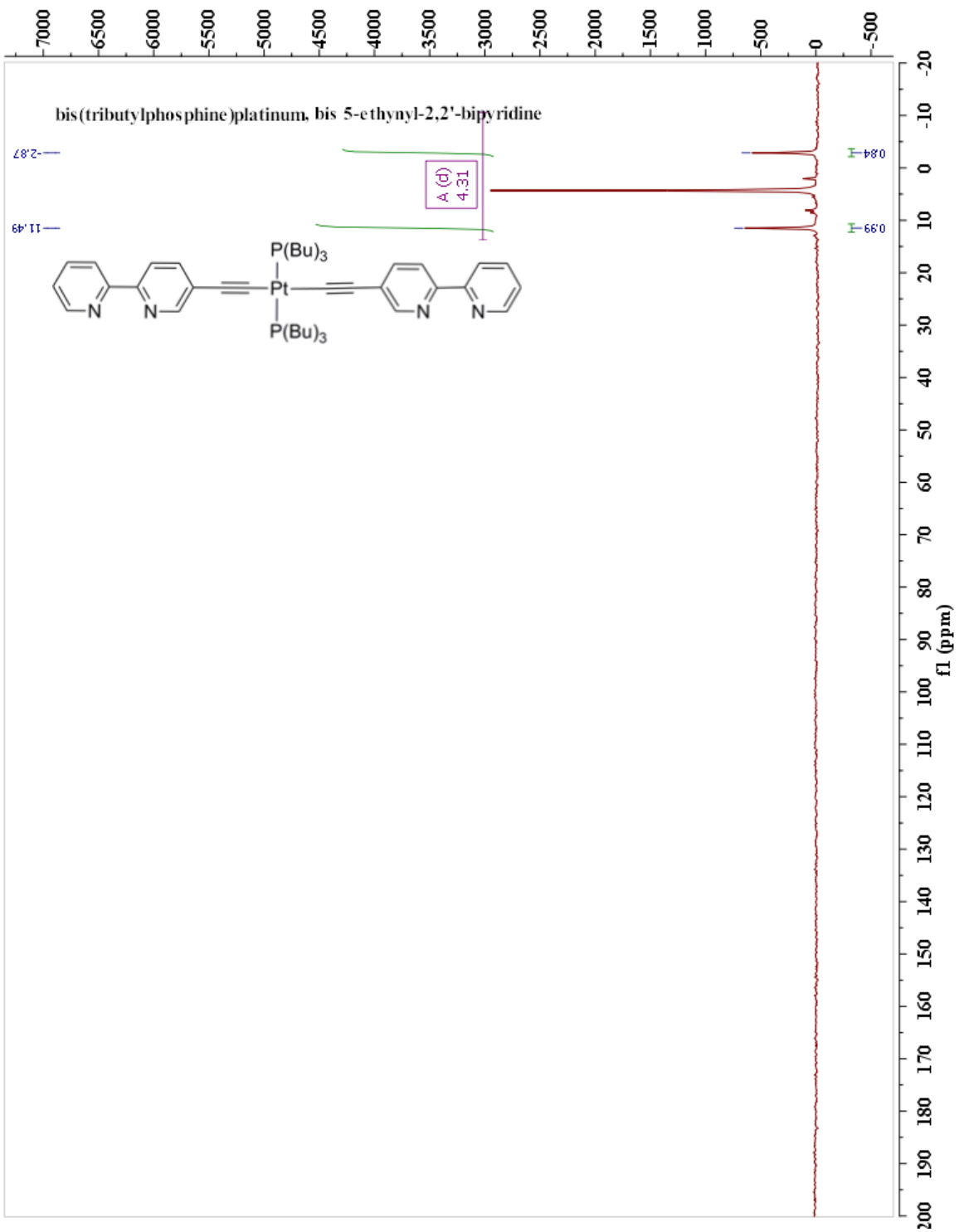

Figure S26: ^{1}H NMR data for **[Ir(ppy)$_2$(5-ethynyl-2,2'-bipyridine)] Hexafluorophosphate (1):**

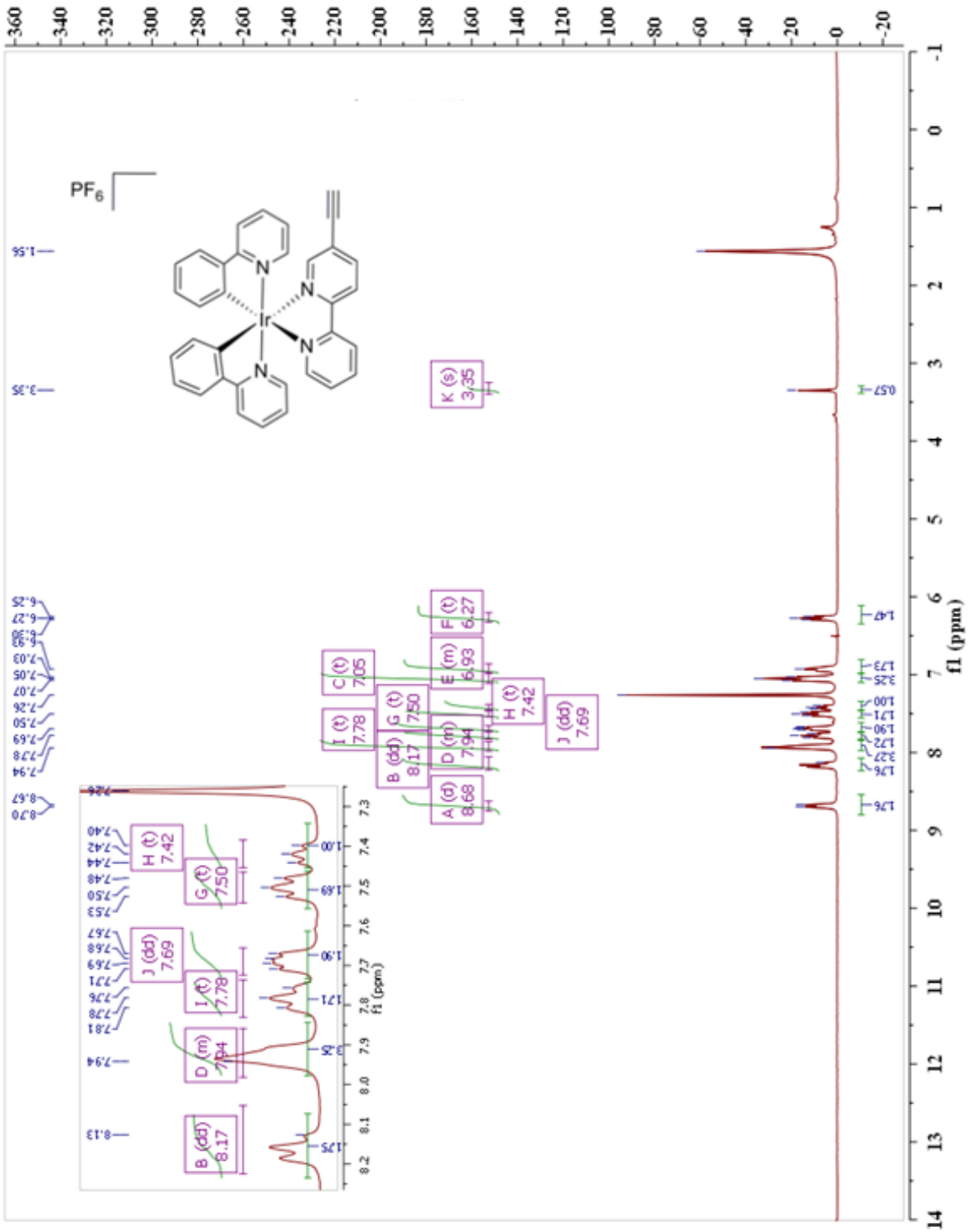

Figure S27: ^{13}C NMR data for **[Ir(ppy)$_2$(5-ethynyl-2,2'-bipyridine)] Hexafluorophosphate (1):**

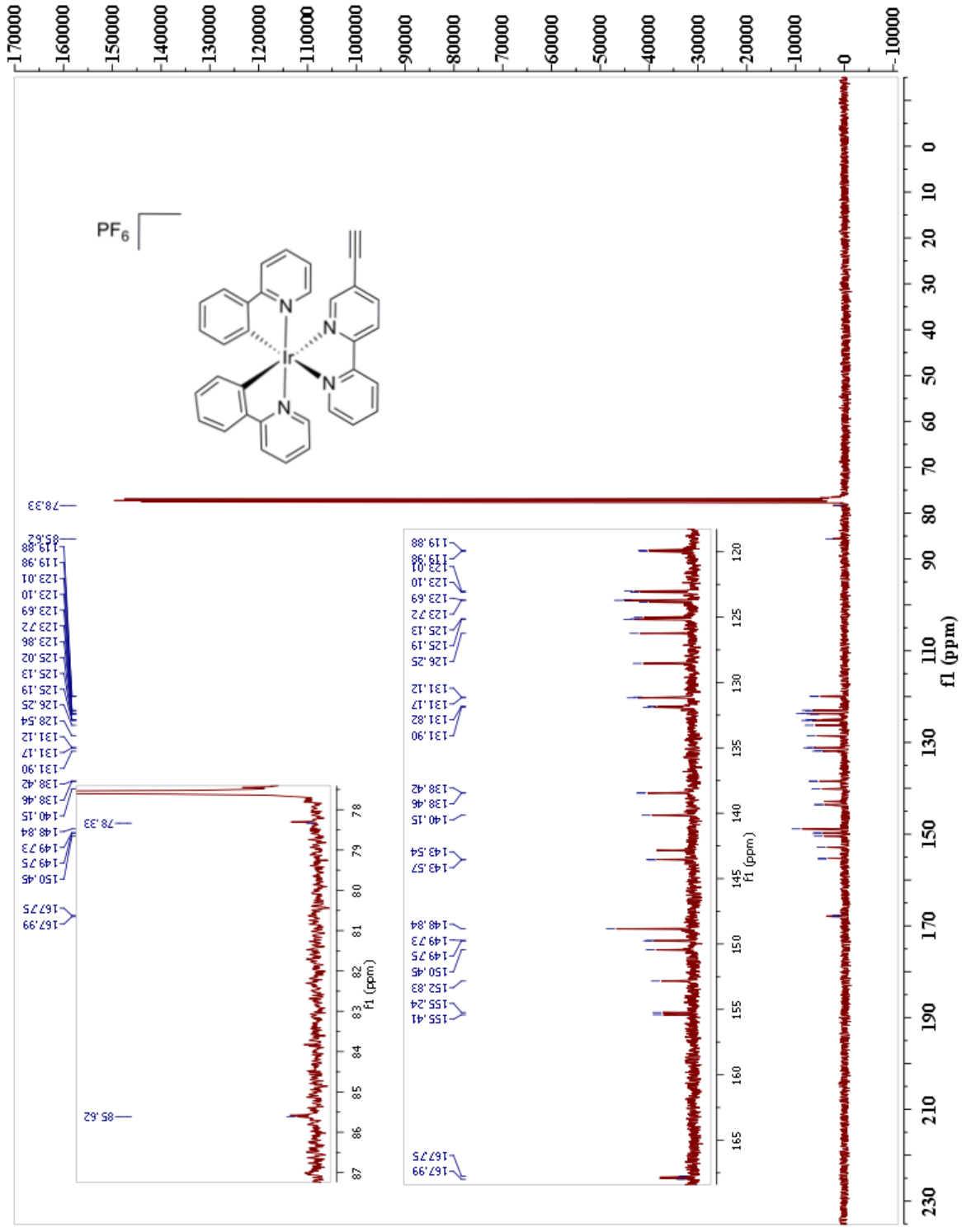

Figure S28: ^{1}H NMR data for ***trans*-[Ir(ppy)$_2$(5-Ethynyl-2,2'-bipyridine)]-4-tolylethynyl-bis(tri-*n*-butylphosphine)platinum Hexafluorophosphate (3):**

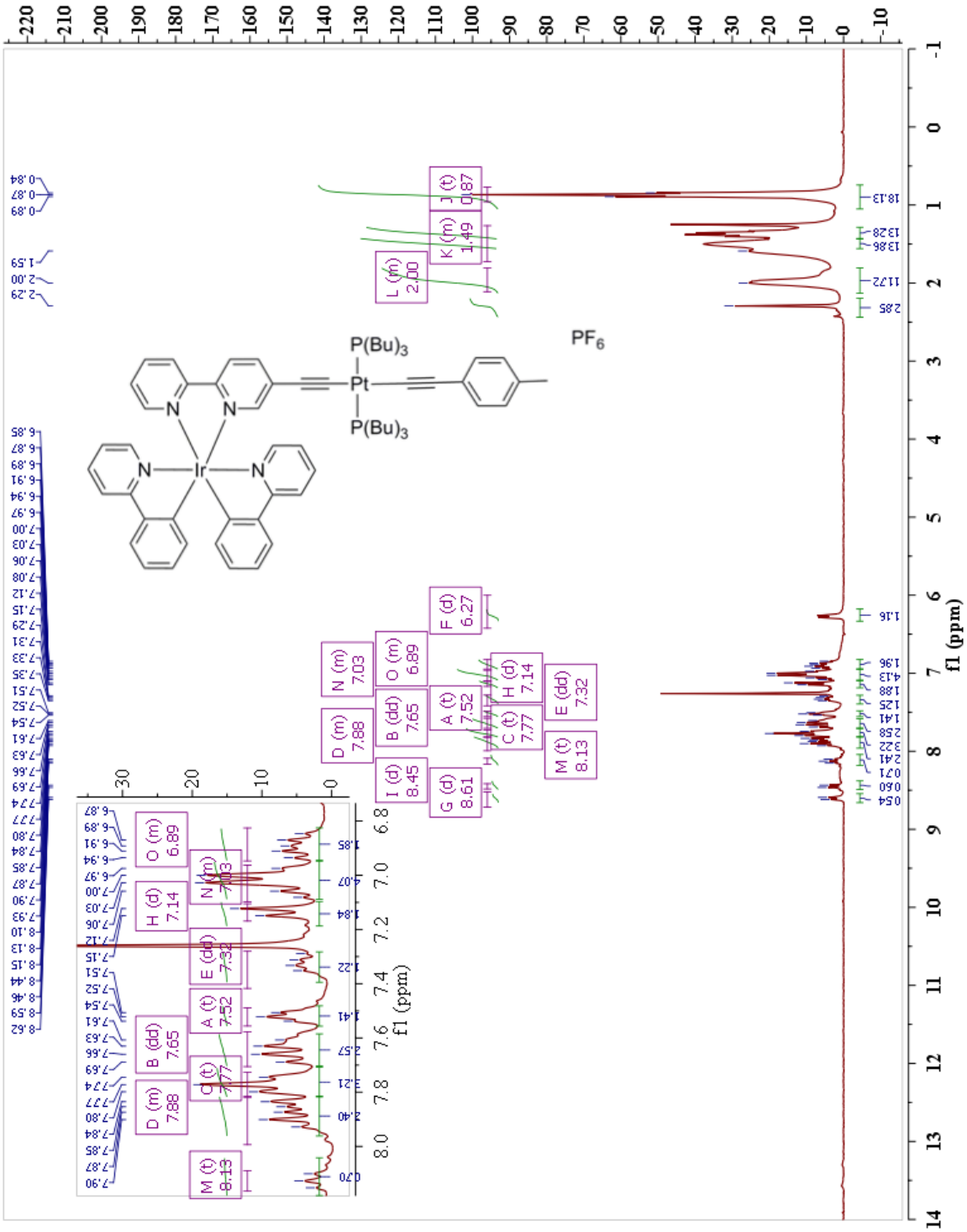

Figure S29: ^{13}C NMR data for ***trans*-[Ir(ppy)$_2$(5-Ethynyl-2,2'-bipyridine)]-4-tolylethynyl-bis(tri-*n*-butylphosphine)platinum Hexafluorophosphate (3):**

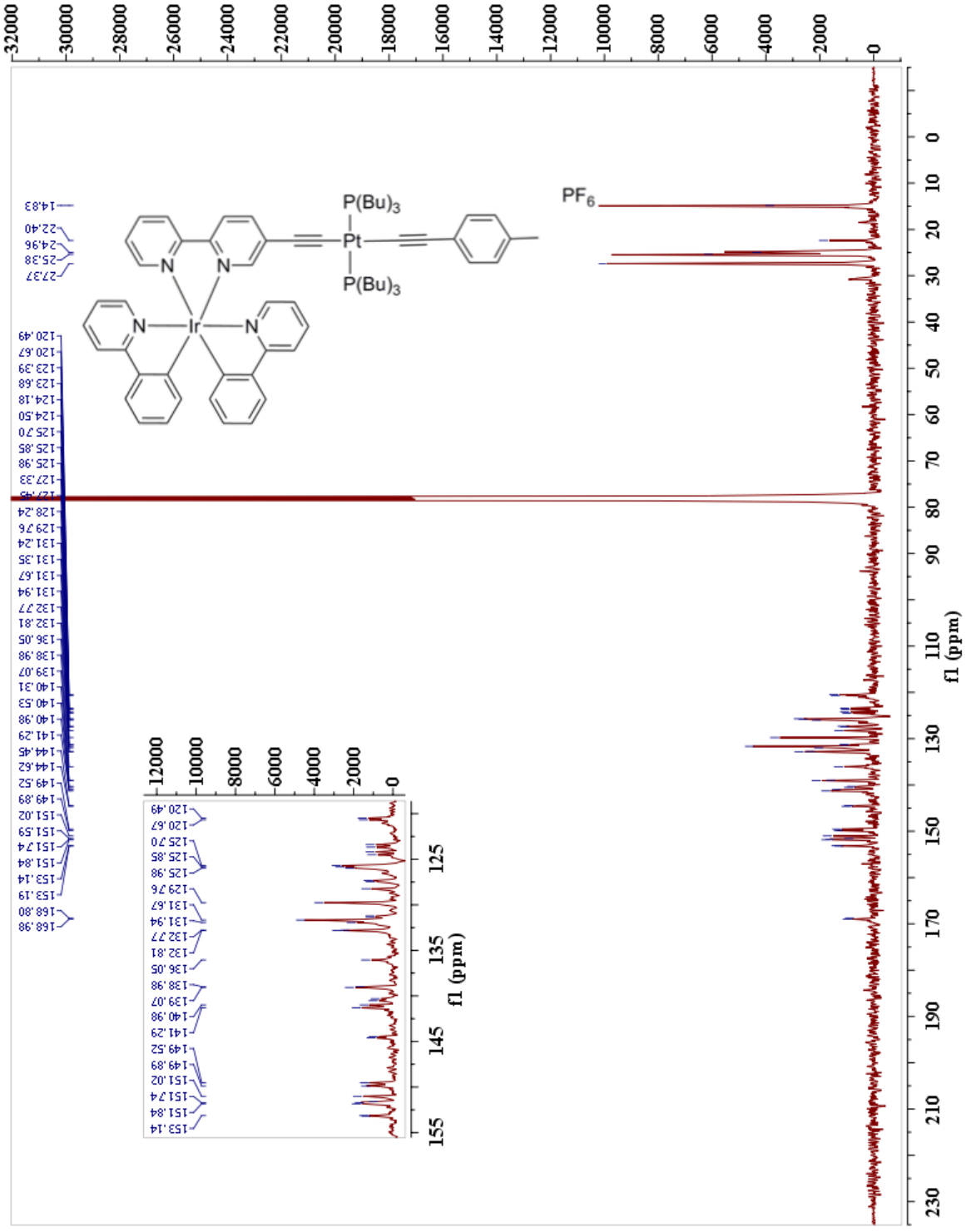

Figure S30: ^{31}P NMR data for ***trans*-[Ir(ppy)$_2$(5-Ethynyl-2,2'-bipyridine)]-4-tolylethynyl-bis(tri-*n*-butylphosphine)platinum Hexafluorophosphate (3):**

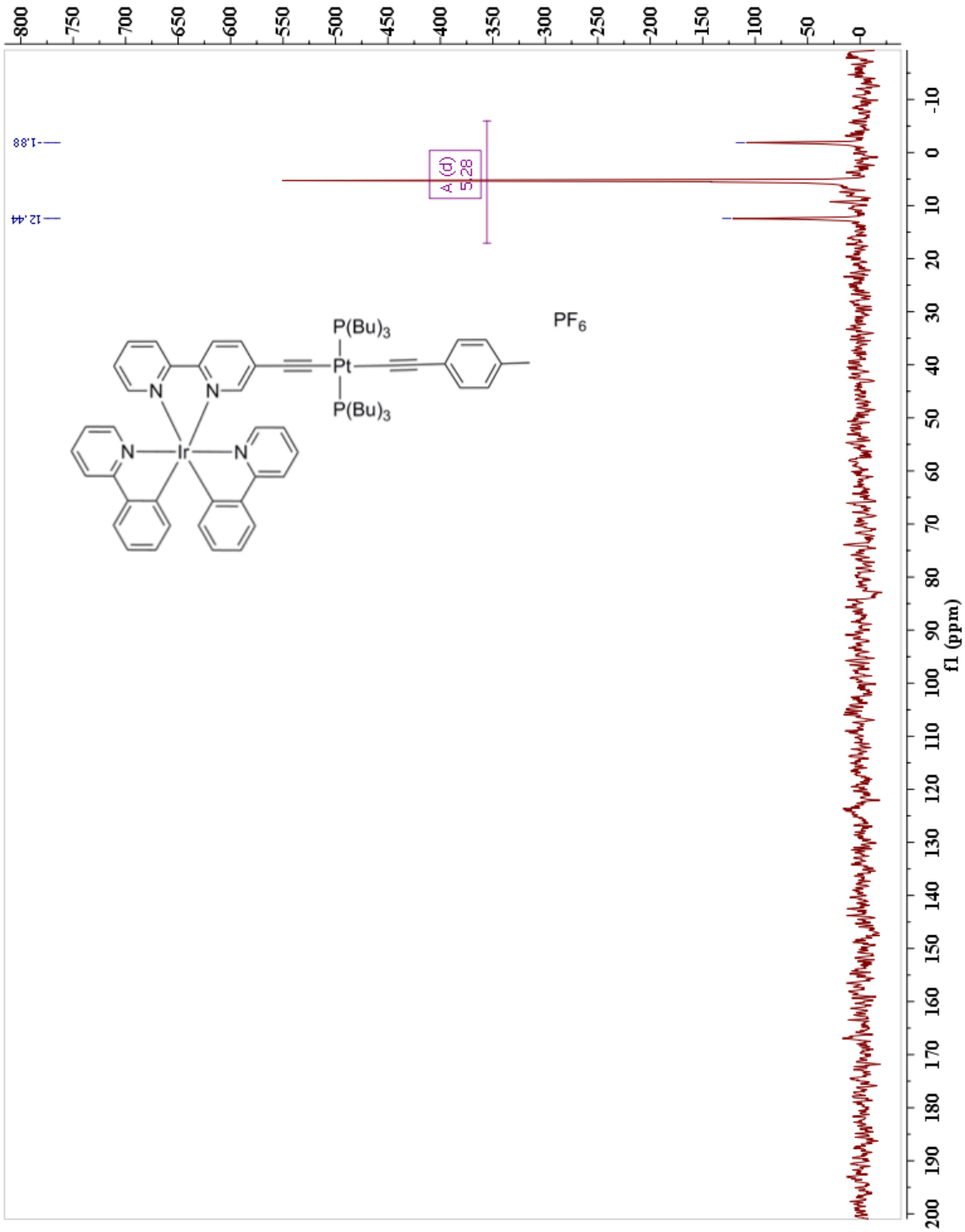

Figure S31: ^{1}H NMR data for ***trans*-bis[Ir(ppy)$_2$(5-Ethynyl-2,2'-bipyridine)]-bis(tri-*n*-butylphosphine)platinum Hexafluorophosphate (4):**

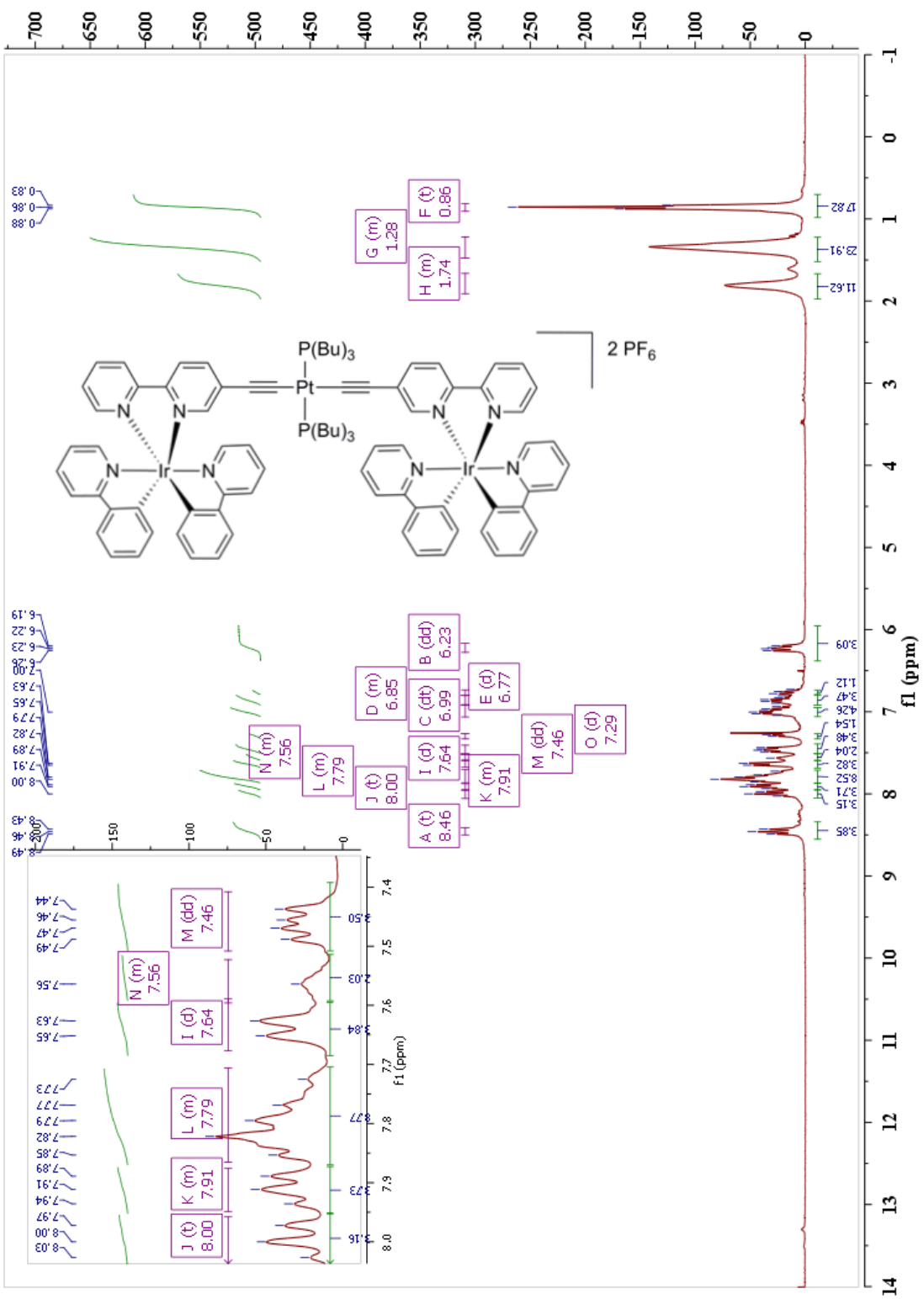

Figure S32: ^{13}C NMR data for ***trans*-bis[Ir(ppy)$_2$(5-Ethynyl-2,2'-bipyridine)]-bis(tri-*n*-butylphosphine)platinum Hexafluorophosphate (4):**

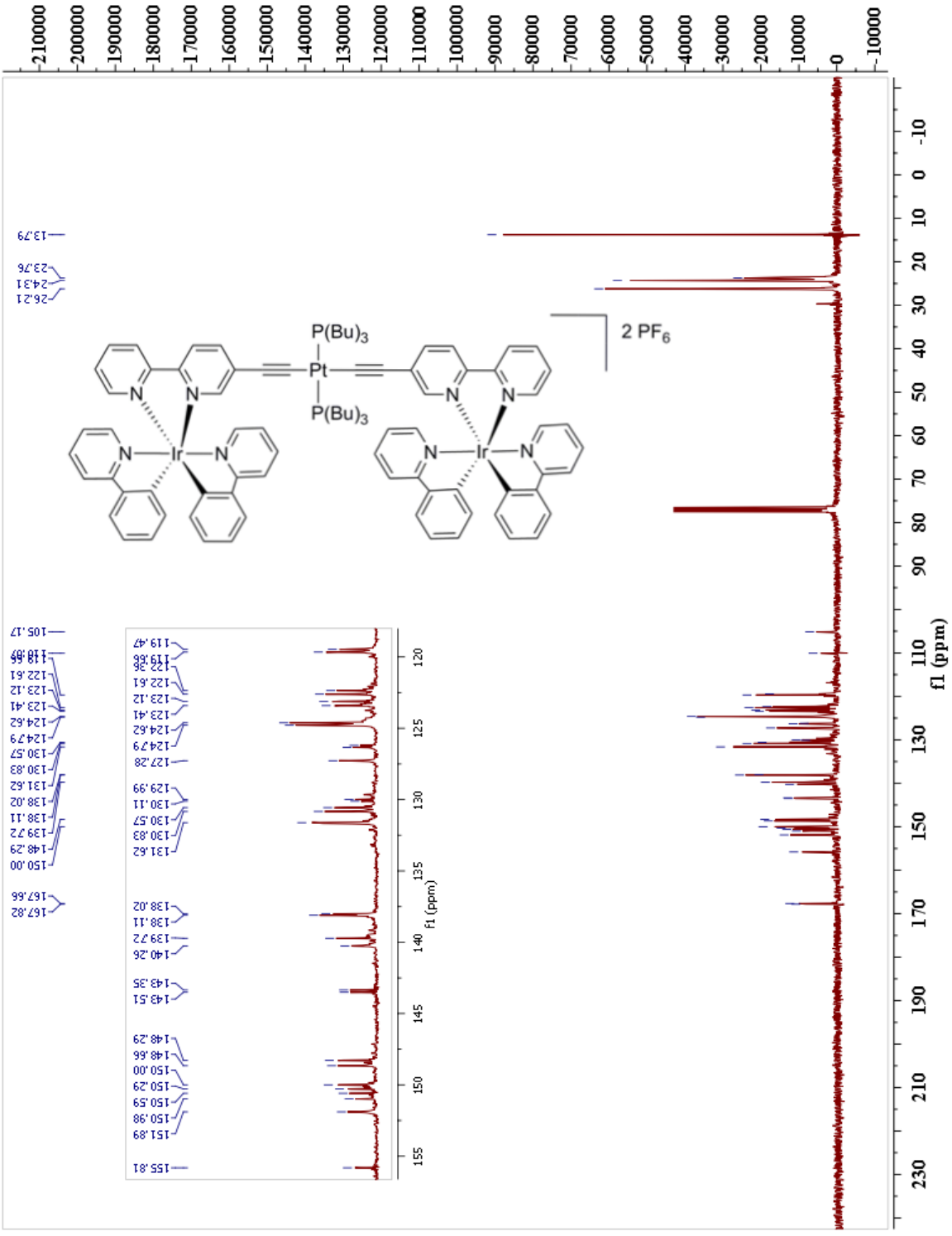

Figure S33: ^{31}P NMR data for ***trans*-bis[Ir(ppy)$_2$(5-Ethynyl-2,2'-bipyridine)]-bis(tri-*n*-butylphosphine)platinum Hexafluorophosphate (4):**

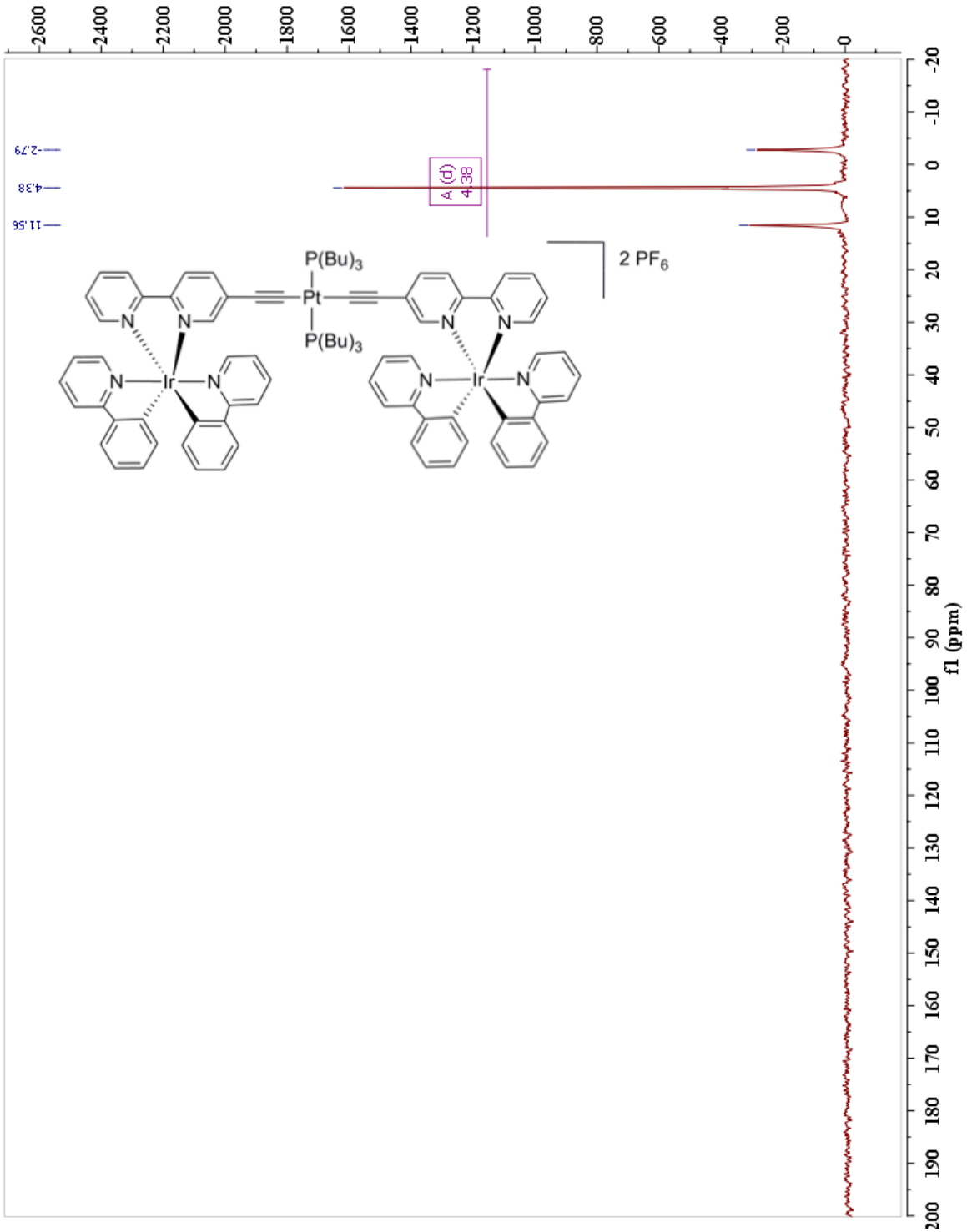

References:

(1). G. B. Kauffman, L. A. Teter and J. E. Huheey, in *Inorg. Synth.*, John Wiley & Sons, Inc., 2007, pp. 245-249.
(2). W. L. F. Armarego and D. D. Perrin, *Purification of Laboratory Chemicals, 3rd edition*, Pergamon Press, Oxford, 1988.
(3). M. Nonoyama, *Bull. Chem. Soc. Japan*, 1974, **47**, 767.
(4). (a) N. E. Leadbeater and B. J. Tominack, *Tetrahedron Lett.*, 2003, **44**, 8653-8656; (b) Y. Wang, B. Huang, S. Sheng and M. Cai, *J. Chem. Res.*, 2007, **2007**, 728-732.
(5). U. Lehmann and A. D. Schlüter, *Eur. J. Org. Chem.*, 2000, **2000**, 3483-3487.
(6). J. J. Song and N. K. Yee, *J. Org. Chem.*, 2000, **66**, 605-608.
(7). S.-H. Kim and R. D. Rieke, *Tetrahedron Lett.*, 2009, **50**, 5329-5331.
(8). A. Lützen and M. Hapke, *Eur. J. Org. Chem.*, 2002, **2002**, 2292-2297.
(9). V. Grosshenny, F. M. Romero and R. Ziessel, *J. Org. Chem.*, 1997, **62**, 1491-1500.
(10). A. A. Rachford, R. Ziessel, T. Bura, P. Retailleau and F. N. Castellano, *Inorg. Chem.*, 2010, **49**, 3730-3736.
(11). G. A. Crosby and J. N. Demas, *J. Phys. Chem.*, 1971, **75**, 991-1024.
(12). S. Fery-Forgues and D. Lavabre, *J. Chem. Educ.*, 1999, **76**, 1260.
(13). H. Ishida, S. Tobita, Y. Hasegawa, R. Katoh and K. Nozaki, *Coord. Chem. Rev.*, 2010, **254**, 2449-2458.
(14). M. J. Frisch, G. W. Trucks, H. B. Schlegel, G. E. Scuseria, M. A. Robb, J. R. Cheeseman, V. G. Zakrzewski, J. A. Montgomery, R. E. Stratmann, J. C. Burant, S. Dapprich, M. J.M., A. D. Daniels, K. N. Kudin, M. C. Strain, O. Farkas, J. Tomasi, V. Barone, M. Cossi, R. Cammi, B. Mennucci, C. Pomelli, C. Adamo, S. Clifford, J. Ochterski, G. A. Peterson, P. Y. Ayala, Q. Cui, K. Morokuma, A. Malik, A. D. Rabuck, K. Raghavachari, J. B. Foresman, J. Cioslowski, J. V. Ortiz, A. G. Baboul, B. B. Stefanov, G. Liu, A. Liashenko, P. Piskorz, I. Komaromi, R. Gomperts, R. L. Martin, M. Challacombe, P. M. W. Gill, B. G. Johnson, W. Chen, M. W. Wong, J. L. Andres, M. Head-Gordon, E. S. Replogle and J. A. Pople, *Gaussian 98 (Revision A.6)*, Gaussian Inc., Pittsburgh, PA, 1998.
(15). (a) P. Hohenberg and W. Kohn, *Phys. Rev.* , 1964, **136**, B864; (b) W. Kohn and L. J. Sham, *Phys. Rev.*, 1965, **140**, A1133; (c) in *The Challenge of d and f Electrons,*, eds. D. R. Salahub and M. C. Zerner, ACS, Washington, DC, 1989; (d) R. G. Parr and W. Yang, *Density-functional theory of atoms and molecules*, Oxford Univ. Press, Oxford, 1989.
(16). (a) R. E. Stratmann, G. E. Scuseria and M. J. Frisch, *J. Chem. Phys.*, 1998, **109**, 8218; (b) R. Bauernschmitt and R. Ahlrichs, *Chem. Phys. Lett.*, 1996, **256**, 454; (c) M. E. Casida, C. Jamorski, K. C. Casida and D. R. Salahub, *J. Chem. Phys.*, 1998, **108**, 4439.
(17). (a) A. D. Becke, *J. Chem. Phys.*, 1993, **98**, 5648-5652; (b) C. Lee, W. Yang and R. G. Parr, *Phys. Rev. B*, 1988, **37**, 785-789; (c) B. Miehlich, A. Savin, H. Stoll and H. Preuss, *Chem. Phys. Lett.*, 1989, **157**, 200-206.
(18). (a) J. S. Binkley, J. A. Pople and W. J. Hehre, *J. Am. Chem. Soc.*, 1980, **102**, 939; (b) M. S. Gordon, J. S. Binkley, J. A. Pople, W. J. Pietro and W. J. Hehre, *J. Am. Chem. Soc.*, 1982, **104**, 2797; (c) W. J. Pietro, M. M. Francl, W. J. Hehre, D. J. Defrees, J. A. Pople and J. S. Binkley, *J. Am. Chem. Soc.*, 1982, **104**, 5039; (d) K. D. Dobbs and W. J. Hehre, *J. Comp. Chem.* , 1986, **7**, 359; (e) K. D. Dobbs and W. J. Hehre, *J. Comp. Chem.* , 1987, **8**, 861; (f) K. D. Dobbs and W. J. Hehre, *J. Comp. Chem.* , 1987, **8**, 880.

(19). (a) W. J. Stevens, W. J. Basch and M. Krauss, *J. Chem. Phys.*, 1984, **81**, 6026; (b) W. J. Stevens, M. Krauss, H. Basch and P. G. Jasien, *Can. J. Chem.*, 1992, **70**, 612; (c) T. R. Cundari and W. J. Stevens, *J. Chem. Phys.*, 1993, **98**, 5555-5565.
(20). (a) M. S. Lowry, W. R. Hudson, R. A. Pascal Jr. and S. Bernhard, *J. Am. Chem. Soc.*, 2004, **126**, 14129-14135; (b) S. Ladouceur, D. Fortin and E. Zysman-Colman, *Inorg. Chem.*, 2010, **49**, 5625-5641.
(21). N. M. O'Boyle, *GaussSum 2.0*, Dublin City University; Dubin Ireland, 2006.
(22). J. Tomasi, B. Mennucci and R. Cammi, *Chem. Rev.*, 2005, **105**, 2999-3094.